1967

An investigation of the performance and mixing phenomena associated with a supersonic exhauster interacting with subsonic secondary flow.

Monroe, Philip Alvah

Monterey, California. U.S. Naval Postgraduate School

AN INVESTIGATION OF THE PERFORMANCE AND MIXING PHENOMENA ASSOCIATED WITH A SUPERSONIC EXHAUSTER INTERACTING WITH SUBSONIC SECONDARY FLOW

PHILIP ALVAH MONROE

AN INVESTIGATION OF THE PERFORMANCE AND MIXING PHENOMENA ASSOCIATED WITH A SUPERSONIC EXHAUSTER INTERACTING WITH SUBSONIC SECONDARY FLOW

by

Philip Alvah Monroe
Lieutenant Commander, United States Navy
B.A., Cornell University, 1957

Submitted in partial fulfillment of the
requirements for the degree of

AERONAUTICAL ENGINEER

from the

NAVAL POSTGRADUATE SCHOOL
September 1967

ABSTRACT

The Transonic Turbine Test Rig at the Naval Postgraduate School, Monterey, California, uses a supersonic jet exhauster to lower the turbine exit static pressure and thus increase pressure ratios available for turbine testing. Exhauster operation results in interaction between two co-flowing streams of air. The primary air is supersonic and the secondary air, subsonic. This thesis is an experimental study of the mixing process that occurs between the two streams in a cylindrical mixing chamber. In addition, a theoretical model of the exhauster performance based on polytropic efficiencies and conservation of momentum was programmed, and the predicted values were compared to test results.

Thesis by: Philip A. Monroe entitled An Investigation of the Performance and Mising Phenomena Associated with a Supersonic Exhauster Interacting with Subsonic Secondary Flow

ERRATA SHEET

Page 16, lines 15/16	Hyphenate "meas - ured" vice "mea - sured"
Page 17, lines 10/11	Hyphenate "meas - uring" vice "mea - suring"
Page 17, line 11/12	Hyphenate "manom - eter" vice "mano - meter"
Page 18, line 5	Change the comma to a semicolon before the word "hence"
Page 21, lines 13/14	"pecu - liar" not "pecul - iar"
Page 22, lines 1/2	Hyphenate "second - ary" vice "secon - dary"
Page 34, lines 6/7	Hyphenate "stat - ic" vice "sta - tic"
Page 36, lines 16/17	Hyphenate "stat - ic" vice "sta - tic"
Page 39, last line	"abscissa" vice "absissa"
Page 46, lower	Hyphenate "viscos - ity" vice "visco - sity"
Page 51, lines 15/16	Insert semi-colons instead of commas in the compound sentence. The comma in line 17 remains unchanged.
Page 53, lines 15/16	Hyphenate "second - ary" vice "secon - dary"
Page 56, line 20	"affected" vice "effected"
Page 57, lines 6/7	"restrict - ed" vice "restric - ted"
Page 58, ref. 2, lines 4/5	"Post - Graduate" should be "Post - graduate"
Page 77, middle right	In tabulation of PTN/P_{atm}, the word "NOZZEL" should read "NOZZLE"
Page 103, lines 8/9	Hyphenate "stat - ic" vice "sta - tic"
Page 110, bottom line	"outside to" should read "outside of the..."

TABLE OF CONTENTS

LIST OF TABLES

LIST OF ILLUSTRATIONS

LIST OF ILLUSTRATIONS (CONT'D)

TABLE OF SYMBOLS

Symbol	
A	Cross sectional area ($in.^2$)
D	Diameter (in.)
F_f	Viscous shear force (lb_f)
g	Universal gravitational constant (32.174 lbm-ft/lb_f-sec^2)
h_w	Differential pressure across flow measuring taps (in. H_20)
J	Conversion factor (778.16 ft-lb/BTU)
K	Discharge coefficient (dimensionless)
L	Length (in.)
M	Mach number
$\dot{m}$	Mass flow rate (slugs/sec)
M1-M14	Mixing pipe stations
n	Number of throttlings in labyrinth
n	Polytropic exponent
P	Pressure (psia.)
R	Gas constant for air (53.35 ft-lb_f/lbm-^oR)
R	Recovery factor (dimensionless)
R_e	Reynolds number (dimensionless)
r	Radius (in.)
T	Temperature (^oR)
TTTR	Transonic Turbine Test Rig
V	Velocity (ft/sec)
$\dot{w}$	Mass flow rate (lbm/sec)
Y_1	Expansion coefficient (dimensionless)

Greek Letters

α	Flow nozzle coefficient of thermal expansion (dimensionless)
α	Labyrinth discharge coefficient for a single throttling (dimensionless)
γ	Specific heat ratio, c_p/c_v (dimensionless)
δ	Boundary layer thickness
η	Efficiency
ν	Kinematic viscosity (ft/sec^2)
ρ	Density (lbm/ft^3)
Φ	Non-dimensional flow function
$\bar{\tau}$	Average shear (lb/ft^2)

Subscripts

atm	Atmospheric condition
aw	Adiabatic wall
c	Diffuser polytropic exponent or efficiency
d	Secondary flow polytropic exponent or efficiency
ex	Exit
is	Isentropic process
n	Nozzle air
p	Polytropic
s	Static conditions
s	Surface area
sl	Shaft labyrinth
t	Total

Subscripts (Cont'd)

t	Polytropic exponent or efficiency to nozzle throat
t	Secondary air
x	Axial position from hypothetical source
x	Conditions before shock
y	Conditions after shock
o	Stagnation condition
1	Inlet condition - flow function
1	Condition upstream of flow measuring nozzle - flow rate calculation
1	Nozzle polytropic exponent or efficiency to exit
2	Station of interest

1. Introduction

Exhausters are being incorporated into the design of many systems because of the simplicity of their design and the absence of moving parts. Air augmentation of rocket thrust, torpedo drag reduction innovations, use as a jet pump in aircraft for fuel transfer or boundary layer control are significant applications.

The Transonic Turbine Test Rig (TTTR) installed at the Propulsion Laboratory of the Naval Postgraduate School uses a supersonic exhauster system to increase the range of turbine pressure ratios available for testing. The test turbine is enclosed in a hood. A compressor can provide a maximum turbine inlet total pressure of 43 psia giving a maximum turbine pressure ratio ($P_{t_{inlet}}/P_{s_{exit}}$) of about 3 when exhausting to the atmosphere. Since the turbine uses only part of the mass flow furnished by the compressor, the remainder can be used to drive the exhauster which produces a vacuum in the hood and thereby increases the turbine pressure ratio.

Very little information is available on the mixing phenomena encountered with supersonic exhausters. Abramovich[1] provides extensive information for the case of an incompressible free jet and associated turbulent mixing. He includes test work accomplished, and theory developed,

---

[1]Abramovich, G. N., The Theory of Turbulent Jets (Cambridge, Massachusetts: The MIT Press, Massachusetts Institute of Technology, 1963), Part I, "Turbulent Jets in Incompressible Fluid."

by Prandtl and Tollmien. The effect of compressibility on turbulence is very complicated however, and simplifications of the problem must be introduced to develop approximate solutions.

This thesis is a study of the supersonic exhauster system used with the TTTR. Objectives of the investigation were to determine the hood total pressure variation with drive nozzle total pressure for a given secondary flow rate,and to study the mixing and turbulent interchange that occurs between the two co-flowing streams in the mixing pipe. Main topics include: traverse probe design, experimental results of the ejector test series, a computer prediction program of exhauster performance based on polytropic processes and conservation of momentum, empirical determination of polytropic efficiencies, and an attempt to determine from test data the losses due to mixing and turbulent interchange between the two streams of air.

A summary of the general properties of turbulent jets, including terminology used to describe the different mixing regions that occur with restricted jet operation and co-flowing streams, is given in Appendix D. The terms ejector and exhauster are used interchangeably throughout this thesis.

The author is most appreciative of the guidance, counsel and encouragement provided by Professor M. H. Vavra, the laboratory assistance given by Mr. J. E. Hammer, and the probe fabrication work of Mr. T. B. Dunton.

2. Installation.

The TTTR installation is shown schematically in Fig. 1, and Fig. 2 is a photograph of the turbine hood and exhauster assembly. High pressure air is supplied by an Allis-Chalmers VA 312 compressor and enters Tank 1. Air to the turbine passes from Tank 1 through a calibrated flow measurement nozzle and enters Tank 2. The amount of air to the turbine is controlled by a manual valve; an electrically operated exhauster inlet valve controls the drive nozzle total pressure (PTN). More detailed descriptions of the TTTR and its operating performance are given by Eckert[2] and by Commons.[3]

The exhauster section of the TTTR is shown in greater detail in Fig. 3. Important features are the arrangement of twelve mixing tube static pressure taps (M2 - M13), the Kiel probe to measure drive nozzle total temperature (TTN) and total pressure, and the secondary air static pressure taps just prior to entry into the mixing pipe. Secondary air is defined as the air that enters the mixing pipe from the turbine hood. To obtain the mixing pipe static pressures, four taps are equally spaced circumferentially at

---

[2]Eckert, R. H., Performance Analysis and Initial Tests of a Transonic Turbine Test Rig (Aeronautical Engineer's Thesis, U. S. Naval Postgraduate School, Monterey, California, May 1966), Section 2, "Installation."

[3]Commons, P. M., Instrumentation of the Transonic Turbine Test Rig to Determine the Performance of Turbine Inlet Guide Vanes Through the Application of the Momentum and Moment of Momentum Equations (Master's Thesis, U. S. Naval Postgraduate School, Monterey, California, 1967), Section 2, "Installation."

each location and commoned to obtain an average reading. Secondary air static pressures are measured by three taps at each location, equally spaced circumferentially and commoned.

One section of the mixing pipe was modified by cutting a 3 inch by 1/4 inch slit at 3 locations to provide ingress and egress of a traverse probe. The slits were designed to place the traverse probe total pressure opening at the same distance from the drive nozzle exit as the mixing pipe wall static pressure; that is, in the plane of the wall static pressure taps for a given axial location. Seals were also fabricated to prevent leakages, with or without the traverse probe in position.

Secondary air total temperature (TTD) is measured with a modified Kiel probe. Hood total pressure (PTD) is measured by eight static pressure ports that are commoned to obtain an average value. The secondary air is essentially that which passes from Tank 2 to the turbine. It is augmented by a small amount that enters the shaft labyrinth seal of the hood. Dimensions of the shaft labyrinth shown in Fig. 4 differ from those given by Eckert[4] due to increasing shaft clearance from 0.005 inch to 0.020 inch. A thermocouple is placed at the labyrinth entrance to measure the total temperature (TTC) of the leakage air.

Drive nozzle I, the exhauster drive nozzle designed for the TTTR, is shown in Fig. 5 with detailed measurements.

---

[4]Eckert, op. cit., Fig. 4, p. 25.

Drive nozzle II, a smaller nozzle with the same area ratio (A_{throat}/A_{exit}), was designed and built to investigate the effects of different primary and secondary flow areas, and smaller primary flow rate, on the mixing process and on hood total pressure. Details of Drive nozzle II are shown in Fig. 6. Design calculations were made to insure a uniformly decreasing secondary flow area for the new nozzle.

All temperatures are measured using standard Iron - Constantan or Cromel - Alumel thermocouples with an ice bath as reference. Differential pressures across the flow measuring nozzle are measured in inches of water on a manometer board with 0.1 inch gradations. Mixing tube static pressures are measured against atmospheric pressure with a Texas Instruments Fused Quartz Pressure Gage. All other pressures are measured in inches of mercury against atmospheric pressure as reference using 96 inch long manometer tubes with 0.1 inch gradations. A check of static pressure readings between the Texas Instrument gage and the mercury manometers produced values within 0.5 per cent of each other.

3. Probe Design.

In order to study the mixing of two co-flowing streams, velocity traverses were desired at a number of axial locations. Naviaux[5] attempted to obtain this information but

[5]Naviaux, J. C., Transonic Turbine Test Rig Exhauster System Tests and Tests of a Reaction Turbine (Master's Thesis, U. S. Naval Postgraduate School, Monterey, California, December 1966), Section 4, "Test Results."

experienced difficulty in obtaining reliable data. During his tests the probe had excessive vibration, the static pressure probe used had the pressure ports only 2 diameters away from the probe tip, and a thermocouple was not incorporated, hence, the differences in stagnation temperatures between the two streams could not be measured.

For the ejector tests, the four probes of Fig. 7 were designed and built to obtain traverse information; two were pressure probes with a thermocouple and two were hot wire probes. Probe I was the only successful instrument and all traverse information was obtained with it.

Probe I is shown with its significant dimensions in Fig. 8. Criteria presented by Gettelman and Krause[6] concerning static port location for maximum accuracy were strictly adhered to. Best results are obtained when the static ports are 4 - 6 sensing element diameters away from the tip, and greater than 8 support diameters away from the support. These minimum criteria produce static pressure readings within 5.0 per cent of the velocity head at Mach 0.9 and 3.5 per cent at Mach 0.5. Mr. E. Keener of NASA Ames Laboratories assured the author that the error decreases in supersonic conditions.

---

[6]Gettelman, C. C. and Krause, L. N., Considerations Entering into the Selection of Probes for Pressure Measurement in Jet Engines (ISA Proceedings Vol. 7, Aeronautic Instrumentation - Session II), pp. 134-137.

The blockage of probe I is 4.3 per cent of the mixing pipe area. Tests[7] show that a blockage effect based on ratio of support diameter to duct or jet diameter can induce an error as large as 8.0 per cent for conditions and dimensions used in the ejector tests. The error, however, causes a measurement that is too large in a circular duct and a measurement that is too small in a jet. This difference in direction of the measurement error probably leads to a partial cancellation of the blockage error at mixing stations near the drive nozzle for the exhauster system. The exact effect and variations with axial position were not evaluated.

The thermocouple of probe I was placed in the support 0.5 inch above the pressure element. This position was chosen to avoid a second extended sensing arm which could induce errors due to probe interactions. The thermocouple is exposed to the stream by a 0.160 inch diameter hole. A 0.040 inch diameter hole in the after side provides air circulation. Total temperature measurements at mixing pipe station M1 were less than 2.0 per cent different than those obtained for the primary and secondary flow before entry to the mixing pipe.

The probe vibration problem was eliminated by installation of two 4 inch x 6 inch box supports contoured to fit the outside surface of the mixing pipe. Each box was

---

[7] Krause, L. N. and Gettelman, C. C., Effect of Interaction Among Probes, Supports, Ducts, Walls and Jet Boundaries on Pressure Measurements in Ducts and Jets (ISA Proceedings Vol. 7, Aeronautic Instrumentation - Session II), Fig. 4, p. 140.

fitted with a 3 inch teflon bushing to provide probe support over a long distance. This eliminated the pivot point about which a probe would tend to oscillate. The assembly is shown in detail in Fig. 9 and pictured in Fig. 10. The design proved very successful.

The mixing process is primarily a function of axial location in the mixing pipe. Probe I has a 3 inch axial distance between the position where the total pressure is taken and the thermocouple. Because significant gradients in total temperature exist, particularly near the drive nozzle, probe II was designed to obtain the temperature nearer to the total pressure opening. An exposed thermocouple was placed in a position 1/2 inch aft of the static pressure ports.

Testing of probe II produced expected results in the subsonic secondary flow. In the supersonic region of the primary flow, the test data were irregular both for static pressures and temperatures. However, lower temperatures were recorded whereas in actuality the primary flow had a higher total temperature than the secondary flow. The lower temperature reading occurred because an exposed thermocouple in supersonic flow measures an adiabatic wall temperature. Shapiro[8] introduces the energy equation to describe the

---

[8]Shapiro, A. H., The Dynamics and Thermodynamics of Compressible Fluid Flow Volume II (New York: The Ronald Press Company, 1954), pp. 1034-1036.

relationship between the adiabatic wall or recovery temperature T_{aw}, the static temperature T_s, and velocity V that must exist in the boundary layer over such an exposed thermocouple.

$$T_{aw} = T_s + R\frac{V^2}{2c_p}$$

R is the recovery factor that has been shown in many experiments[9] to be equal to the square root of the Prandtl number or 0.85 in laminar flow. Probe II could be used in supersonic flows only if the velocity were known and actual temperature, the quantity to be determined from measurement. This temperature was needed in the ejector tests to determine velocity so probe II was not applicable.

An attempt was made to verify the shape of the peculiar velocity profiles obtained at axial stations M1 - M3 by using a hot wire anemometer. The results of such a test would be qualitative because of the temperature difference between the primary and secondary streams. However, the difference in total temperature never exceeded 80°F. With the hot wire temperature at 1200 °F, results within 10 per cent accuracy could still be obtained. This would be sufficiently accurate to confirm the velocity profile obtained with probe I.

Probe III is shown in Fig. 7. It is a hot wire mounted on vertical arms attached to 1/4 inch tubing. On each

---

[9] Ibid., pp. 1070 - 1072.

of six tests the wire maintained its integrity in the secondary flow but broke as soon as the primary jet was encountered. It is possible that the hot wire broke because of vibrations of the thin vertical arms to which the wires were attached.

Probe IV, shown in Fig. 7, was designed such that the arms to which the wire was attached were stronger and oriented parallel to the flow. Both changes were made to dampen arm vibration. The probe was placed in the center stream before the exhauster was operated. The air flows through the turbine and drive nozzle were slowly increased, but the wire broke at velocities far below those experienced during normal exhauster operating conditions.

4. Description of Test Runs.

Tests were made to determine the hood total pressure variation as a function of drive nozzle total pressure and secondary flow rate, to establish the exhauster performance, to obtain the variation of mixing pipe static pressure as a function of drive nozzle total pressure and secondary flow rate, and to study the interaction of the two co-flowing streams by obtaining velocity profiles at different axial positions of the mixing pipe. Testing was accomplished with two different drive nozzles in order to compare the effect of variation of the primary flow rate and secondary flow annulus area on the problem.

A total of 34 runs was carried out between February and September 1967. Exhauster performance and mixing pipe

static pressure rise were obtained for drive nozzle total pressure ratios (PTN/P_{atm}) of 2.65, 2.45, 2.18, 1.90, and 1.63 and for secondary flow rates of 4 and 2 lbm/sec.

The TTTR was set in the following manner. Equation 1 given in Sec. 5, entitled "Data Reduction", is the equation used to determine actual flow rate through the flow measuring nozzle. Using average values for α, K, and Y_1 and with D_2 known for the TTTR installation, an expression for the differential pressure h_w across the pressure taps was obtained.

$$h_w \cong \left[\frac{\dot{w}}{2.18} \sqrt{\frac{T_1}{P_1}} \right]^2$$

$\dot{w}$ = desired secondary flow rate

p_1 = static pressure at upstream tap

T_1 = fluid temperature at upstream tap

For each test condition, the drive nozzle total pressure was set by hand. After allowing time for stabilization of conditions, readings of the calibrated flow measuring nozzle total temperature T_1 and pressure p_1 were taken, and an h_w calculated that corresponds to the desired flow rate. By adjusting the turbine inlet valve, this value of h_w was set. Flow rate regulation to within 0.05 lbm/sec of the desired amount was obtained.

There was no attempt made to precisely regulate either primary or secondary air temperature due to the large number of variables and valve settings involved. Turbine testing

being carried out concurrent with the ejector tests created different turbine efficiencies and operating conditions which made temperature variations difficult to regulate.

The analysis of early test results showed that traverse probe position significantly affected hood total pressure and secondary flow polytropic efficiencies. The probe was removed during final tests to obtain exhauster performance and mixing pipe static pressure rise.

Velocity traverses were initially made at mixing stations M1, M2, M3, M4, M6, M7, and M8 of Fig. 3 for a pressure ratio PTN/P_{atm} of 2.18, and secondary flow rates $\dot{w}_t$ of 4, 3, and 2 lbm/sec. Data points were taken in 1/2 inch radial increments at stations M6 - M8. Due to large gradients in total temperature and pressure, the increment was changed to 1/4 inch for stations M2 - M4 and to 1/10 inch at M1. Additional traverses were obtained at M1 and M4 for $\dot{w}_t$ of 4 lbm/sec and PTN/P_{atm} of 2.65 and 1.63.

It was not possible to change the traverse probe position without shutting down the exhauster system. After restart and stabilization of the system, the new operating conditions could vary in total temperature up to 3 degrees from the previous run. The consequence was considered secondary compared to the effect probe position had on exhauster operation.

Testing with probe II in run 17 produced total pressures different from those obtained with probe I for the same operating conditions. Investigation of the equipment

showed a leak in the traverse probe total pressure tubing. The effect of the leak became noticeable with probe II because of its smaller total pressure opening. After repairs, a retest of data points indicated the leak had existed during all traverse tests.

The planned test program was revised and retests initiated. Final tests included obtaining the hood total pressure and mixing pipe static pressure rise versus drive nozzle total pressure, for secondary flow rates of 4 and 2 lbm/sec. Velocity traverses were taken at stations M1 - M8 (less M5) for $\dot{w}_t$ of 4 and PTN/P_{atm} of 2.18. The tests were carried out for both drive nozzles.

Several attempts to verify the velocity profile at station M1 with a hot wire anemometer proved futile. The wire could not withstand the impact of the primary stream and broke immediately upon insertion in every test.

5. Data Reduction.

Secondary Flow

Secondary flow rates were measured by a flow nozzle between tanks 1 and 2. The basic formula for flow rate in lbm/sec was given by Eckert[10] to be

$$\dot{w} = 0.115\, D_2^2 \propto K Y_1 \sqrt{\frac{P_1 h_w}{T_1}} \qquad (1)$$

[10] Eckert, op. cit., Eq. 145, p. 98.

D_2 = nozzle throat diameter (in.)

α = coefficient of thermal expansion based on D_2^2 (dimensionless)

K = discharge coefficient (dimensionless)

Y_1 = expansion coefficient (dimensionless)

p_1 = static pressure at upstream tap (in. Hg.)

T_1 = fluid temperature at upstream tap (^{o}R)

h_w = differential pressure across taps (in. H_2O)

Values for α were determined as outlined by Eckert.[11] The expansion factor Y_1 was changed to that given by the ASME Power Test Codes.[12] Discharge coefficient K was found by Naviaux[13] to be a function of Reynolds number. Naviaux plotted nozzle flow coefficient versus Reynolds number and by curve fitting obtained an eighth order polynomial for K, with Reynolds number the independent variable. Computation of the polynomial showed that even the highest order terms produce large corrections for K. For R_e of 11.31 X 10^5 the seventh order correction was +1168.857

---

[11] Ibid., pp. 98-99.

[12] Flow Measurement, Supplement to ASME Power Test Codes, New York: ASME, 1959, Chap. 4, Part 5, p. 74.

[13] Naviaux, op. cit., p. 35.

and the eighth order term -96.291. Because values of K were determined by Naviaux to be in the small range from 1.00 to 1.05, the polynomial with such large corrections was considered inappropriate, and K was varied in steps of 0.01 as a function of R_e using Naviaux's graphical results as a reference.[14]

The method used for estimating the leak rate through the shaft labyrinth was developed by Egli[15] and revised by Eckert[16] to apply to the TTTR installation.

$$\dot{W}_{SL} = \alpha \varphi_S \frac{A P_{t_0}}{\sqrt{T_{t_0}}} \sqrt{\frac{g}{R}} \tag{2}$$

and

$$\varphi_S = \left[\frac{1 - (p/p_{t_0})^2}{n + \frac{2}{\gamma} \ln (p_{t_0}/p)} \right]^{1/2} \tag{3}$$

α = discharge coefficient for a single throttling (dimensionless)

α = 0.76 from Egli for present installation

A = cross sectional area of seal passage (in.^{2})

---

[14] Ibid., Fig. 19, p. 68.

[15] Egli, A. "The Leakage of Steam Through Labyrinth Seals," Transactions of ASME, V. 57, 1935, pp. 115 - 122.

[16] Eckert, op. cit., pp. 103 - 105.

P_{t_o} = total pressure at seal entrance (psia)

p = static pressure at seal exit (psia)

T_{t_o} = total temperature at seal entrance (^{o}R)

n = number of throttlings

The calculation of secondary flow rate was accomplished with computer program SECFLO which is shown in Appendix C.

Velocity

The velocity profile data reduction was accomplished by the computer program VELOCITY. Total temperature, total pressure and static pressure were measured. The pressure ratio was tested for supersonic or subsonic conditions. For supersonic flow, the Rayleigh Pitot tube formula[17] was used.

$$\frac{P_{o_y}}{P_x} = \frac{\left(\frac{\gamma+1}{2} M_x^2\right)^{\frac{\gamma}{\gamma-1}}}{\left(\frac{2\gamma}{\gamma+1} M_x^2 - \frac{\gamma-1}{\gamma+1}\right)^{\frac{1}{\gamma-1}}} \tag{4}$$

For subsonic conditions, the standard compressible flow relation was used.

$$\frac{P_o}{P} = \left(1 + \frac{\gamma-1}{2} M^2\right)^{\frac{\gamma}{\gamma-1}} \tag{5}$$

---

[17] Shapiro, A. H., The Dynamics and Thermodynamics of Compressible Fluid Flow Volume I (New York: The Ronald Press Company, 1954), p. 118.

In either case, Mach number was solved by iteration and converted to velocity with the measured total temperature, using:

$$\frac{T_o}{T} = 1 + \frac{\gamma-1}{2} M^2 \quad \Longrightarrow \quad T = \frac{T_o}{1 + \frac{\gamma-1}{2} M^2} \tag{6}$$

$$c_p T_o = c_p T + \frac{V^2}{2gJ} \quad \Longrightarrow \quad V = \sqrt{2gJc_p(T_o - T)} \tag{7}$$

The computer program used for the reduction is given in Appendix C.

6. Exhauster Performance Prediction.

An analysis of the exhauster performance to predict the hood total pressure, for specified drive nozzle total temperature and total pressure, and secondary air mass flow rate and total temperature, has been carried out by Vavra[18] in the TTTR preliminary design calculations, and used by Naviaux.[19] However, both analyses assume that the drive nozzle is operating at design conditions, and the static pressure at the entrance to the mixing section is constant in radial direction. Considering the many variables in the

---

[18] Vavra, M. H., Theoretical Evaluation of Exhauster System of Transonic Turbine Test Rig (TN65T, U.S. Naval Postgraduate School, Monterey, California, 1965), pp. 16 - 21.

[19] Naviaux, op. cit., pp. 22 - 27.

physical set-up of the TTTR, such as turbine efficiency, RPM, secondary air mass flow rate and total temperature, and the range of drive nozzle total pressures available, it seems unlikely that the nozzle will operate always at design conditions. Test data plotted in Fig. 29 indicate a static pressure gradient at station M1, located just 9/16 inch from the nozzle exit. Therefore, the possibility of a discontinuity in static pressure between the nozzle exit (area A1) and the secondary flow annulus (area A1T) at the start of the mixing section is contained in the present development. This hypothesis is supported by Jaumotte[20] who indicated that the classic hypothesis that assumes uniformity of the static pressure in the initial section of mixing is wrong. In the cited reference it is stated also that the laws governing the pressures in the two fluids and the factors which influence them are not yet well understood.

The complete revised analysis of exhauster performance is included as Appendix A. Appendix B gives the computer program used to calculate prediction maps of exhauster performance over its operating range. The pertinent steps of the analysis are outlined below with the notations corresponding to those of Fig. 3.

---

[20]Engle, M. O., Some Problems in the Design and Operation of Jet Ejectors, Proceedings of the Institution of Mechanical Engineers Steam Plant Group (London, England, No. 133, 1963), p. 350.

Polytropic process relations as well as non-dimensional flow functions are used. These are taken from Vavra.[21] For an expansion process

$$\frac{\dot{w}\sqrt{T_{t_1}}}{A_2 P_{t_1}}\sqrt{\frac{R}{g}} = \Phi_e = \sqrt{\frac{2\gamma}{\gamma-1}\left[\left(\frac{P_2}{P_{t_1}}\right)^{2/n} - \left(\frac{P_2}{P_{t_1}}\right)^{\frac{n+1}{n}}\right]} \qquad (8)$$

where

$$n = \frac{\gamma}{\gamma - \eta_p(\gamma-1)}$$

n = polytropic exponent

η_p = polytropic efficiency $\frac{dT}{dT_{is}}$

γ = ratio of specific heats

$\dot{w}$ = flow rate (lbm/sec)

T_{t_o} = inlet stagnation temperature (^oR)

A_2 = flow area at station of interest ($in.^2$)

P_{t_o} = inlet stagnation pressure (psia)

P_2 = static pressure at station of interest (psia)

g = universal gravitation constant ($lbm\text{-}ft/lb\text{-}sec^2$)

Subscript 1 refers to inlet conditions

Subscript 2 refers to station of interest

---

[21] Vavra, M. H., Problems of Fluid Mechanics in Radial Turbomachines (Rhode-Saint-Genese, Belgium: Von Kármán Institute for Fluid Dynamics, 1965), VKI Course Note 55a, pp. 22 - 35.

For a compression process

$$\frac{\dot{w}\sqrt{T_1}}{P_1 A_2}\sqrt{\frac{R}{g}} = \Phi_c = \sqrt{\frac{2\gamma}{\gamma-1}\left[\frac{T_{t_1}}{T_1}\left(\frac{P_2}{P_1}\right)^{2/n} - \left(\frac{P_2}{P_1}\right)^{\frac{n+1}{n}}\right]} \tag{9}$$

P_1 = static pressure at 1 (psia)

$$n = \frac{\gamma \eta_p}{1-\gamma(1-\eta_p)}$$

For a choked nozzle

$$\Phi_{choked} = \left(\frac{2}{n+1}\right)^{\frac{1}{n-1}}\sqrt{\frac{2\gamma}{\gamma-1}\left(\frac{n-1}{n+1}\right)} \tag{10}$$

Initially, polytropic efficiencies were assumed to be constant over the operating range of the exhauster. The determination or estimation of the values used is described in Sec. 8 entitled "Determination of Polytropic Exponents."

Drive Nozzle

The flow functions from the nozzle entrance to the throat (Φ_n), and from the nozzle entrance to the exit (Φ_{ex}), are

$$\Phi_n = \frac{\dot{w}_n\sqrt{T_{T_N}}}{A_T P_{TN}}\sqrt{\frac{R}{g}} \tag{11}$$

$$\Phi_{ex} = \frac{\dot{w}_n\sqrt{T_{TN}}}{A_1 P_{TN}}\sqrt{\frac{R}{g}} \tag{12}$$

The relationship

$$\Phi_n A_T = \Phi_{ex} A_1 \tag{13}$$

exists, and

$$\Phi_{ex} = \Phi_n \frac{A_T}{A_1} \tag{14}$$

Expressing the exit flow function in terms of a pressure ratio

$$\Phi_{ex} = \sqrt{\frac{2\gamma}{\gamma-1}\left[\left(\frac{P_{IN}}{P_{TN}}\right)^{2/n} - \left(\frac{P_{IN}}{P_{TN}}\right)^{\frac{n+1}{n}}\right]} \tag{15}$$

With Φ_{ex} given by Eq. 14 and PTN an initial condition, PlN may be solved by iteration. With PlN, the quantities TlN, VlN, and $\dot{w}_n$ may then be obtained.

Secondary Flow

For the expansion process from the hood to the mixing pipe annulus area, there is

$$\frac{\dot{w}_T\sqrt{T_{TD}}}{A_{IT}\,P_{TD}}\sqrt{\frac{R}{g}} = \Phi_d = \sqrt{\frac{2\gamma}{\gamma-1}\left[\left(\frac{P_{IT}}{P_{TD}}\right)^{2/n_d} - \left(\frac{P_{IT}}{P_{TD}}\right)^{\frac{n_d+1}{n_d}}\right]} \tag{16}$$

With secondary flow rate and hood total temperature known, a value of PlT is assumed and PTD calculated by iteration and matching. For the assumed PlT and corresponding PTD, the values of TlT and VlT can be calculated.

Mixing Pipe

With the values calculated for the drive nozzle and for assumed secondary air flow conditions, the momentum equation was used for the region within the mixing pipe to obtain conditions at the diffuser entrance. The basic equation is

$$\left(\frac{\dot{w}_n + \dot{w}_T}{g}\right)V_2 - \frac{\dot{w}_n}{g}V_{IN} - \frac{\dot{w}_T}{g}V_{IT} = (PIT)AIT + (PIN)AI - (P2)A2 - F_f \qquad (17)$$

Assumptions include uniform velocity profiles, uniform static pressure distribution over each area, and adiabatic flow. The term F_f represents the viscous shear force imposed by the wall on the moving fluid. Estimation of the magnitude of this force is outlined by Naviaux. In the calculation, the resultant pressure drop produced by F_f is determined by a single iteration of Eq. 17.

In Eq. 17, P_2 and V_2 are unknown. With continuity, the pressure P_2 can be expressed with the known quantities and V_2, which leaves one equation to be solved with the unknown quantity V_2. With V_2, all conditions at the diffuser entrance can be obtained.

Diffuser

For the compression in the subsonic diffuser

$$\frac{\dot{w}\sqrt{T_2}}{A_3 P_2}\sqrt{\frac{R}{g}} = \Phi_c = \sqrt{\frac{2\gamma}{\gamma-1}\left[\frac{T_{T2}}{T_2}\left(\frac{P_3}{P_2}\right)^{2/n_c} - \left(\frac{P_3}{P_2}\right)^{\frac{n_c+1}{n_c}}\right]} \qquad (18)$$

The pressure P_3 is obtained by iteration; and if it does not match atmospheric conditions, a new value of P1T for the secondary air must be assumed and the calculation repeated.

7. Test Results and Discussion.

Hood Total Pressure

Tests of the exhauster system were conducted to measure the hood total pressure obtained over the operating range of the drive nozzle. Runs were made at a secondary flow rate of 4 and 2 lbm/sec for each drive nozzle.

Two attempts to obtain the information were discarded. Run 11 was made with the traverse probe at station M2 of the mixing pipe. Comparison with other test data showed that hood total pressure was increased by as much as 1 inch of mercury with the traverse probe installed, particularly when the probe was close to the drive nozzle. The increase in hood pressure is the result of losses due to shock waves that attach to the probe, the drag of the probe in the stream, and the wake formed behind the probe. Run 29 with drive nozzle II was not used due to the discovery that a large seal in the hood had not been properly installed. Run 18 and 22 for drive nozzle I and run 32 for drive nozzle II were successful. The results are plotted in Fig. 11.

The graph shows that for the same secondary flow rate, drive nozzle I creates a lower hood total pressure than nozzle II. This occurs primarily because nozzle I has a throat area of 10.42 $in.^2$ and nozzle II a throat area of

8.29 $in.^2$ so that with choked conditions, about 1.51 lbm/sec greater flow rate of primary air exists with nozzle I. Hence, its driving momentum flow is larger.

For drive nozzle I, a lower hood pressure resulted for a smaller secondary flow rate at a given drive nozzle pressure ratio. In a relative sense, the effect is the same as described above. For the same drive nozzle pressure, which establishes the mass flow rate and momentum flow of the primary nozzle, it is possible to produce lower pressures in the hood for smaller secondary flow rates.

Mixing Pipe Static Pressure Rise

Mixing pipe static pressures were recorded for each pressure ratio PTN/P_{atm} and flow rate. Graphs showing the static pressure variation as a function of distance from the drive nozzle exit are given in Figs. 12, 13, and 14. In general, there occurs a rapid increase in the static pressure along the initial region of the mixing pipe. In the main mixing zone where the primary and secondary core regions have disappeared, there is a slight but steady decrease in static pressure in each case, except for $PTN/P_{atm} = 2.65$ in Fig. 12. The exception could be due to the fact that incomplete mixing has occurred in the mixing pipe for the extreme condition tested. This point is the greatest drive nozzle pressure ratio used and lowest hood total pressure produced during testing. As expected, the static pressure rises in the diffuser to the atmospheric pressure at the exit.

No attempt was made to predict analytically the mixing pipe static pressure as a function of axial location. Due to the extremely complex nature of the flow which includes mixing, turbulence, and shocks in this region, the momentum equation used in the exhauster prediction analysis is applied only for the whole mixing pipe to obtain average conditions ahead of the diffuser. The rapid rise of static pressure in the initial region is due to the slowing down of the supersonic stream as it mixes with the subsonic secondary air. Also present is a series of expansions and shock waves to equalize the static pressure between the two flows. A possible extension of this thesis would be to devise a mixing chamber for Schlieren photographic study of the mixing phenomena in compressible flow.

The slight but steady decrease in static pressure in the main mixing zone indicates the loss of available energy due to losses caused by the shear forces in the flow and the continued turbulent interchange between particles.

Figures 13 and 14 show that at L/D of about 4, the wall static pressure is higher for a drive nozzle total pressure ratio of 2.45 than for 2.18. This condition repeated itself on 4 different occasions, but each time the manometer board was very unstable with pressure variations at stations M1 - M3 up to plus or minus 3 in. Hg. observed out of 6 - 8 in. Hg. vacuum. The unsteady condition was not reflected in the hood total pressure. It appeared to be the result of a shock moving fore and aft in the initial

region of the mixing pipe. A very definite sound variation was heard while operating at this condition which would tend to support the hypothesis of an unstable shock movement.

Velocity Profiles

Velocity profiles obtained with probe I for drive nozzle I are shown in Figs. 15 through 19, and those for drive nozzle II in Fig. 20. There occur large gradients between the two co-flowing streams at station M1 and considerable non-uniformities of the velocity profiles. Both of these effects decrease with increase in axial distance from the drive nozzle.

The non-uniformity of velocity profile had been expected because of Naviaux's results[22] but not to the degree observed in the ejector tests. However, Naviaux did not traverse closer than 4 inches to the drive nozzle, whereas at station M1 the traverse total pressure opening is only 9/16 inch from the drive nozzle exit plane.

The unusual profiles are probably caused by the shock structure that actually exists in the flow. A full discussion with sketches of the possible pattern is included in Sec. 10. Essentially, the presence of internal oblique and normal shocks causes sharp gradients in pressure and velocity in the flow with accompanied differences in flow directions. The large peak in static pressure shown in Fig. 29

[22] Naviaux, op. cit., Fig. 3, p. 52.

for station M1 is probably due to a large radial velocity component in the mixing zone at this radial position.

Abramovich cites experiments by Zhestkov[23] for a free jet operating at off-design conditions. The results are similar to the ejector tests with regard to the decrease in velocity in the center of the primary jet, compared to that in the jet's boundaries. By comparing the velocity profiles at stations M1, M2, and M3 it is apparent that the secondary air increases in velocity and the secondary core region decreases in size. The primary stream velocity decreases and the primary core area decreases as the mixing zone increases in size.

Interesting results were obtained by non-dimensionalizing the velocity profiles obtained in the main mixing region of the mixing pipe, in the manner given by Abramovich[24] for compressible flows. The main mixing region is the part of the mixing pipe where the "core" flows of primary and secondary air have disappeared. Appendix D describes the regions more fully. Abramovich uses the ordinate V/V_{ax} where V is the velocity at a given location, V_{ax} is the axial velocity. For the absissa,

$$\bar{\eta} = \frac{y}{2.27\, y_c}$$

---

[23] Abramovich, op. cit., pp. 335 - 338.

[24] Ibid., pp. 275 - 276.

where y and y_c represent the coordinate of the point which corresponds to an arbitrary value of the dimensionless velocity, and the coordinate where the velocity is 1/2 the axial velocity, respectfully. Figures 21 and 22 graph the result. In both cases a single profile is obtained.

Station M4 is not inside the main mixing region with drive nozzle I, but it is with drive nozzle II. Figure 23 shows that the non-dimensional profile at station M4 for nozzle I deviates from the single profile obtained by non-dimensionalizing the velocity profiles of stations M6 - M8. From these results, it appears that a sufficient condition to determine the start of the main mixing region in a restricted jet is to determine where the velocity profile may be non-dimensionalized to a single profile. The following paragraphs discuss the mixing regions in greater detail.

Mixing Zone

The shape of the mixing zone determined from the velocity profiles is shown in Figs. 24 and 25 for nozzle I and nozzle II, respectively. This is at best an approximation because of the limited number of traverse positions in the initial mixing region. The mixing zone appears to touch the mixing pipe wall at an L/D of 3.78 for nozzle I, and 4.71 for nozzle II. D is the nozzle exit diameter.

Victorin[25] carried out a series of experiments using water as the driven and driving fluid and determined that the velocity distribution in the mixing chamber behaved in the same fashion as a circular wake with the width proportional to $x^{1/3}$, where x is the axial position. The assumption is made that the primary fluid emanates at a point source at $x = 0$ located at a position upstream of the nozzle so that the velocity distribution would have spread to match the nozzle exit dimensions. Calculations of the theoretical distance $x^{1/3}$, to predict where the mixing zone meets the mixing pipe wall, gave an L/D of 8.27 for nozzle I, and 9.71 for nozzle II. These conditions are shown in Fig. 26.

It appears from the traverse information that the outward spread of the mixing zone occurs at a faster rate than the incompressible approximation. From the test data obtained, a closer approximation for the spread of a jet in compressible flow would be $y = x^{2/5}$. The relation predicts that mixing zone touches the pipe wall at an L/D of 3.87 for nozzle I, and 4.86 for nozzle II.

From the traverse data from runs 4 - 17 it can be concluded that the shape of the mixing zone is independent of secondary air mass flow rate. This conclusion is valid even though a leak existed in the traverse probe total

---

[25]Victorin, K., Investigation of Turbulent Mixing Processes, NACA TM 10 96, 1946.

pressure line during these runs. The leak did not affect the radial position of the steep total pressure gradient observed in test data. The radial position where the steep gradient in total pressure occurred was invariant as the secondary flow rate was set at 4, 3, and 2 lbm/sec.

8. Determination of Polytropic Exponents.

General

The theoretical model which has been assumed for the prediction of exhauster performance uses flow functions with polytropic exponents to describe the flow in four regions of the exhauster; namely, nozzle entrance to nozzle throat (n_t), nozzle entrance to nozzle exit (n_1), secondary air from the hood to the annulus at the start of the mixing pipe (n_d), and the compression process in the diffuser (n_c). The relationship between polytropic efficiencies (η) and polytropic exponents (n), for an expansion process, is

$$n_e = \frac{\gamma}{\gamma - \eta_e(\gamma-1)} \qquad \eta_e = \left(\frac{\gamma}{\gamma-1}\right)\left(\frac{n_e-1}{n_e}\right)$$

and for a compression process

$$n_c = \frac{\gamma \eta_c}{1-\gamma(1-\eta_c)} \qquad \eta_c = \left(\frac{n_c}{1-n_c}\right)\left(\frac{1-\gamma}{\gamma}\right)$$

Eckert[26] assumed polytropic efficiencies to be:

$\eta_T = 0.975$, $\eta_1 = 0.925$, $\eta_d = 0.90$, and $\eta_c = 0.70$.

Secondary Flow

Tests were conducted to determine n_d and η_d for the secondary flow. Secondary flow rate ($\dot{w}_t$) was maintained at 4 lbm/sec, and drive nozzle total pressure ratio PTN/P_{atm} was set at 2.65, 2.45, 2.18, 1.90, and 1.63. The flow function for this expansion is

$$\frac{\dot{w}_T \sqrt{T_{TD}}}{A_{1T} P_{TD}} \sqrt{\frac{R}{g}} = \Phi_D = \sqrt{\frac{2\gamma}{\gamma-1}\left[\left(\frac{P_{1T}}{P_{TD}}\right)^{2/n_d} - \left(\frac{P_{1T}}{P_{TD}}\right)^{\frac{n_d+1}{n_d}}\right]} \qquad (19)$$

Quantities on the left were either measured or are constants. The pressures on the right were measured. n_d was determined by iteration in computer program PDLY. Results of the tests are given in Table I. For 4 lbm/sec secondary flow rate, the average values are $n_d = 1.32$ and $\eta_d = 0.85$ for the supersonic operating range of the exhauster. Conditions during the test were stable.

Initial testing to determine n_d for secondary flow rate of 2 lbm/sec was not immediately successful. In two separate tests, results showed polytropic exponents from 1.08 up to 1.41, and one value of 1.61 which is impossible

---

[26]Eckert, op. cit., p. 93.

since n_d cannot be larger than $\gamma = 1.41$. During the test, annulus static pressure was unsteady and an average reading was used for data reduction. Figure 13 indicates that an unusual condition exists in the mixing pipe between pressure ratios of 2.45 and 2.18. The curves showing mixing pipe static pressures cross each other for the given conditions. This phenomenon repeated itself on four separate occasions.

In order to determine the effect of a small error in the annulus static pressure readings, the computer program POLY was used. Values for hood total temperature, total pressure, and secondary flow rate were held constant and values of annulus static pressure varied in increments of 0.1 inch mercury or 0.05 psia. The result is given in Table II. It is evident that annulus static pressure is critical to the calculation of n_d since a change of $\pm$ 0.1 psia from the test value changes n_d between 1.39 and 1.24. In the final test it was attempted to take all readings simultaneously. Results of this test are considered accurate and are given in Table III. They show that n_d is about 1.28, with η_d equal to 0.84. The tests showed that the polytropic efficiency was independent of drive nozzle total pressure but dependent on secondary flow rate.

Diffuser

Diffuser polytropic efficiency was determined empirically from the static pressure rise between the mixing pipe

station M9 to the diffuser exit for all operating conditions tested. Figure 27 is a graph of the diffuser static pressure rise for secondary flow rates of 4 and 2 lbm/sec for different pressure ratios of drive nozzle total pressure and atmospheric pressure.

Initially, the exhauster performance prediction program was used with the actual exhauster operating conditions as inputs and with a diffuser efficiency $\eta_c = 0.7$ as assumed by Eckert. The predicted static pressure rise from M7 to atmospheric conditions based on η_c of 0.70 is plotted also in Fig. 27 for 4 and 2 lbm/sec secondary flow, showing that the diffuser efficiency is larger than 0.7. A diffuser efficiency of 0.90 was assumed, and the results of the calculated static pressure rise in the diffuser is shown in Fig. 28. Agreement between calculated and actual diffuser static pressure rise is good, but the graph shows that there is a small variation of diffuser efficiency with drive nozzle total pressure ratio. A diffuser efficiency of 0.90 very accurately predicts the performance at the lower drive nozzle total pressure ratios up to about 2.1 but underestimates the performance at the higher pressure ratios. The prediction program was altered to vary η_c with drive nozzle total pressure. Values used for diffuser efficiency at different drive nozzle total pressure ratios are shown in Table IV. The results of calculated pressure rise in the diffuser compared to test data are in Fig. 28. The curves show good agreement between calculated and test results.

It was noted also that the diffuser efficiency varied slightly with secondary flow rate. This effect is small and need not be taken into account in the simplified model used for the prediction program.

9. Determination of Average Shear and Friction Coefficient.

Mathematical solutions do not exist that exactly predict the conditions in a flow as complicated as that in the mixing tube of the exhauster. However, it was attempted to establish a value for the average shear stresses in the flow by an approximate method. Such an approximation was obtained by not attempting to satisfy the hydrodynamic differential equations for each particle but by integrating the profile distributions obtained in laboratory tests and hence solving the momentum equation for the flow between two stations. The momentum equation

$$\int_{①} V_1 \, d\dot{m}_1 + \int_{①} P_1 \, dA_1 = \int_{②} V_2 \, d\dot{m}_2 + \int_{②} P_2 \, dA_2 + \bar{\tau} A_s \qquad (20)$$

where: 1 represents conditions at the upstream station

2 represents conditions at the downstream station

A_s = surface area of the mixing pipe between stations

can be used, but in turbulent flow with large velocity gradients $\bar{\tau}$ consists of the "true shear" due to the viscosity of the fluid, and the "apparent shear" due to the losses produced by the turbulent interchange of fluid particles.

Prandtl states[27] that except in layers directly next to the wall, the true shear is small enough to be neglected in comparison to the apparent shear. The approach assumes axisymmetric flow, a perfect gas, axial velocities everywhere and steady flow, with gravitational effects being ignored. Equation 20 is used for the profiles of velocity, pressure (total and static), and temperature measured at stations M1, M4, and M8.

With the pressures in psi and r in inches, there are

$$dA = 2\pi r\,dr$$

$$d\dot{m} = \rho V\,dA = \frac{144\,p}{gRT}\,V\,2\pi\,\frac{r}{12}\,\frac{dr}{12} = \frac{2\pi}{gR}\left(\frac{pVr\,dr}{T}\right)$$

$$V\,d\dot{m} = \frac{2\pi}{gR}\left(\frac{pV^2 r\,dr}{T}\right)$$

Equation 20 becomes

$$\frac{2\pi}{gR}\int_{①}\frac{p_1 V_1^2}{T_1}r\,dr + \int_{①} p_1\,r\,dr = \frac{2\pi}{gR}\int_{②}\frac{p_2 V_2^2}{T_2}r\,dr + \int_{②} p_2\,r\,dr + \bar{\tau}\,A_s$$

Numerical integration of large scale reproductions of Figs. 29 and 30 gave at station M1

$$\frac{2\pi}{gR}\int_{①}\frac{p_1 V_1^2}{T_1}r\,dr + \int_{①} p_1\,r\,dr = 342.5 + 475.0 = 817.5 \text{ lbs.}$$

---

[27] Prandtl, L., The Mechanics of Viscous Fluids, Aerodynamic Theory (California: Durand Reprinting Committee, California Institute of Technology, January 1943), Vol. III G, p. 135.

at M4

$$\frac{2\pi}{gR}\int_{④}\frac{p_4 V_4^2}{T_4}\,r\,dr + \int_{④} p_4\,r\,dr = 334.4 + 525.5 = 869.9 \text{ lbs.}$$

and at M8

$$\frac{2\pi}{gR}\int_{⑧}\frac{p_8 V_8^2}{T_8}\,r\,dr + \int_{⑧} p_8\,r\,dr = 222.0 + 565.3 = 787.3 \text{ lbs.}$$

The results, which show an increase in momentum from station M1 to M4, must be in error although use of the momentum equation to model the mixing pipe performance and the mathematical integration can be considered correct. The error could have been introduced by the blockage effect of the traverse probe and the variation of the overall exhauster performance with probe position. To illustrate this condition, Table V shows the values of the hood total pressure for the same exhauster operating conditions, but with the traverse probe at different locations. A variation of 1.65 in. Hg. hood total pressure occurs between the conditions where the traverse probe is at station M1, and the probe is completely removed. Another possible reason for the error is that it was not possible to produce exactly the same settings of pressures and temperatures for each traverse since, to change traverse probe locations, it was necessary to shut down the turbine and exhauster. Re-establishment of all previous conditions was extremely difficult. Analysis of the data indicates, however, that this effect should be secondary.

The calculation was continued between station M4 and M8 using the integrated values obtained.

$$F_f = 869.9 - 787.3 = 82.6 \text{ lbs.}$$

$$A_{s_{M_4 - M_8}} = 6.46 \text{ ft}^2$$

$$\bar{\tau} = 8.19 \text{ lbs/ft}^2$$

From the test data and results obtained, the turbulent friction coefficient f was also calculated. Using Vavra,[28] the pressure drop Δp due to friction may be approximated by

$$\Delta P = f \frac{L \bar{\rho} \bar{V}^2}{D 2} \qquad (psf)$$

where f = turbulent friction coefficient (dimensionless)

L = length of pipe (in.)

D = diameter of pipe (in.)

$\bar{\rho}$ = average density between stations (slugs/ft^3)

$\bar{V}$ = average velocity between stations (ft/sec)

with

$$\bar{\rho} = \frac{\bar{P}(144)}{R \bar{T} g} = \frac{8.38}{100} \frac{\bar{P}}{\bar{T}} \qquad (\text{Slugs/ft}^3)$$

$$f = 179.1 \frac{\bar{T} \Delta P}{\bar{P} \bar{V}^2 L}$$

---

[28] Vavra, M. H., Theoretical Evaluation of Exhauster System of Transonic Turbine Test Rig (TN65T, U. S. Naval Postgraduate School, Monterey, California, 1965), p. 26.

The total frictional force may be expressed in terms of a pressure drop

$$F_f = \frac{\pi}{4} \frac{D^2}{144} \Delta p = 0.303 \Delta p \quad (\text{lbs.})$$

With F_f determined, f becomes

$$f = 585 \frac{\overline{T} F_f}{L \overline{p} \overline{V}^2} \tag{21}$$

Average values used to calculate f were: $\overline{T} = 530^{\circ}R$, $\overline{p} = 12.4$ psia, and $\overline{V} = 700$ ft/sec.

$$f = 0.106$$

This is one order of magnitude larger than the friction factor 0.017 predicted by the Moody diagram[29] for commercial steel pipes. The value should have been closer even with velocities of 700 ft/sec. Shapiro cites numerous tests[30] that confirm the use of the incompressible friction formula for conditions up to Mach = 1.0.

The calculations were repeated between M1 and M8. With $F_f = 29.7$ lbs., $L = 86$ in., $\overline{p} = 11.3$ psia, $\overline{T} = 500^{\circ}R$, and $\overline{V} = 750$ ft/sec, Eq. 21 gives

$$f = 0.024$$

This value is still large but has the correct order of magnitude for the friction coefficient.

---

[29] Shapiro, op. cit., Fig. 6.15, p. 184.

[30] Ibid., p. 1071.

The results of the calculations for friction coefficient suggest that the traverse data at station M4 are not accurate. Better results were obtained between M1 and M8 than M4 and M8. No particular quantity in the M4 data was considered unreasonable. The conclusion is that the calculation of an average shear force and friction coefficient for the mixing pipe, using the ejector test data, produced unreliable results.

10. Evaluation and Discussion of Predicted Results.

Actual test conditions were input to the exhauster prediction program to determine a predicted hood total pressure. Three predictions were made: Program EJECT 1 used constant polytropic efficiencies determined from test data for the secondary air and diffuser and an assumed drive nozzle polytropic efficiency of 0.975, EJECT 2 used Eckert's polytropic efficiencies, and EJECT 3 used EJECT 1 efficiencies, except that the diffuser efficiency was varied with drive nozzle total pressure from 0.90 to 0.93. The results of the predictions for drive nozzle I and a comparison with the test results of run 18 are shown in Fig. 31 for 4 lbm/sec secondary flow, and in Fig. 32 for 2 lbm/sec. Appropriate changes were made in the program to reflect the new dimensions of drive nozzle II. The prediction compared to test results is shown in Fig. 32.

The results show that Eckert's assumed polytropic efficiencies greatly underestimate the exhauster performance.

At high drive nozzle pressure ratios, the use of the theoretical prediction program EJECT I with experimentally determined exponents very closely establishes the actual performance of the exhauster. The accuracy of the prediction decreases as drive nozzle pressure ratio decreases. At the low pressure ratios the exhauster performs much better than predicted.

Much of the difference noted above can be attributed to the physical formation of an oblique shock within the drive nozzle for off-design operation. The classical approach to describing nozzle operation notes a third critical pressure which is the exit static pressure that provides design operation. As the receiver static pressure is increased, an oblique shock forms, originating at the exit plane edge. Further increase in static pressure increases the angle of the oblique shock until a normal shock forms in the exit plane for the second critical pressure. Still further increase in pressure causes the normal shock to move from the exit toward the nozzle throat. This idealized flow development does not occur in actuality because of friction and three-dimensional flow effects. The latter, in particular, produce internal oblique shocks which have the effect of extending the shock action over an extended axial distance in the nozzle. Tests conducted by Stodola[31] show internal shock effects over the axial distance of a nozzle.

---

[31]Hall, N. A., Thermodynamics of Fluid Flow (Englewood Cliffs, N. J.: Prentice Hall, Inc., 1951), Fig. 9.5, p. 136.

By removing the mixing pipe and operating as a free jet, the presence of an internal oblique shock in the drive nozzle could be made visible because of condensations of the atmospheric humidity in the primary stream. Figure 33 is a photo of the free jet operation. The oblique shocks originated inside the nozzle and extended outside the nozzle to their intersection with a near normal circular shock in the center area of the nozzle. A sketch of the observed pattern is shown in Fig. 34. With increased drive nozzle pressure, the entire shock structure moved towards the nozzle exit.

To determine the displacement of this shock structure in the drive nozzle under exhauster test conditions, six static pressure taps were arranged in drive nozzle I in positions shown by D1 through D6 in Fig. 35. At a secondary flow of 4 lbm/sec the drive nozzle total pressure was set at values of PTN/P_{atm} of 2.65, 2.45, 2.18, 1.90, and 1.63 to duplicate conditions of run 18. The measured static pressures at the nozzle walls are shown in Fig. 36. They show that the internal shock moves toward the nozzle exit if the pressure ratio is increased. It should be noted that for each condition the pressure at the discharge of the secondary nozzle was below that required for oblique shock formation at the exit plane for isentropic flow theory; that is, the pressure was always less than the 2^{nd} critical pressure.

During the free jet operation it was observed also that the primary jet did not completely fill the exit plane when oblique shocks occurred inside the nozzle. There existed a slowed down region of flow at the outer perimeter of the nozzle discharge that had a radial thickness of 0.5 to 0.75 inch. This phenomenon can be noticed in Fig. 34 and must be responsible for the apparent thickness of the mixing zone at the nozzle exit which is illustrated in Fig. 24.

The order of magnitude of expected boundary layer thickness at the nozzle exit was determined with Eq. 22 which can be used to evaluate the boundary layer thickness on a flat plate in turbulent flow.[32] The Reynolds number applied is based on distance from the nozzle throat to its exit.

$$\frac{\delta}{\ell} = 0.37 \left(\frac{V \ell}{\nu} \right)^{-1/5} \qquad (22)$$

δ = boundary layer thickness

ν = kinematic viscosity (ft/sec^2)

ℓ = distance from throat to exit (ft)

V = velocity (ft/sec)

Based on average conditions

$$\delta \cong 0.07 \text{ inch}$$

This boundary layer thickness is much smaller than the observed distance of about 0.5 to 0.75 inch. The increased

[32] Schlichting, H., Boundary Layer Theory (New York: McGraw Hill Book Co. Inc., 1955), Eq. 2.9, p. 38.

boundary layer thickness must be caused by flow separations from the nozzle walls. This separation is the result of the internal oblique shock structure that exists in the drive nozzle. The nearer the throat the separation occurs, the less of the diverging portion of the nozzle is used to increase Mach number of the flow; that is, full expansion is not realized. The effect is readily apparent by observing average nozzle Mach numbers obtained at station M1 for PTN/P_{atm} of 2.65, 2.18, and 1.63. Test data showed Mach numbers of 2.08, 1.18, and 0.88 respectively. Figure 37 is a sketch of the shock conditions that appear to exist.

The effect of the internal oblique shock and resultant primary flow separation is to raise the static pressure of a portion of the nozzle exit area to the pressure of the static pressure at the discharge of the secondary nozzle. The momentum theorem expressed by Eq. 17 uses in the actual prediction program

$$PSUM \quad A_2 = P_{1N} A_1 + P_{1T} A_{1T}$$

A_2 = mixing pipe area

A_{1T} = secondary flow annulus area

A_1 = nozzle exit area

P_{1N} = nozzle exit plane static pressure

P_{1T} = secondary air static pressure.

In the program the value of PSUM is increased by iteration until the conditions at the diffuser exit match the atmospheric pressure. In the prediction program the assumption is made that P_{1N} and P_{1T} are constant,

respectively, over A_1 and A_{1T}. In reality P_{1N} occurs on an area smaller than A_1, and P_{1T} on an area greater than A_{1T}, for conditions where the internal oblique shock exists. The result is that for a given value of PSUM A_2, the pressure P_{1T} may be smaller than predicted to satisfy the equality. Thus, the hood total pressure would also be lower. This condition should be taken care of in the program for a more correct performance evaluation at low pressure ratios.

11. Conclusions and Recommendations.

The performance analysis of the exhauster system based on polytropic efficiencies and conservation of momentum very closely predicts the exhauster performance with regards to hood total pressure at high drive nozzle pressure ratios. The prediction under-estimates exhauster performance at the low pressure ratios because of the presence of internal oblique shocks in the drive nozzle. Accuracy obtained by the prediction program was the same for drive nozzle II which had dimensions different from nozzle I.

The hood total pressure is significantly effected by the presence of a traverse probe in the mixing pipe. The amount of hood pressure rise is a function of probe position. Therefore, traverse information presented cannot be considered as having been obtained for precisely the same operating conditions.

Traverse profiles near the drive nozzle exhibit steep gradients of pressure, temperature, and velocity. Velocity profiles obtained appeared irregular. The lower centerline velocity is probably due to the shock structure that occurs in the nozzle. It appears that a sufficient condition to determine the start of the main mixing region in a restricted jet is to determine where the velocity profile may be non-dimensionalized to a single profile. Results from flow traverses showed that the initial mixing zone expands radially at a faster rate than predicted by Victorin's incompressible approximation.

Secondary flow polytropic efficiencies are independent of drive nozzle pressure but dependent on secondary flow rate. Diffuser polytropic efficiency is independent of flow rate and slightly dependent on drive nozzle pressure. The diffuser polytropic efficiency is about 0.90 which is considerably higher than the previous estimate of 0.70.

Little test data are available on the behavior of compressible free jets. The facility used for the ejector tests could be adapted to obtain test data for experiments in this area. In addition, further insight into the shock pattern in the drive nozzle and the mixing pipe might be gained if an adaptation for Schlieren photography were designed. A study of the effects of the frictional and three-dimensional effects on shock formation in a circular nozzle is considered the next step necessary to improve the exhauster prediction analysis so that it produces more accurate results for the entire operating range.

BIBLIOGRAPHY

1. Abramovich, G. N., The Theory of Turbulent Jets, The M.I.T. Press, Cambridge, Massachusetts, 1963.

2. Commons, P. M., Instrumentation of the Transonic Turbine Test Rig to Determine the Performance of Turbine Inlet Guide Vanes Through the Application of the Momentum and Moment of Momentum Equations, Thesis, Naval Post-Graduate School, Monterey, Califomia, to be published in September 1967.

3. Eckert, R. H., Performance Analysis and Initial Tests of a Transonic Turbine Test Rig, Thesis, U.S. Naval Postgraduate School, Monterey, California, May, 1966.

4. Eckert, R. H., Determination of Flow Rates Transonic Turbine Test Rig, TN 66T-1, U.S. Naval Postgraduate School, Monterey, California, January, 1966.

5. Egli, A., The Leakage of Steam through Labyrinth Seals. Transactions of the ASME, v. 57, 1935, 115-122.

6. Engle, M. O., Some Problems in the Design and Operation of Jet Ejectors, Proceedings of the Institution of Mechanical Engineers Steam Plant Group. Thermo-dynamics and Fluids Group, Vol. 177, No. 133, 1963, London, England, p. 350.

7. Gettelman, C. C. and Krause, L. N., Considerations Entering into the Selection of Probes for Pressure Measurement in Jet Engines, ISA PROCEEDINGS, Vol. 7.

8. Hall, N. A., Thermodynamics of Fluid Flow, Prentice Hall, Inc., Englewood Cliffs, N. J., 1951.

9. Krause, L. N. and Gettelman, C. C., Effect of Inter-action Among Probes, Supports, Duct Walls and Jet Boundaries on Pressure Measurements in Ducts and Jets, ISA PROCEEDINGS, Vol. 7.

10. Naviaux, J. C., Transonic Turbine Test Rig Exhauster System Tests and Tests of a Reaction Turbine, Thesis, U.S. Naval Postgraduate School, Monterey, California, December, 1966

11. Pai, S., Fluid Dynamics of Jets, D. Van Nostrand Company, Inc., Toronto, New York, London, 1954.

12. Prandtl, L., The Mechanics of Viscous Fluids, Aerodynamic Theory. Durand Reprinting Committee, California Institute of Technology, California, January 1943.

13. Schlichting, H., Boundary Layer Theory, McGraw Hill Book Co. Inc., New York, 1955.

14. Shapiro, A. H., The Dynamics and Thermodynamics of Compressible Fluid Flow Volume I & II, The Ronald Press Company, New York, 1954.

15. Vavra, M. H., Theoretical Evaluation of Exhauster System of Transonic Turbine Test Rig, TN65T, U.S. Naval Postgraduate School, August, 1965.

16. Vavra, M. H., Problems of Fluid Mechanics in Radial Turbomachines (Rhode-Saint-Genese, Belgium, Von Kármán Institute for Fluid Dynamics, 1965) VKI Course Note 55a, pp. 22-35.

17. Victorin, K., Investigation of Turbulent Mixing Processes, NACA TM 10 96, 1946.

Drive Nozzle Total Pressure (PSIA)	Hood Total Temperature (^{o}R)	Hood Total Pressure (PSIA)	Annulus Static Pressure (PSIA)	POLYTROPIC EXPONENT (n_d)
39	523.7	12.73	11.75	1.331
36	521.6	11.77	10.65	1.322
32	519.9	10.46	9.16	1.322
28	514.5	8.99	7.33	1.321
24	511.4	7.99	5.91	1.322

Values Used to Determine

SECONDARY FLOW POLYTROPIC EXPONENT

Secondary Flow Rate - 4 lbm/sec

TABLE I.

ANNULUS STATIC PRESSURE (PSIA)	POLYTROPIC EXPONENT Secondary Flow (n_d)
6.47	1.47
6.42	1.39
6.37	1.34
6.32**	1.30
6.27	1.27
6.22	1.24
6.17	1.22

**Actual Test Reading

VARIATION OF n_d

WITH ASSUMED ANNULUS STATIC PRESSURE

$\dot{W}_T$ = 1.92 lbm/sec TTD = 547.5° PTD = 6.8 PSIA

TABLE II.

Drive Nozzle Total Pressure (PSIA)	Hood Total Temperature (^{o}R)	Hood Total Pressure (PSIA)	Annulus Static Pressure (PSIA)	Polytropic Exponent (n_d)
39	537.9	6.87	6.36	1.28
36	543.3	8.16	7.71	1.27

Values Used to Determine

SECONDARY FLOW POLYTROPIC EXPONENT

Secondary Flow Rate - 2 lbm/sec

TABLE III.

PTN/P_{atm}	η_c
2.65	0.90
2.45	0.91
2.18	0.92
1.90	0.93
1.63	0.94

Variation of Diffuser Polytropic Efficiency

With Drive Nozzle Pressure Ratio

TABLE IV.

Hood Total Pressure $(P_{atm} - P_{hood})$	Traverse Probe Location
-6.9 in. Hg.	M1
-7.0	M2
-7.2	M3
-7.5	M4
-7.85	M5
-8.15	M6
-8.55	No Probe

Hood Total Pressure

versus

Traverse Probe Location

PTN = 32 psia $\dot{w}_t$ = 4 lbm/sec

EJECTOR TESTS

TABLE V.

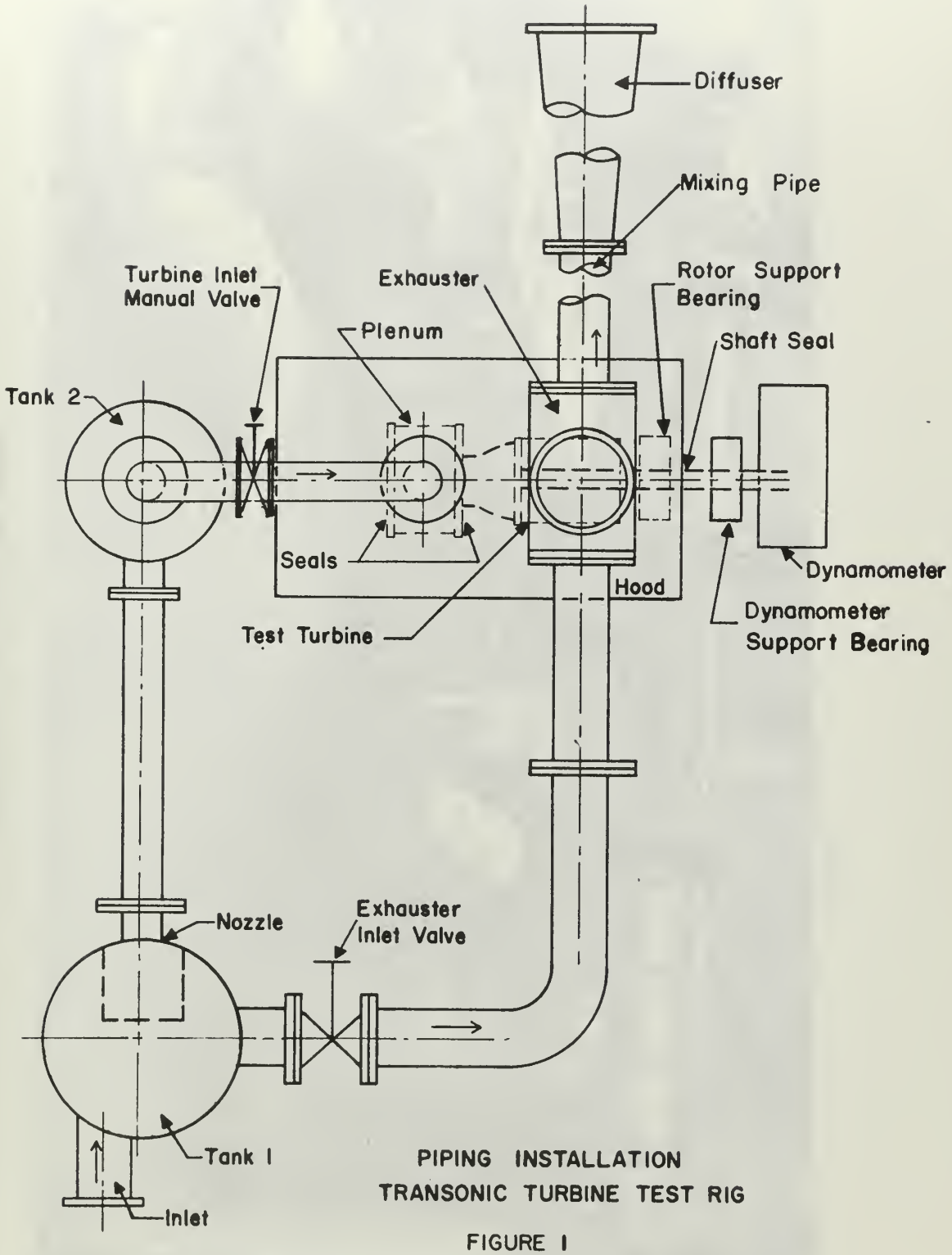

PIPING INSTALLATION
TRANSONIC TURBINE TEST RIG

FIGURE 1

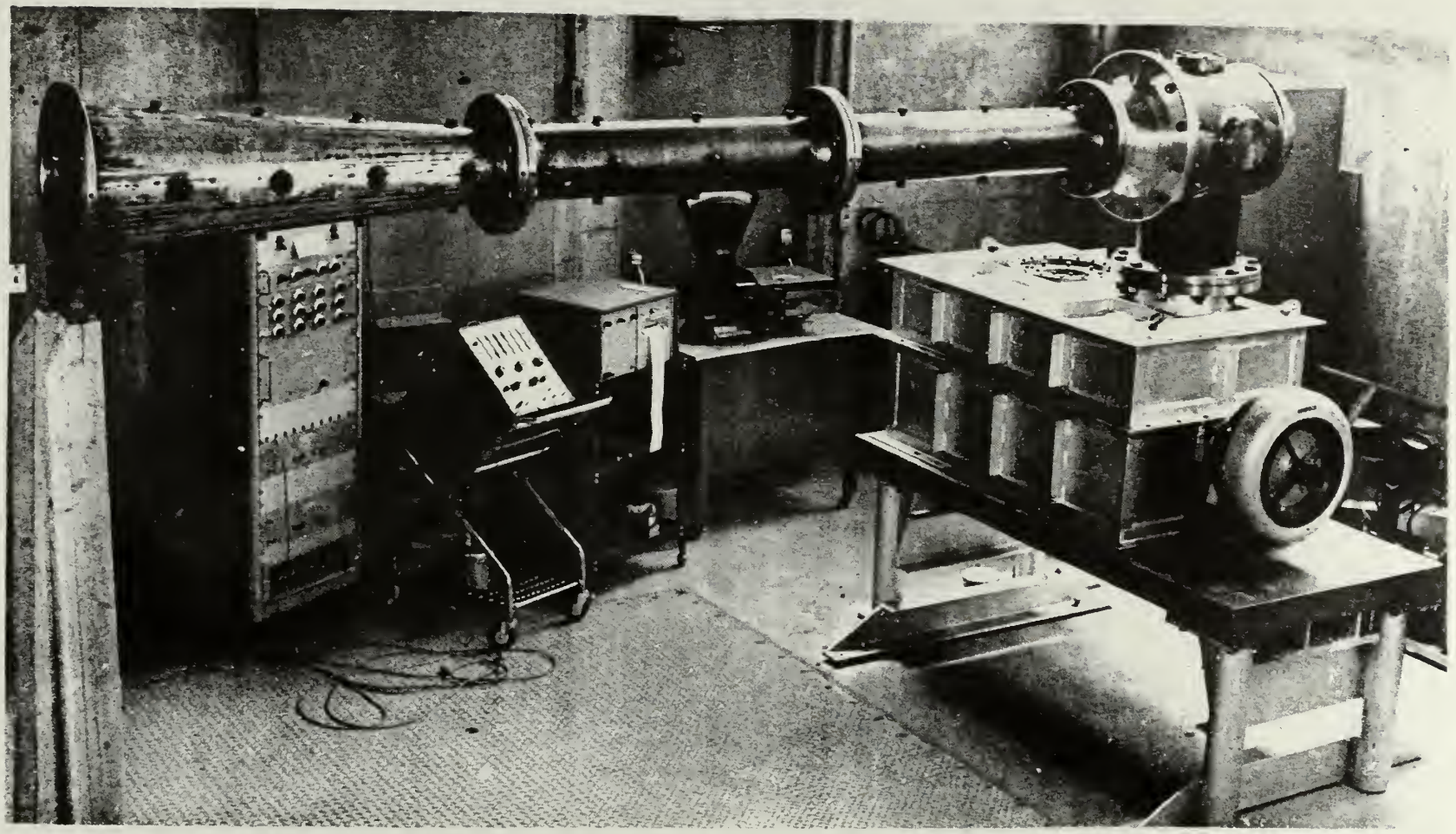

TURBINE HOOD AND EXHAUSTER ASSEMBLY
TRANSONIC TURBINE TEST RIG

FIGURE 2

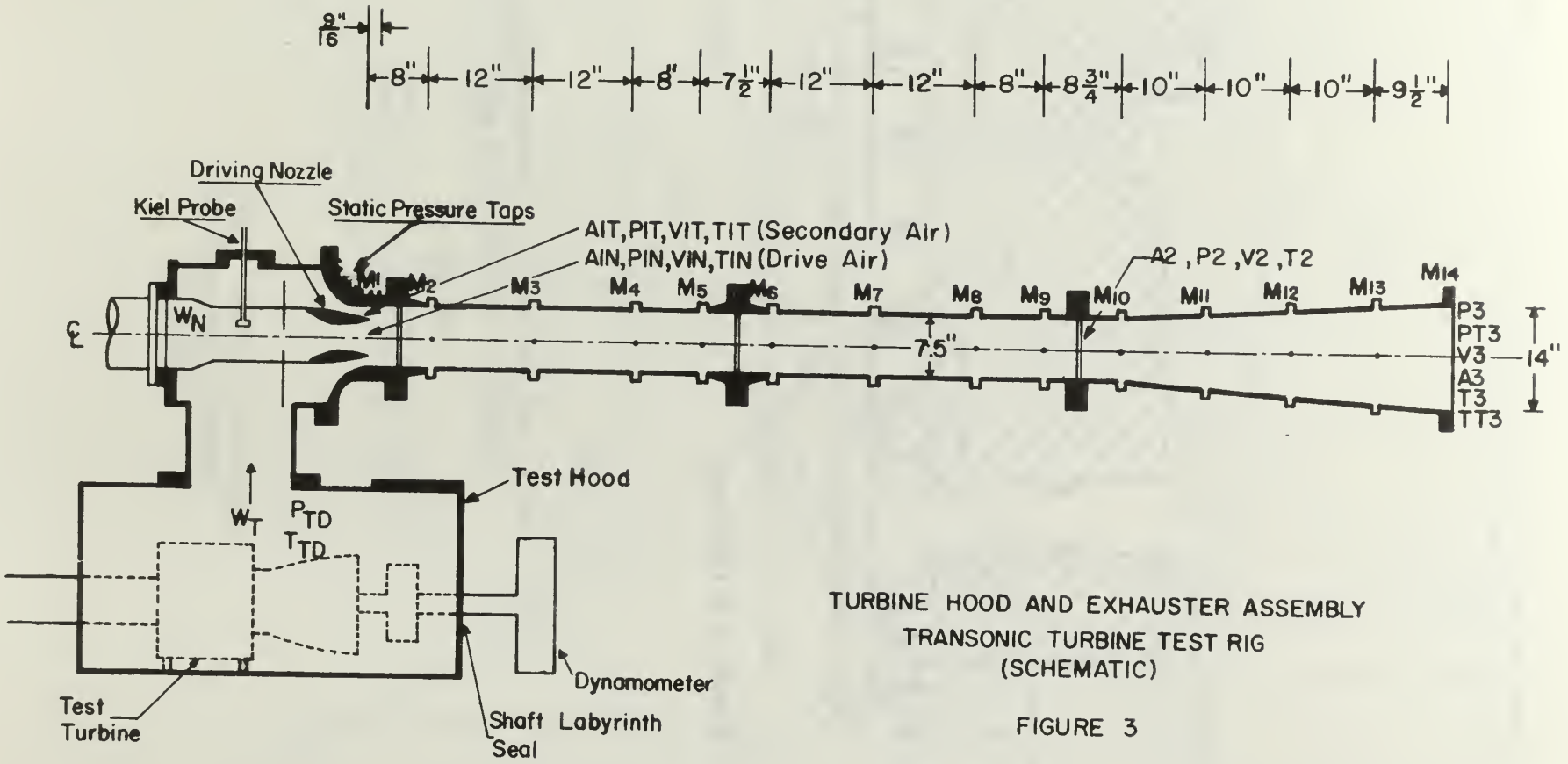

TURBINE HOOD AND EXHAUSTER ASSEMBLY
TRANSONIC TURBINE TEST RIG
(SCHEMATIC)

FIGURE 3

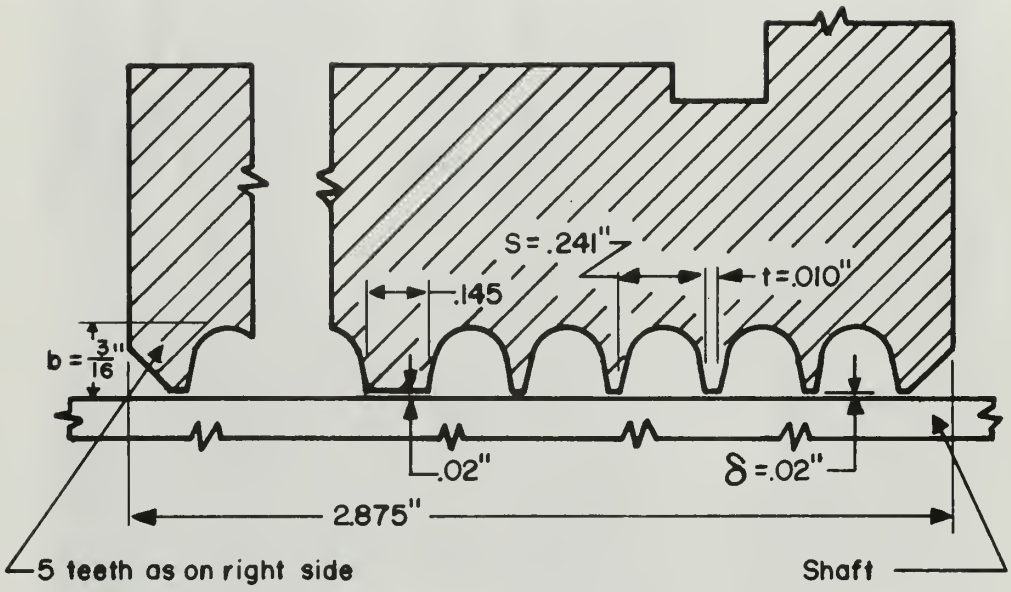

SHAFT LABYRINTH SEAL CONFIGURATION
TRANSONIC TURBINE TEST RIG

FIGURE 4

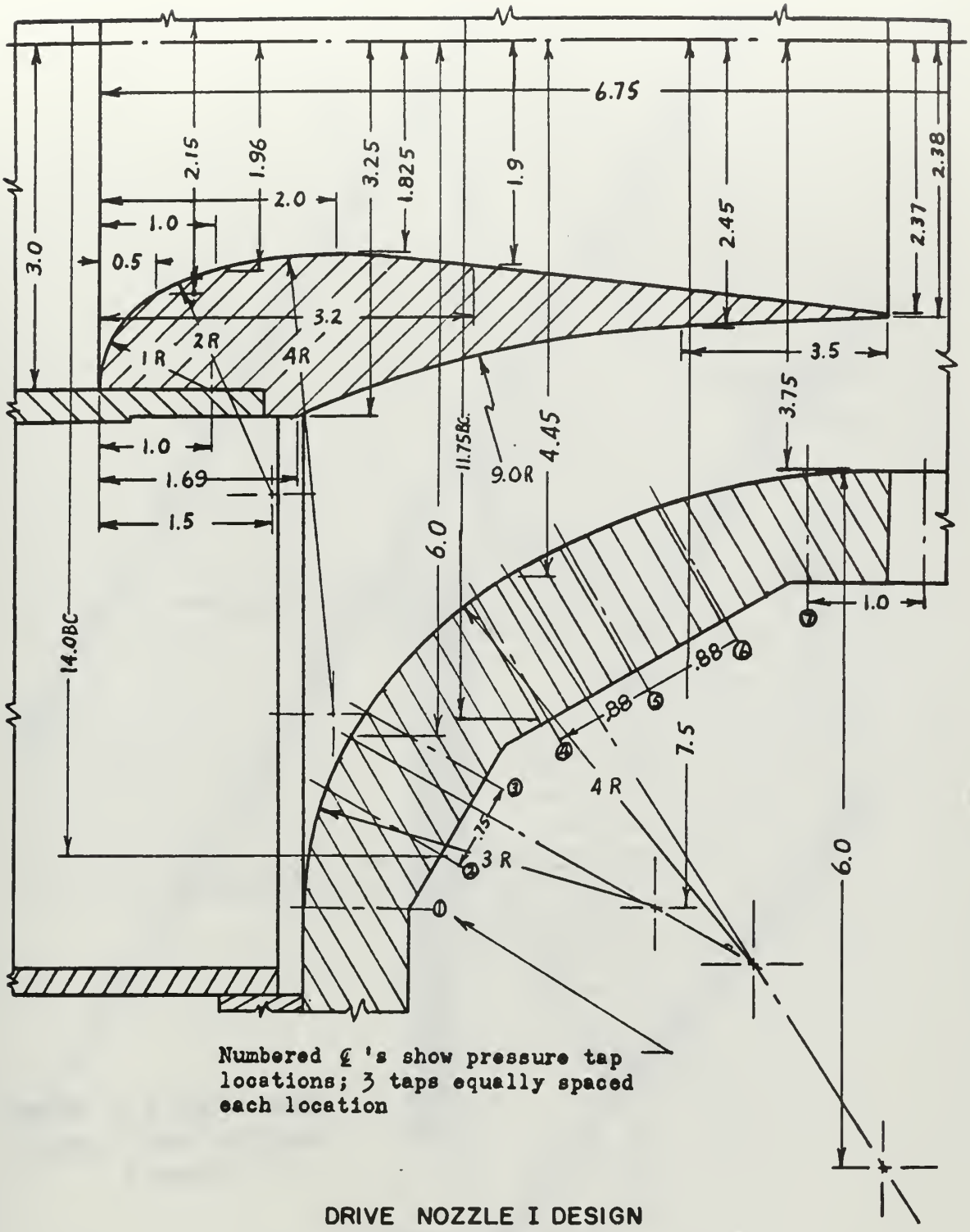

DRIVE NOZZLE I DESIGN
EJECTOR TEST SERIES
FIGURE 5

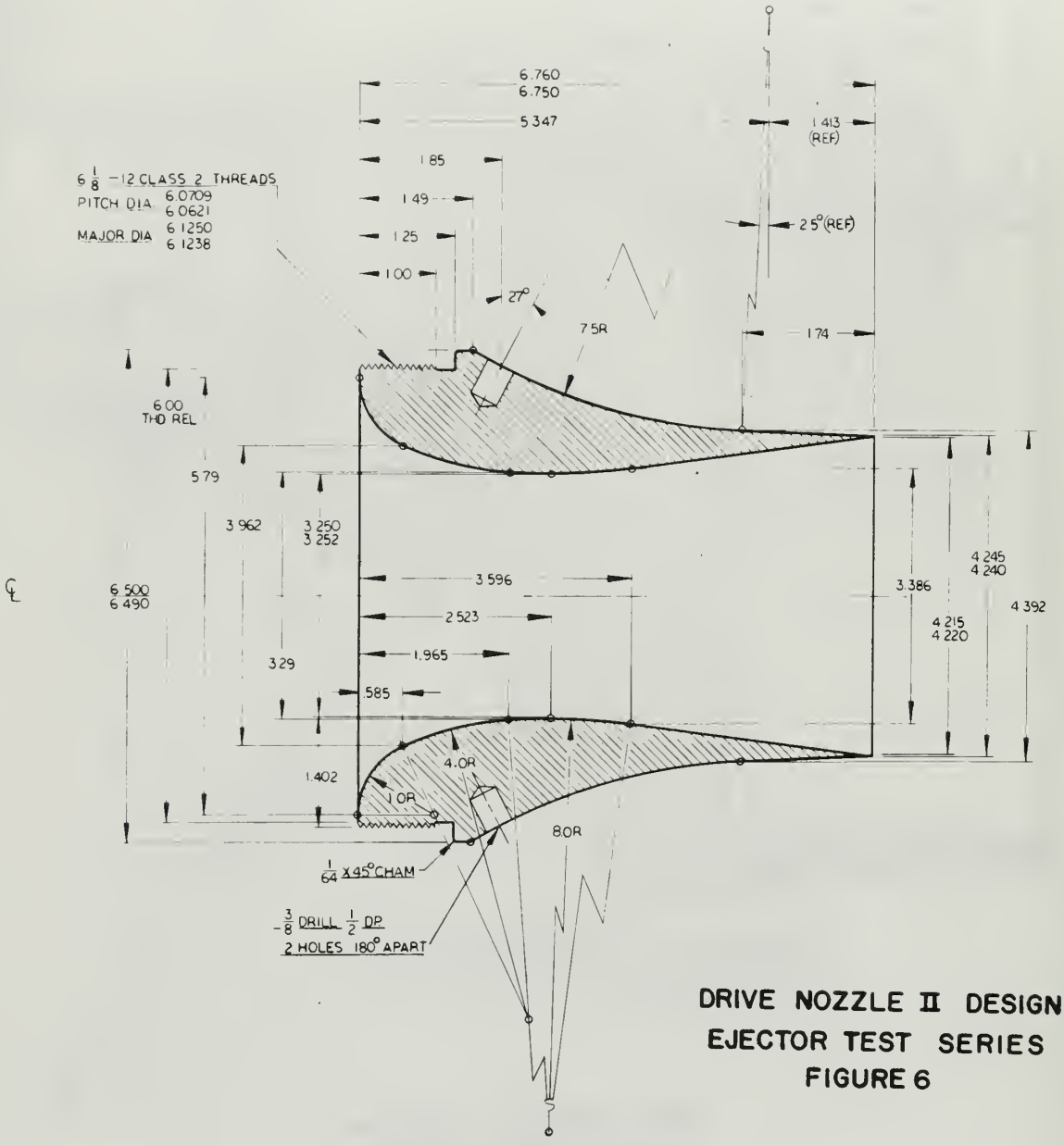

DRIVE NOZZLE II DESIGN
EJECTOR TEST SERIES
FIGURE 6

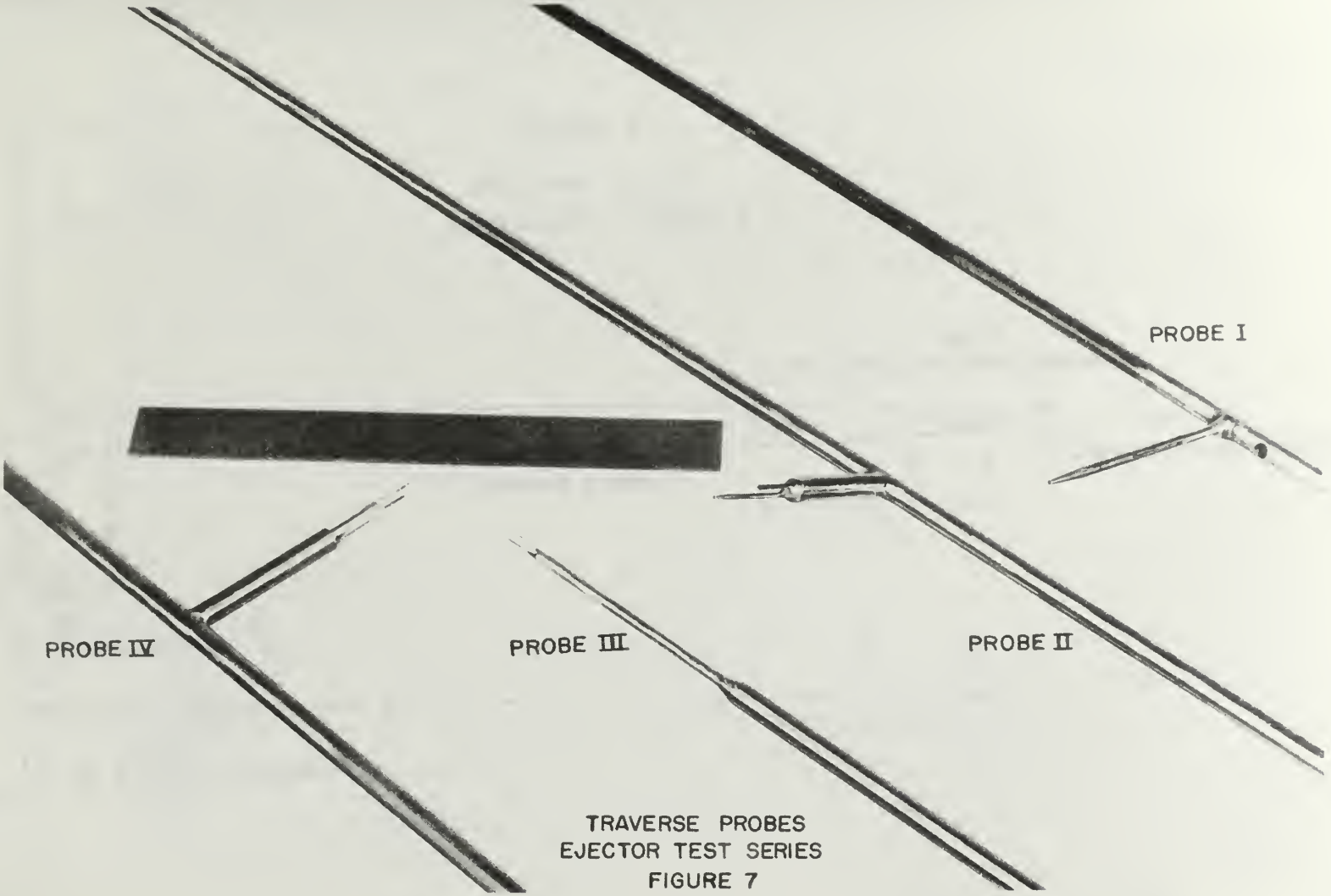

TRAVERSE PROBES
EJECTOR TEST SERIES
FIGURE 7

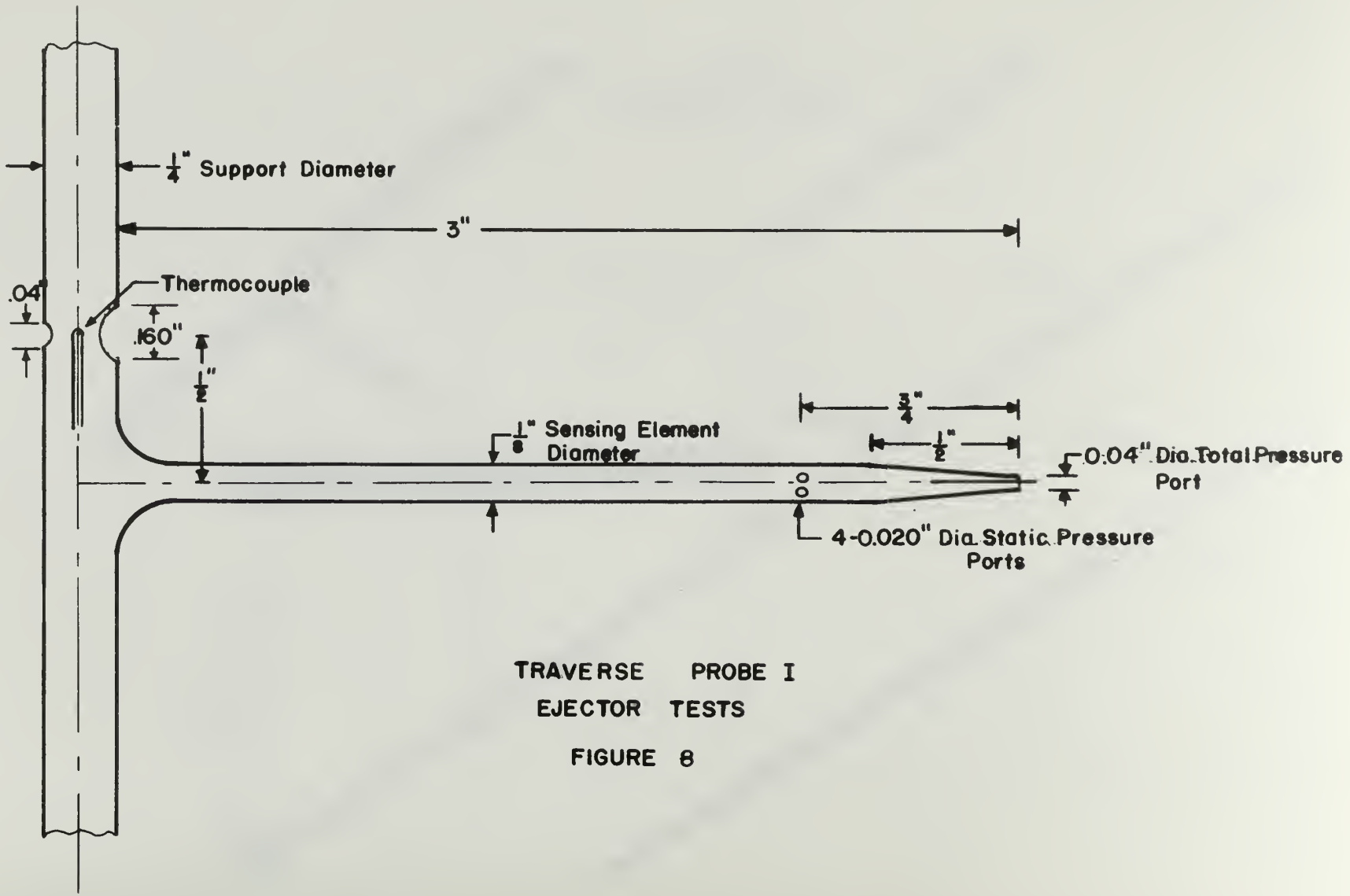

TRAVERSE PROBE I
EJECTOR TESTS

FIGURE 8

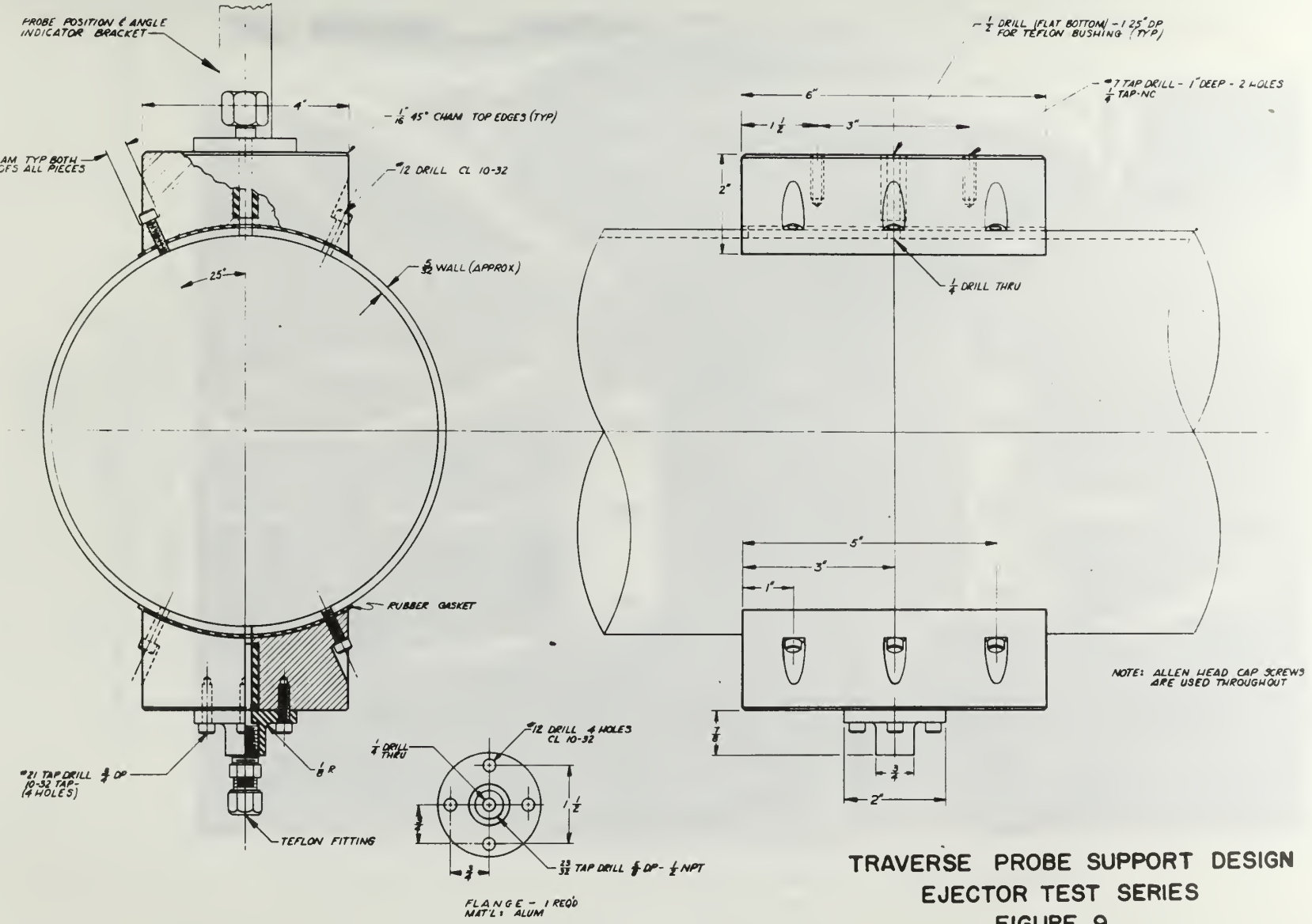

TRAVERSE PROBE SUPPORT DESIGN
EJECTOR TEST SERIES
FIGURE 9

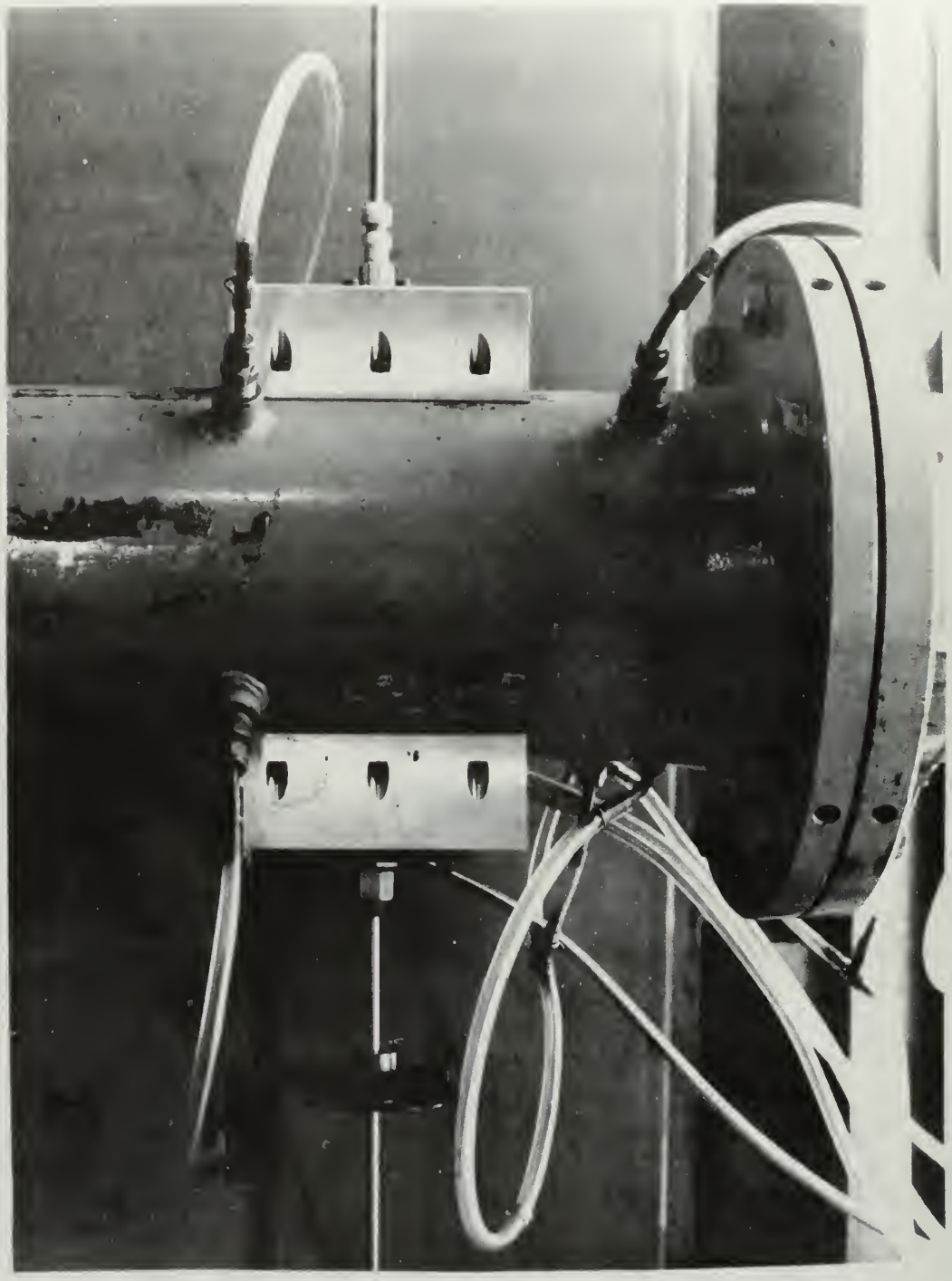

TRAVERSE PROBE INSTALLATION
EJECTOR TEST SERIES
FIGURE 10

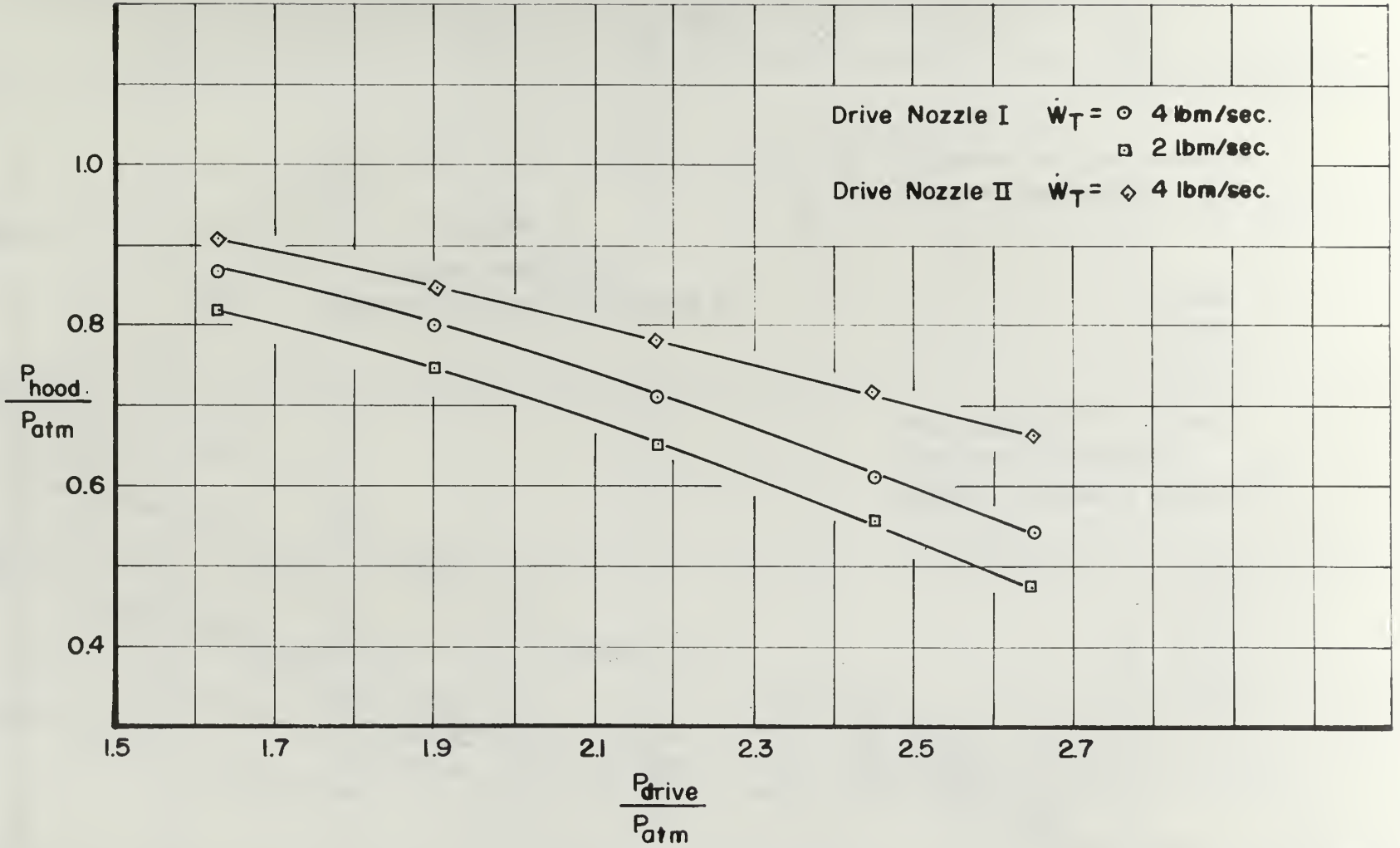

EXHAUSTER PERFORMANCE
HOOD TOTAL PRESSURE VERSUS DRIVE NOZZLE TOTAL PRESSURE
EJECTOR TEST SERIES

FIGURE 11

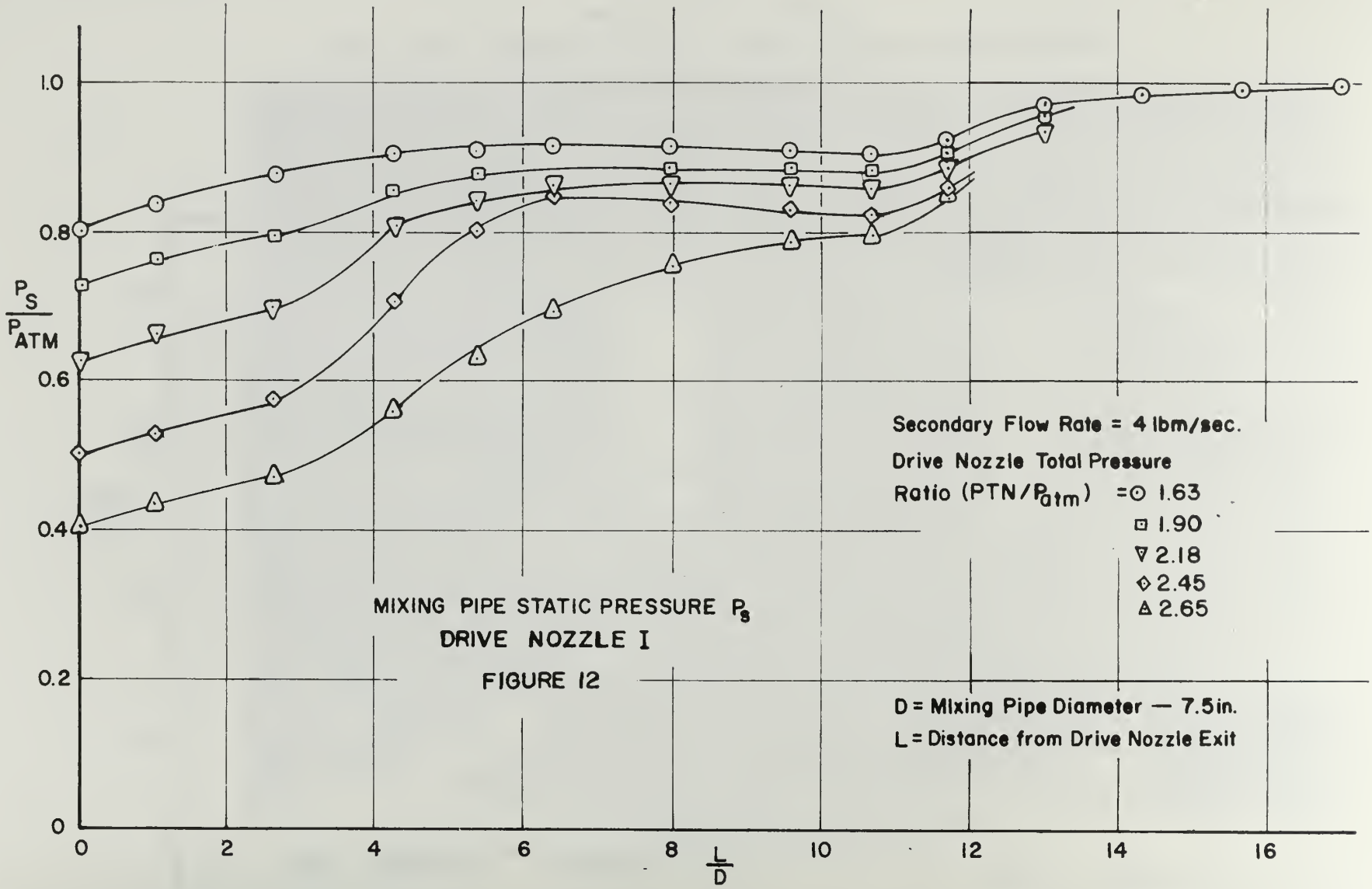
1.0
0.8
0.6
0.4
0.2
0
$\frac{P_S}{P_{ATM}}$
0
2
4
6
8
10
12
14
16
$\frac{L}{D}$
Secondary Flow Rate = 4 lbm/sec.
Drive Nozzle Total Pressure
Ratio (PTN/P_{atm}) = ⊙ 1.63
□ 1.90
▽ 2.18
◇ 2.45
△ 2.65
MIXING PIPE STATIC PRESSURE P_s
DRIVE NOZZLE I
FIGURE 12
D = Mixing Pipe Diameter — 7.5in.
L = Distance from Drive Nozzle Exit

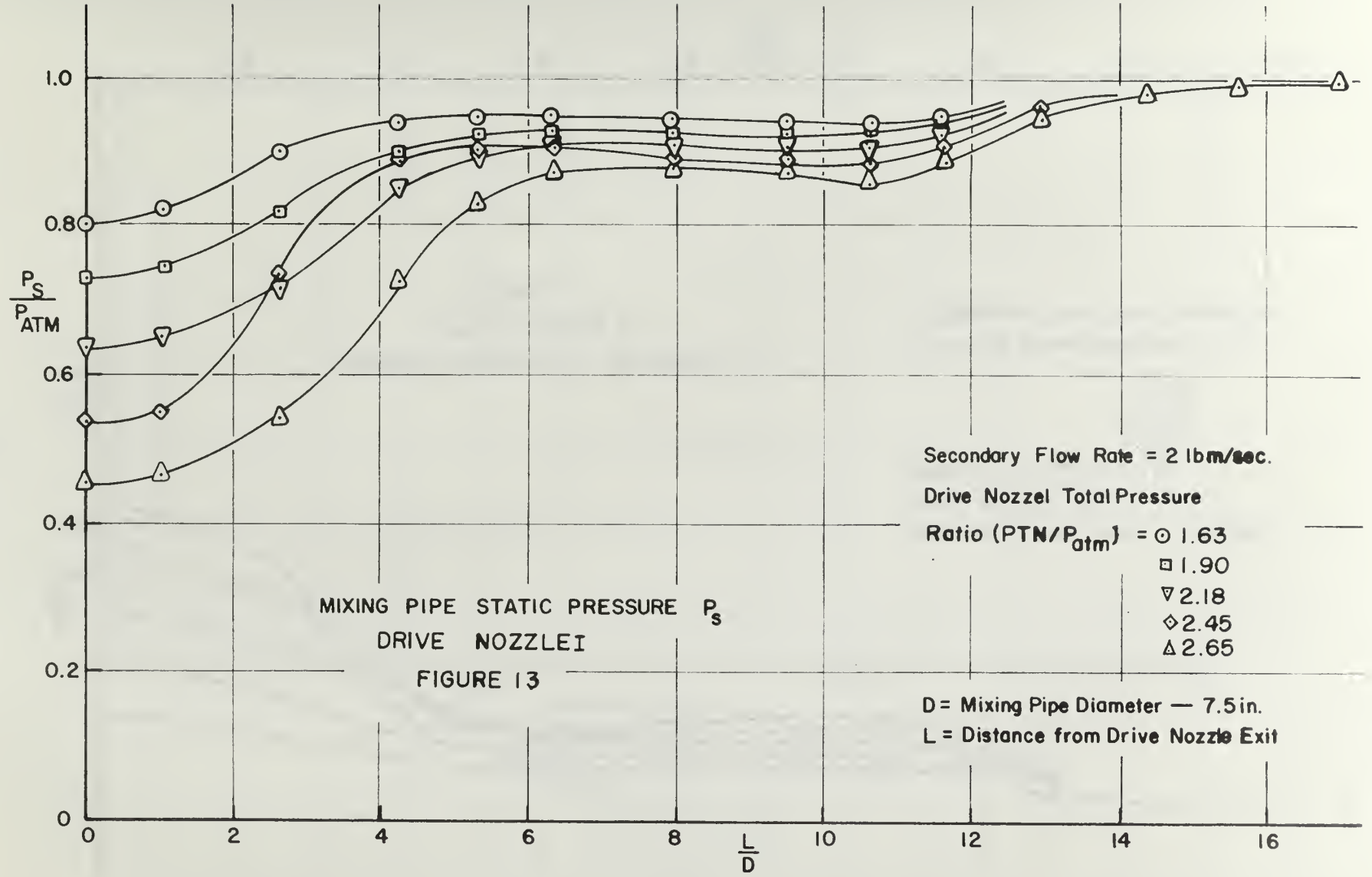

MIXING PIPE STATIC PRESSURE P_s
DRIVE NOZZLEI
FIGURE 13

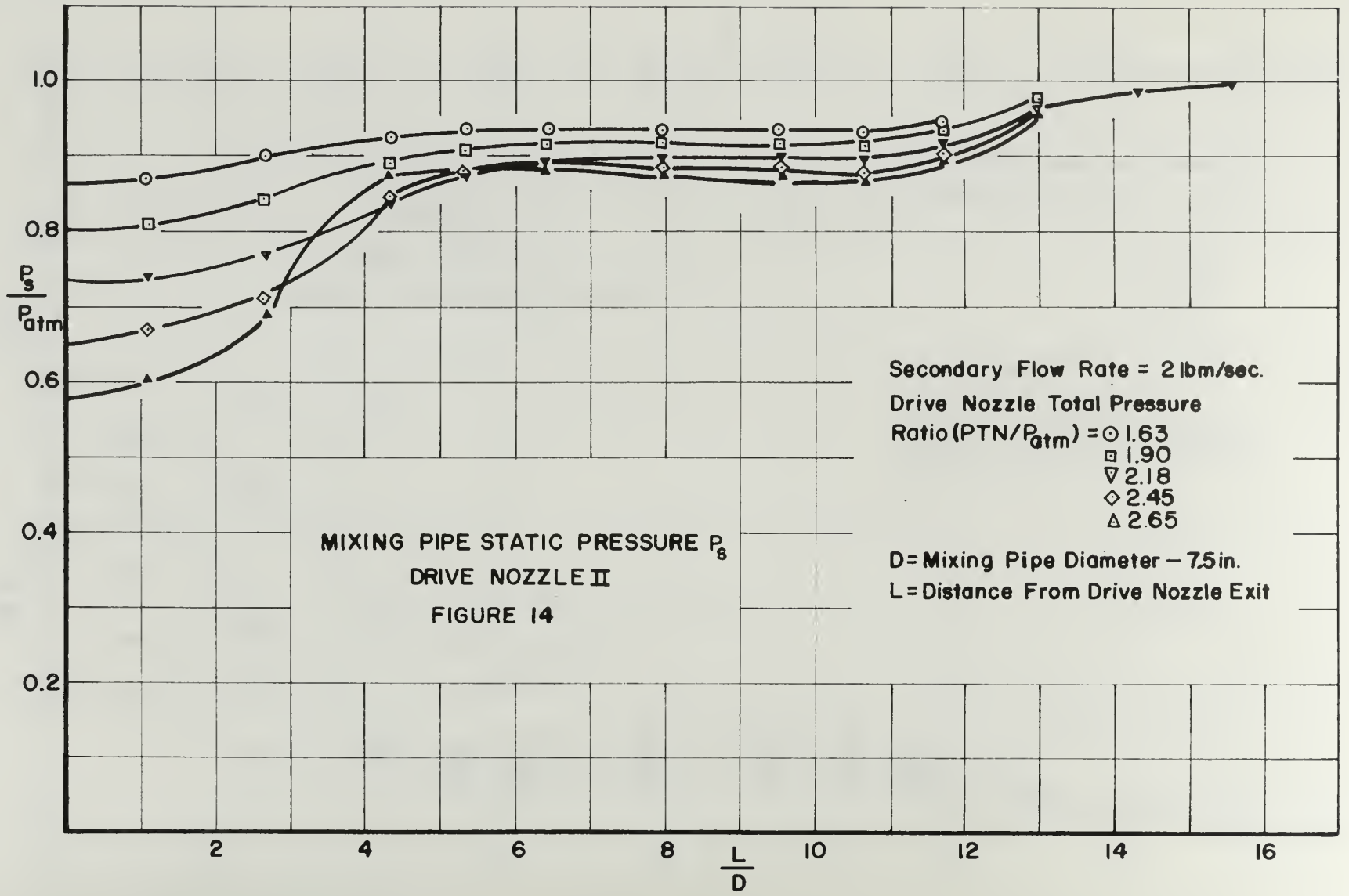
1.0
0.8
$\frac{P_s}{P_{atm}}$
0.6
0.4
0.2
2
4
6
8
$\frac{L}{D}$
10
12
14
16
Secondary Flow Rate = 2 lbm/sec.
Drive Nozzle Total Pressure
Ratio (PTN/P_{atm}) = ⊙ 1.63
□ 1.90
▽ 2.18
◇ 2.45
△ 2.65
D = Mixing Pipe Diameter — 7.5 in.
L = Distance From Drive Nozzle Exit
MIXING PIPE STATIC PRESSURE P_s
DRIVE NOZZLE II
FIGURE 14

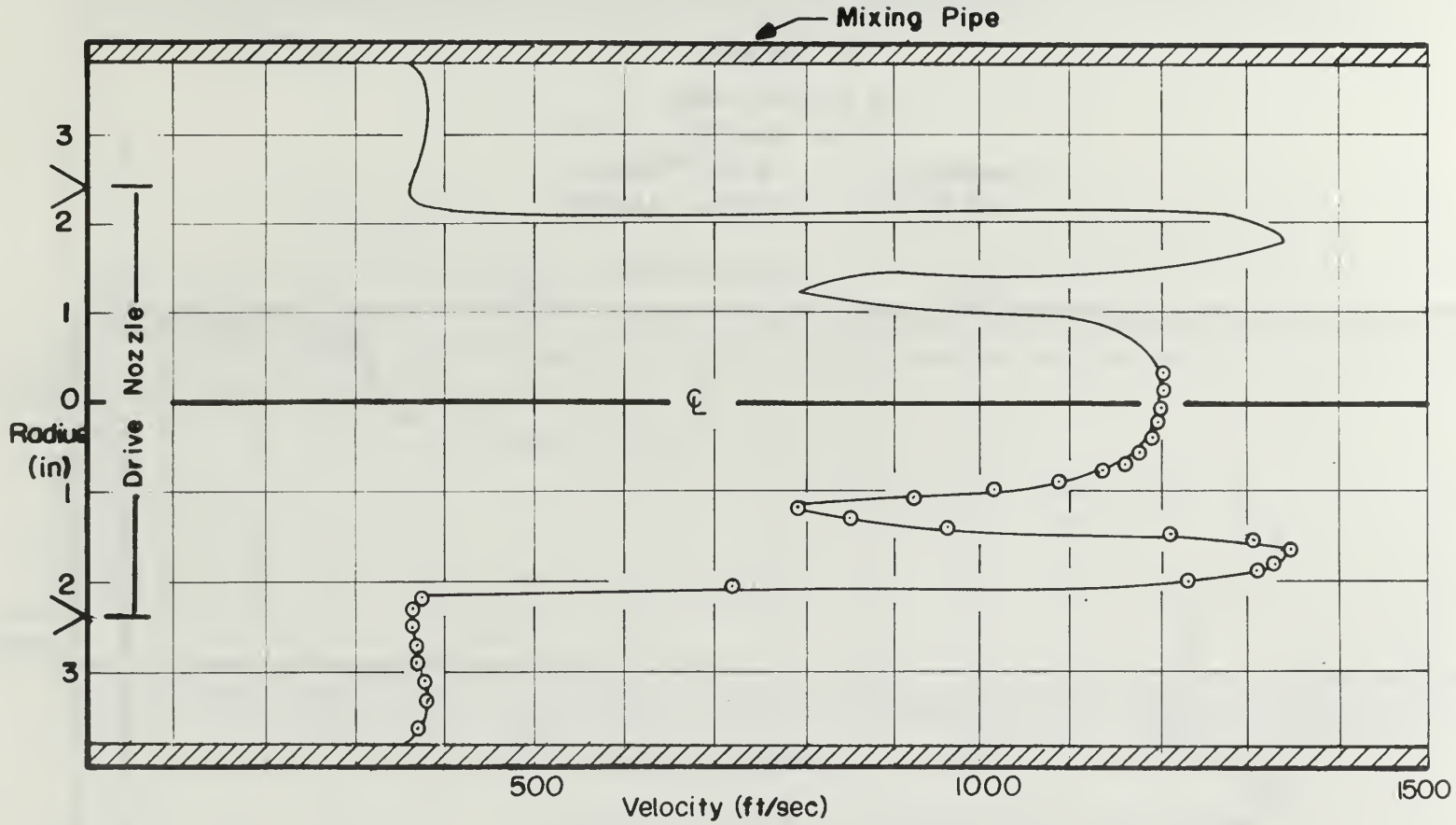

VELOCITY PROFILE – STATION MI
$PTN/P_{atm} = 2.18$ $W_T = 4.0$ lbm/sec.
EJECTOR TESTS
DRIVE NOZZLE 1

FIGURE 15

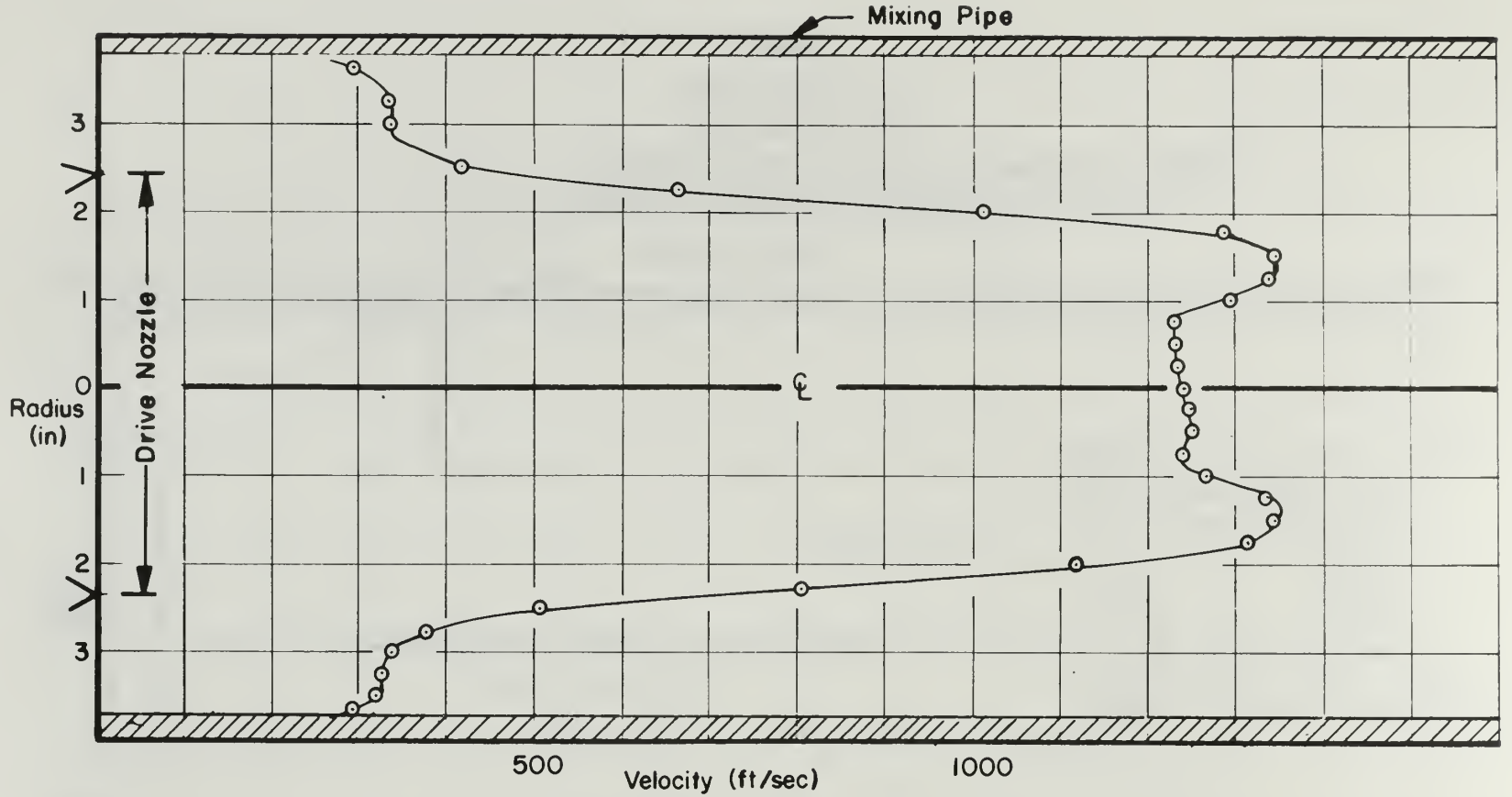

VELOCITY PROFILE — STATION M2
$PTN/P_{atm} = 2.18$ $\dot{w}_T = 4.01 lbm/sec.$
EJECTOR TESTS
DRIVE NOZZLE I

FIGURE 16

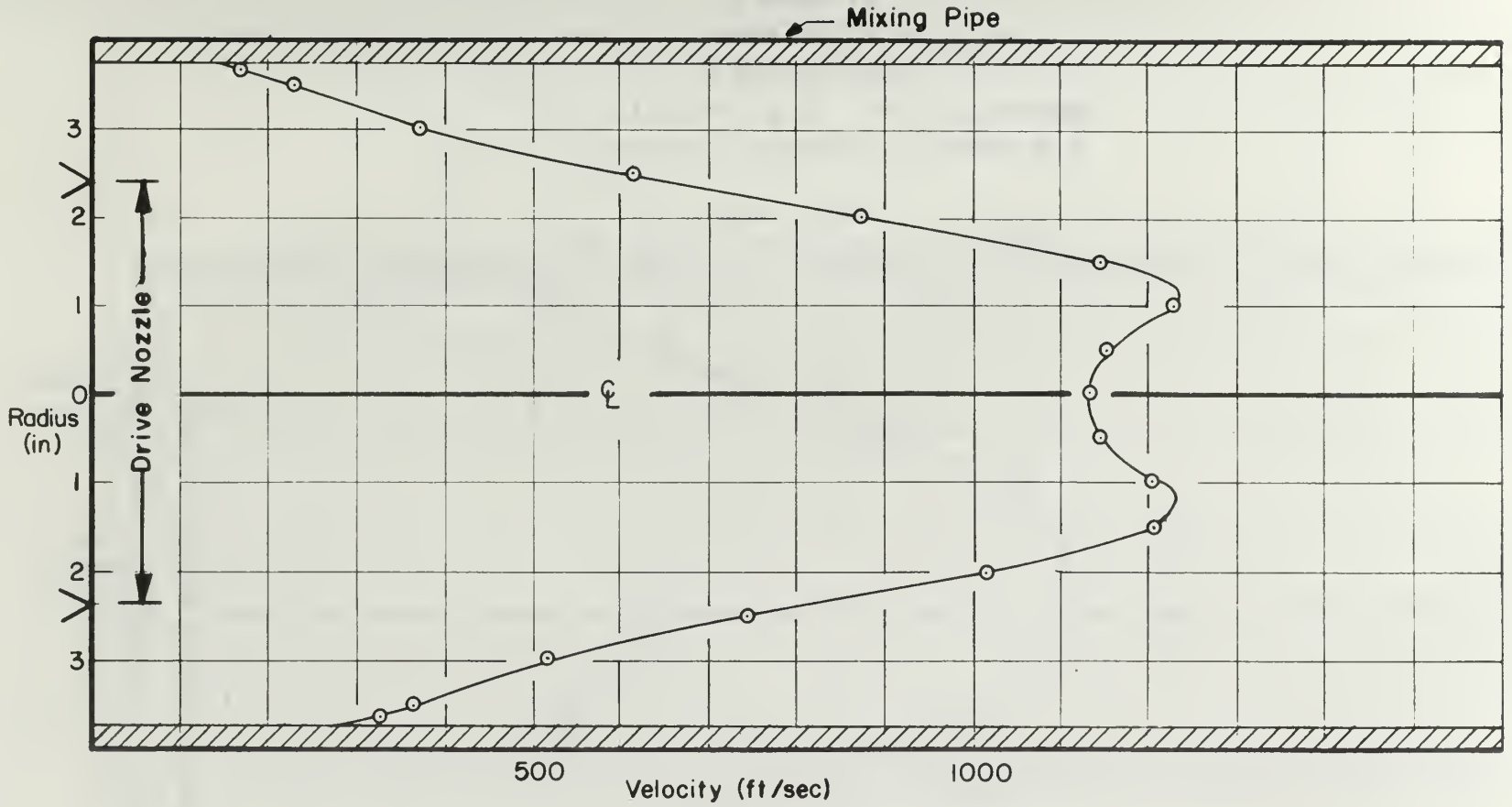

VELOCITY PROFILE – STATION M 3
PTN/P_{atm} = 2.18 $\dot{w}_T$ = 4.01 lbm/sec.
EJECTOR TESTS
DRIVE NOZZLE I

FIGURE 17

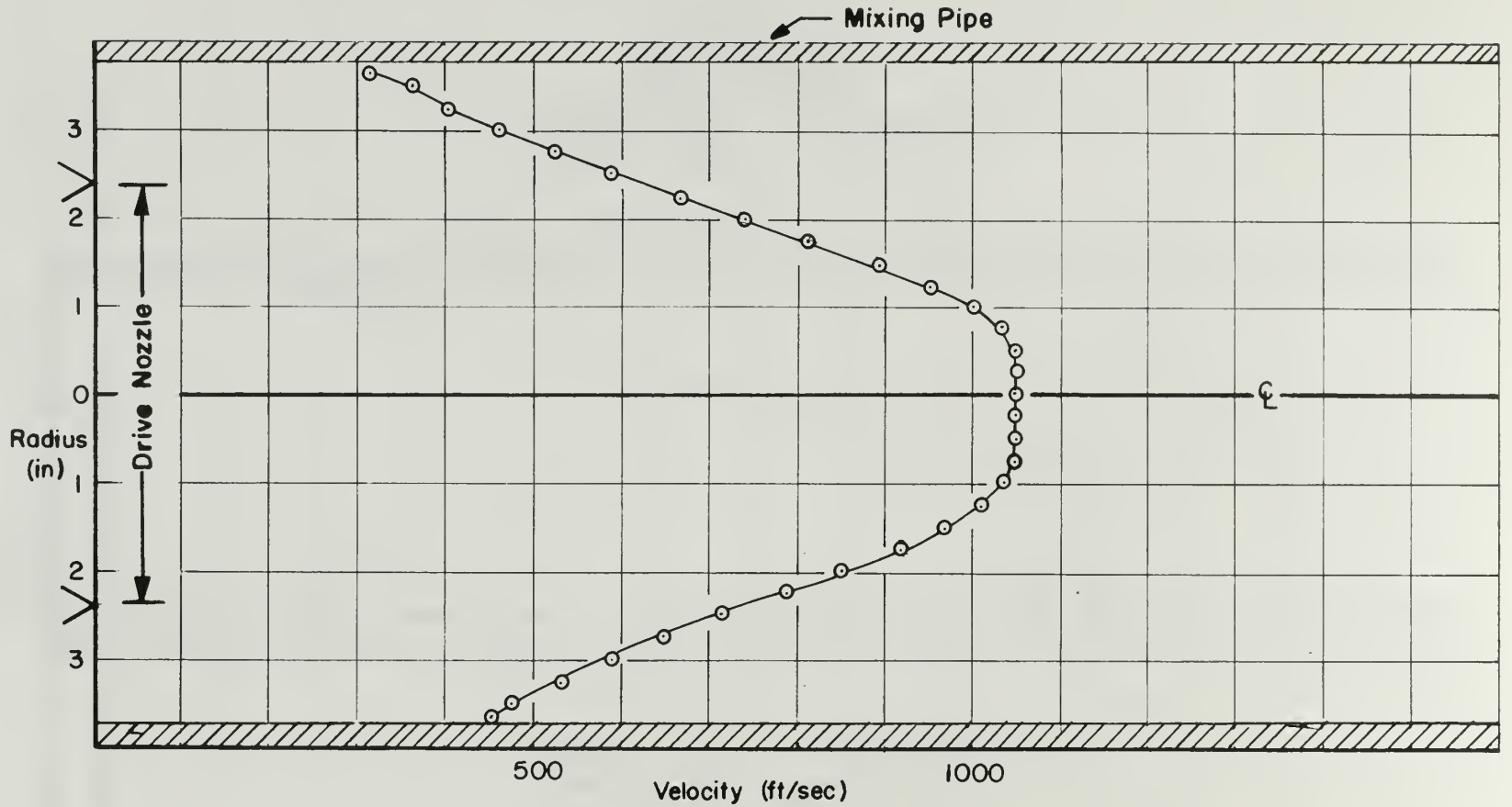

VELOCITY PROFILE – STATION M 4
$PTN/P_{atm} = 2.18$ $\dot{w}_T = 4.0$ lbm/sec.
EJECTOR TESTS
DRIVE NOZZLE I
FIGURE 18

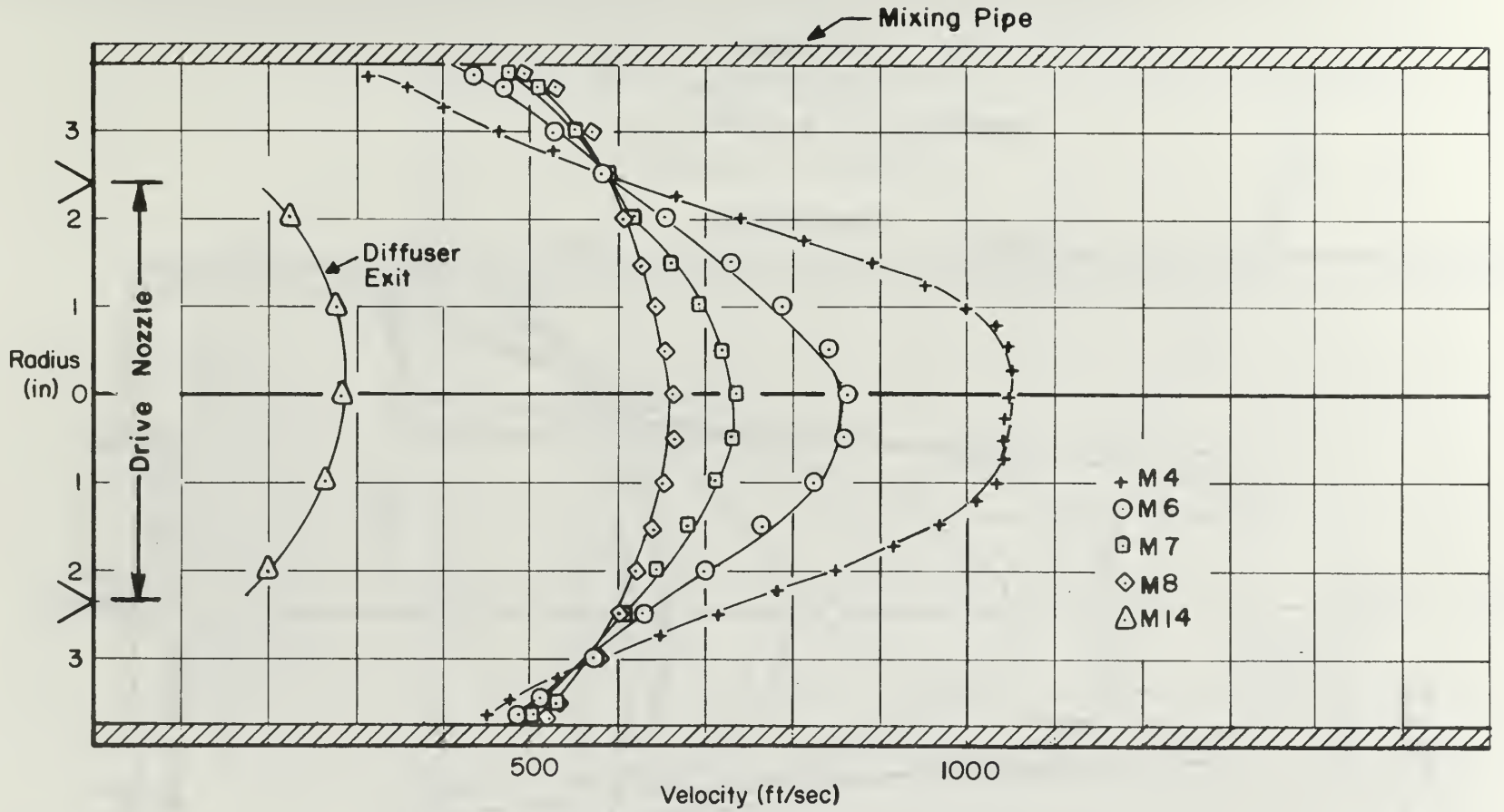

VELOCITY PROFILES- STATIONS M4,6,7,8,14

$PTN/P_{atm} = 2.18$ $\dot{w}_T = 4.0$ lbm/sec.

EJECTOR TESTS

DRIVE NOZZLE I

FIGURE 19

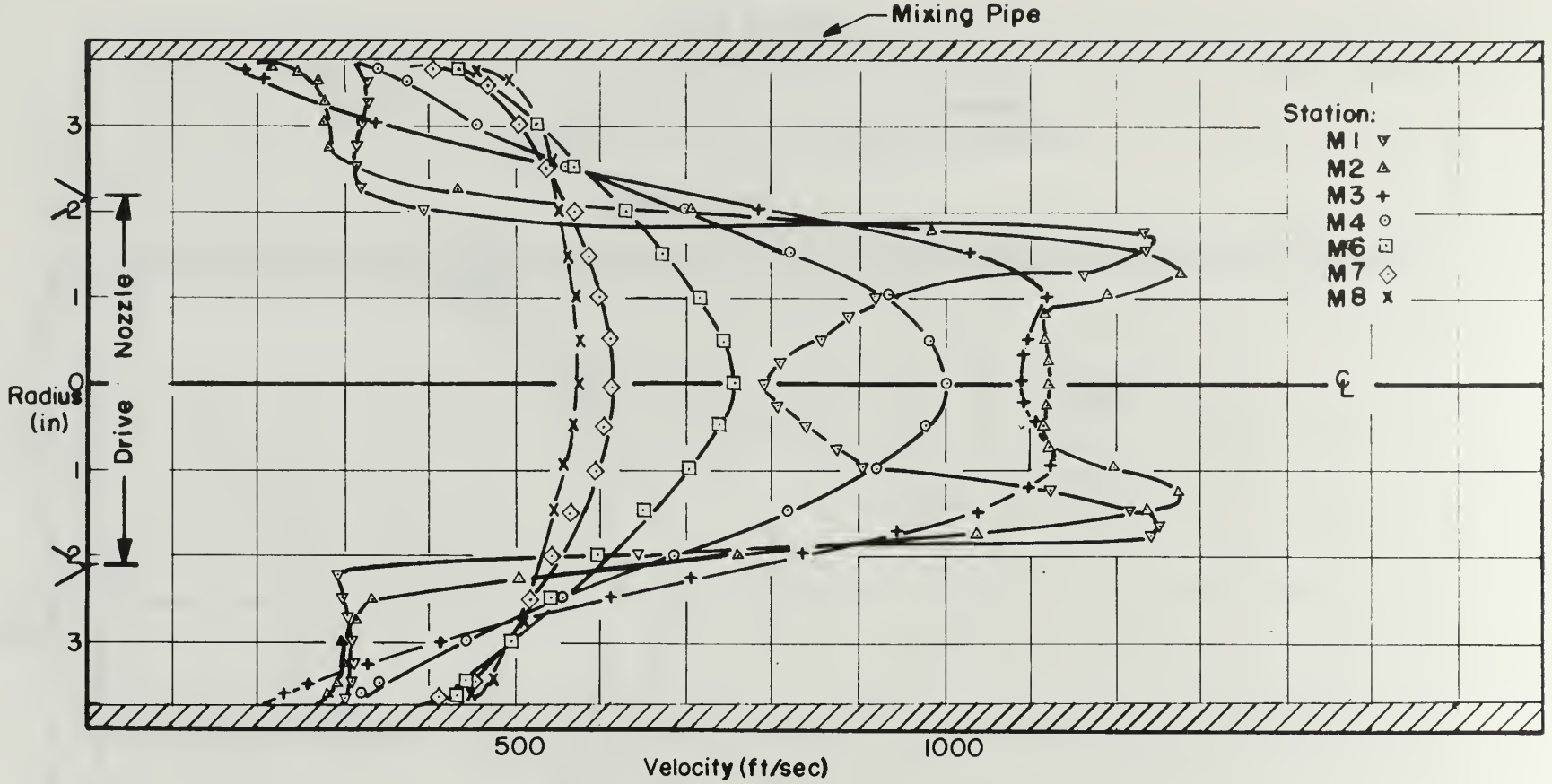

VELOCITY PROFILES
$PTN / P_{atm} = 2.18$ $\dot{w}_T = 4.0$ lbm/sec.
DRIVE NOZZLE II
FIGURE 20

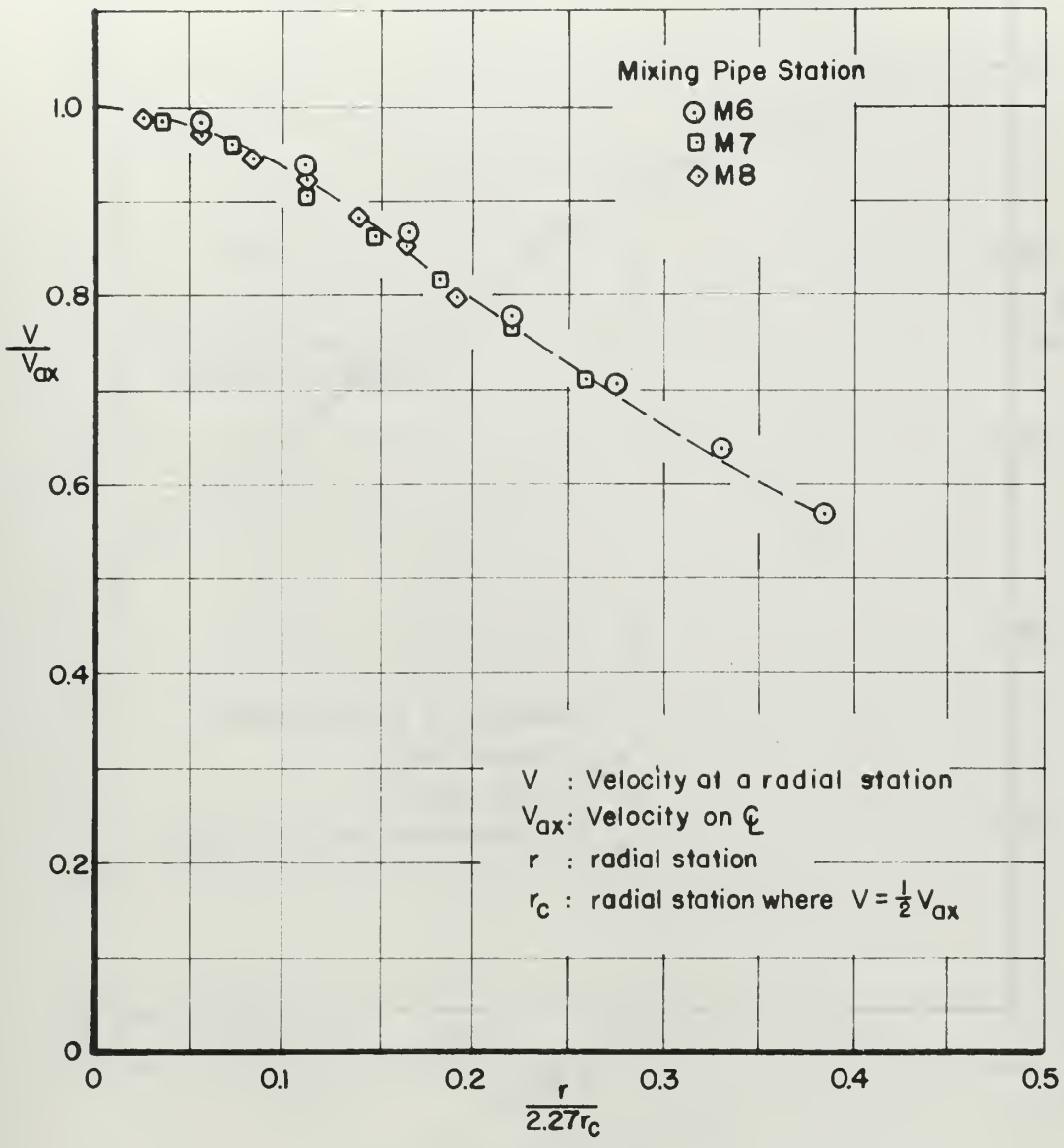

MAIN MIXING REGION
NON-DIMENSIONAL VELOCITY PROFILE
MIXING STATION M5, M6, M7
EJECTOR TEST

FIGURE 21

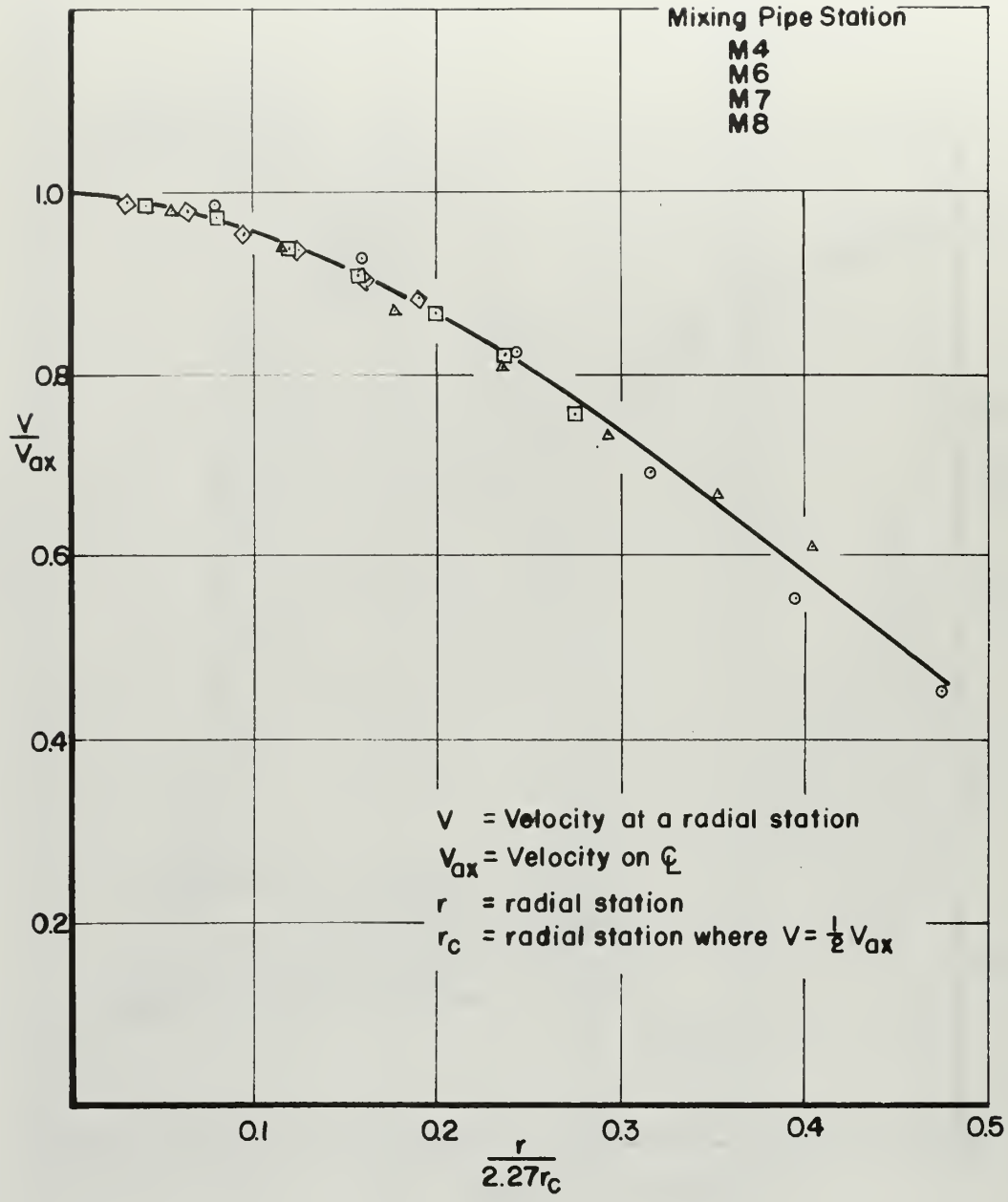

MAIN MIXING REGION
NON-DIMENSIONAL VELOCITY PROFILE
EXHAUSTER NOZZLE 11
PTN/P_{atm} = 2.18 $\dot{w}_T$ = 4.01bm/sec.
FIGURE 22

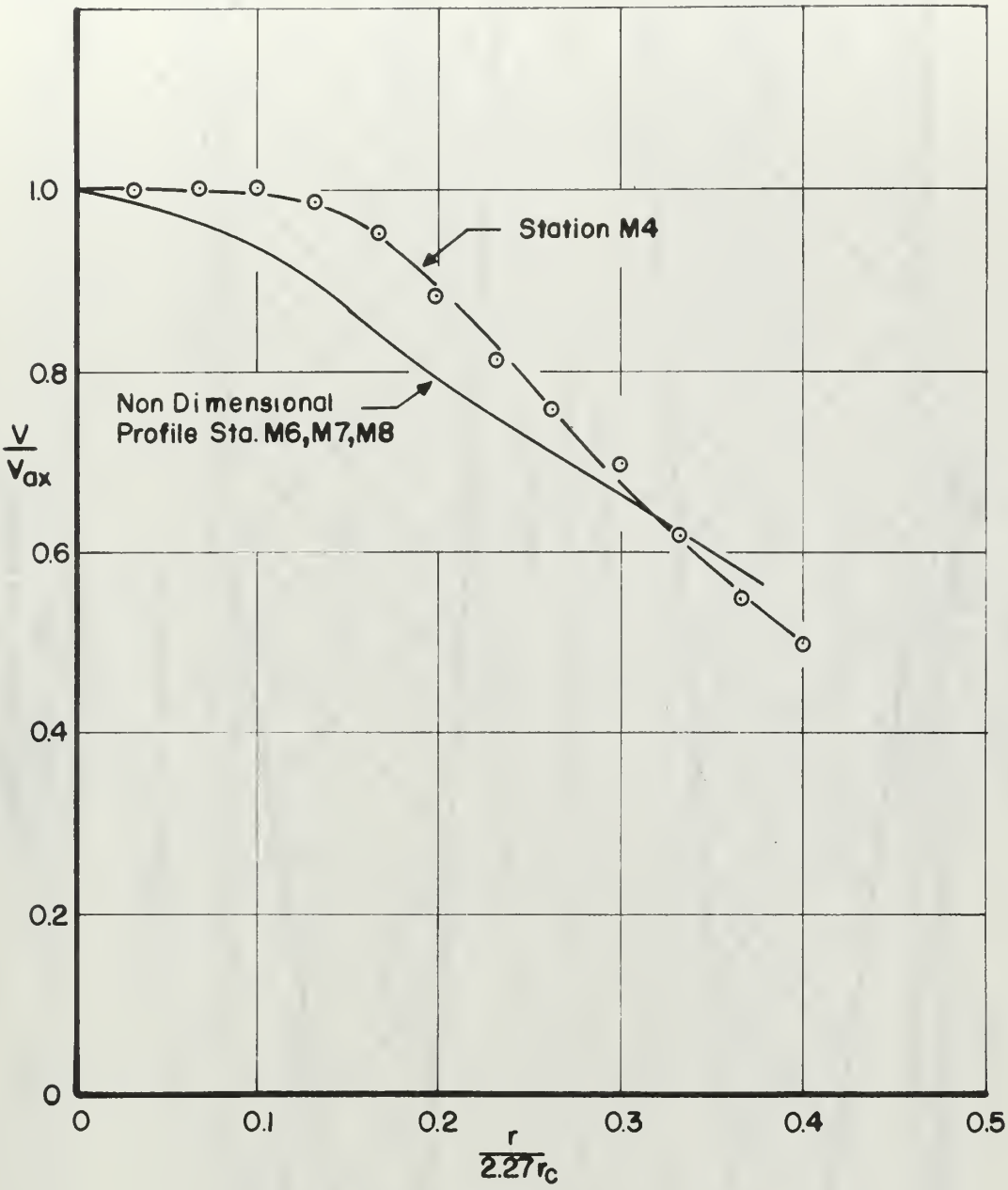

MIXING STATION M4
NON-DIMENSIONAL VELOCITY PROFILE
DRIVE NOZZLE I
FIGURE 23

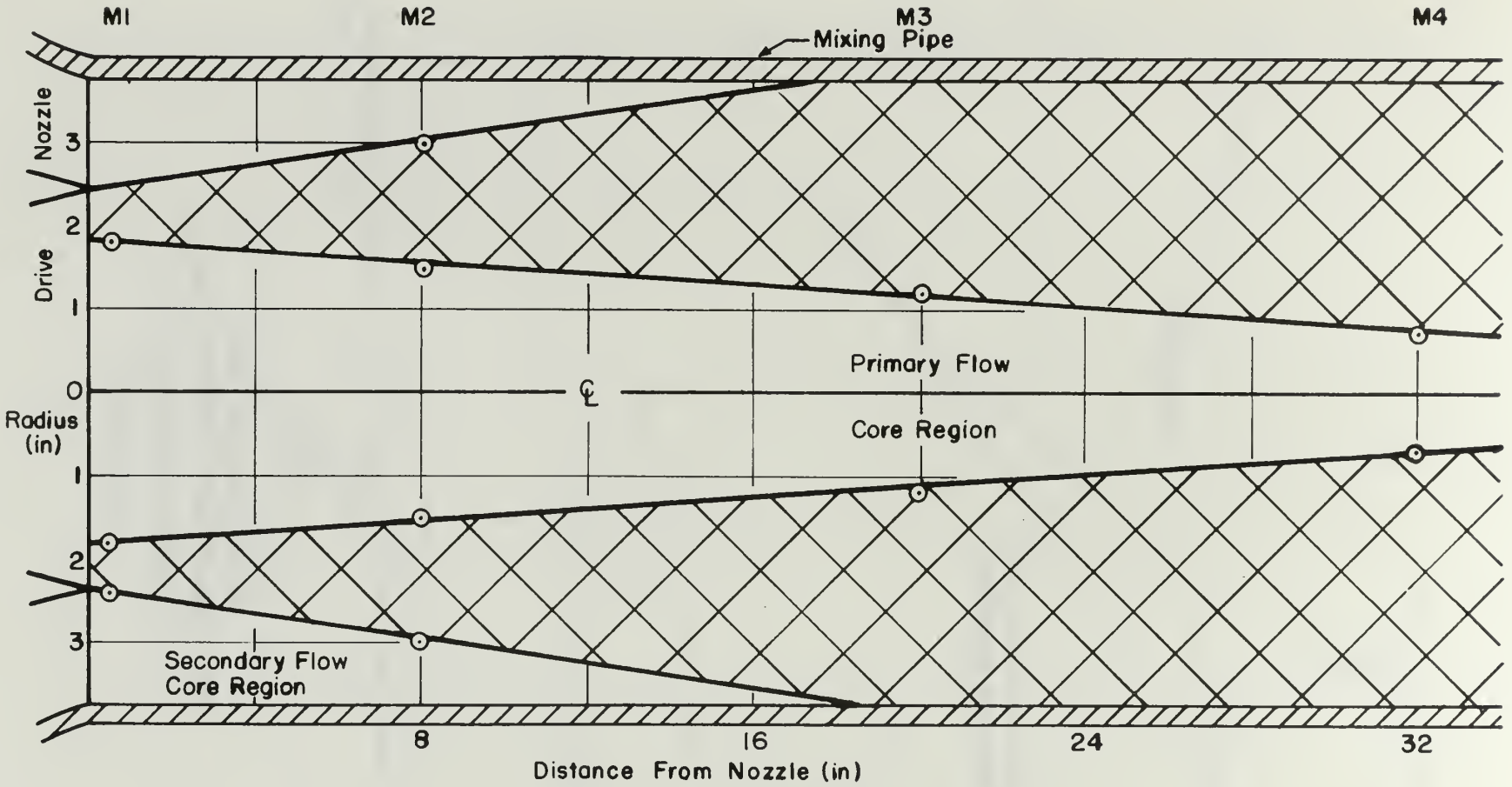

DRIVE NOZZLE I
MIXING ZONE
$PTN/P_{atm}=2.18$ $\dot{w}_T = 4$ lbm/sec.
EJECTOR TESTS

FIGURE 24

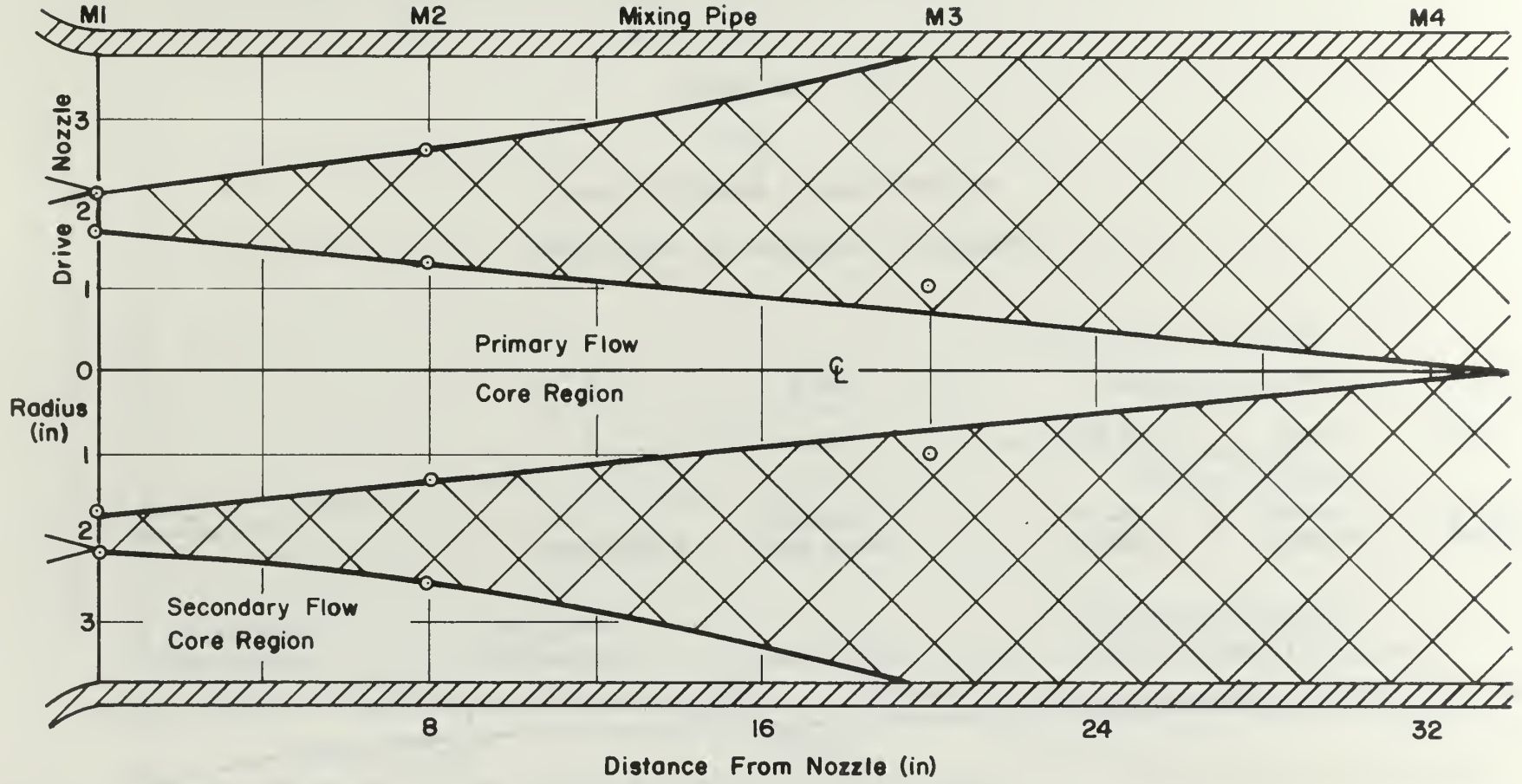

DRIVE NOZZLE II
MIXING ZONE
$PTN/P_{atm} = 2.18$ $\dot{W}_T = 4$ lbm/sec.
EJECTOR TEST
FIGURE 25

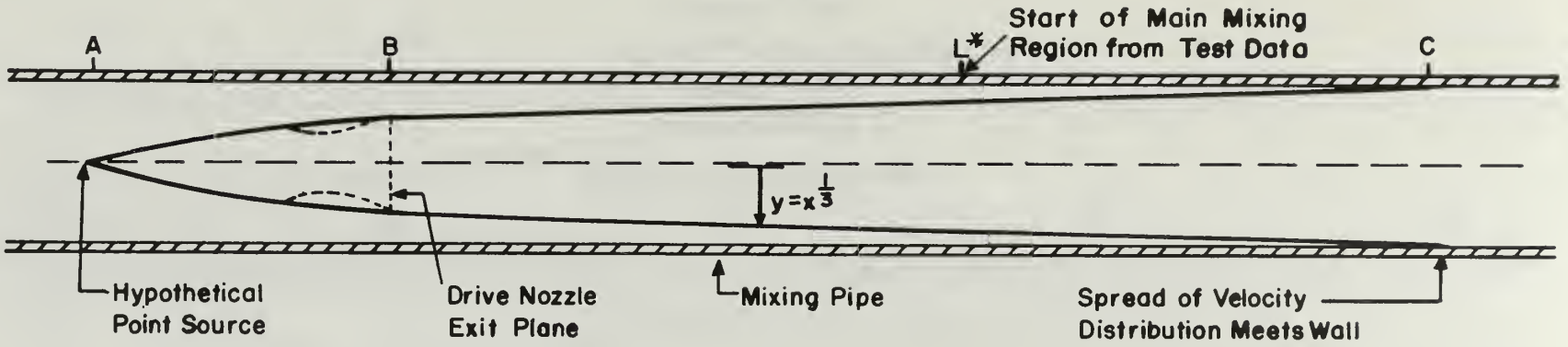

Drive Nozzle	Exit Plane Diameter	Distance A—B	Distance B—C	Distance B—L*
I	4.75"	13.5"	39.3"	18.0"
II	4.25"	9.5"	41.3"	20.0"

PREDICTION OF PRIMARY JET SPREAD

PER VICTORIAN'S APPROXIMATION

$y = x^{\frac{1}{3}}$

FIGURE 26

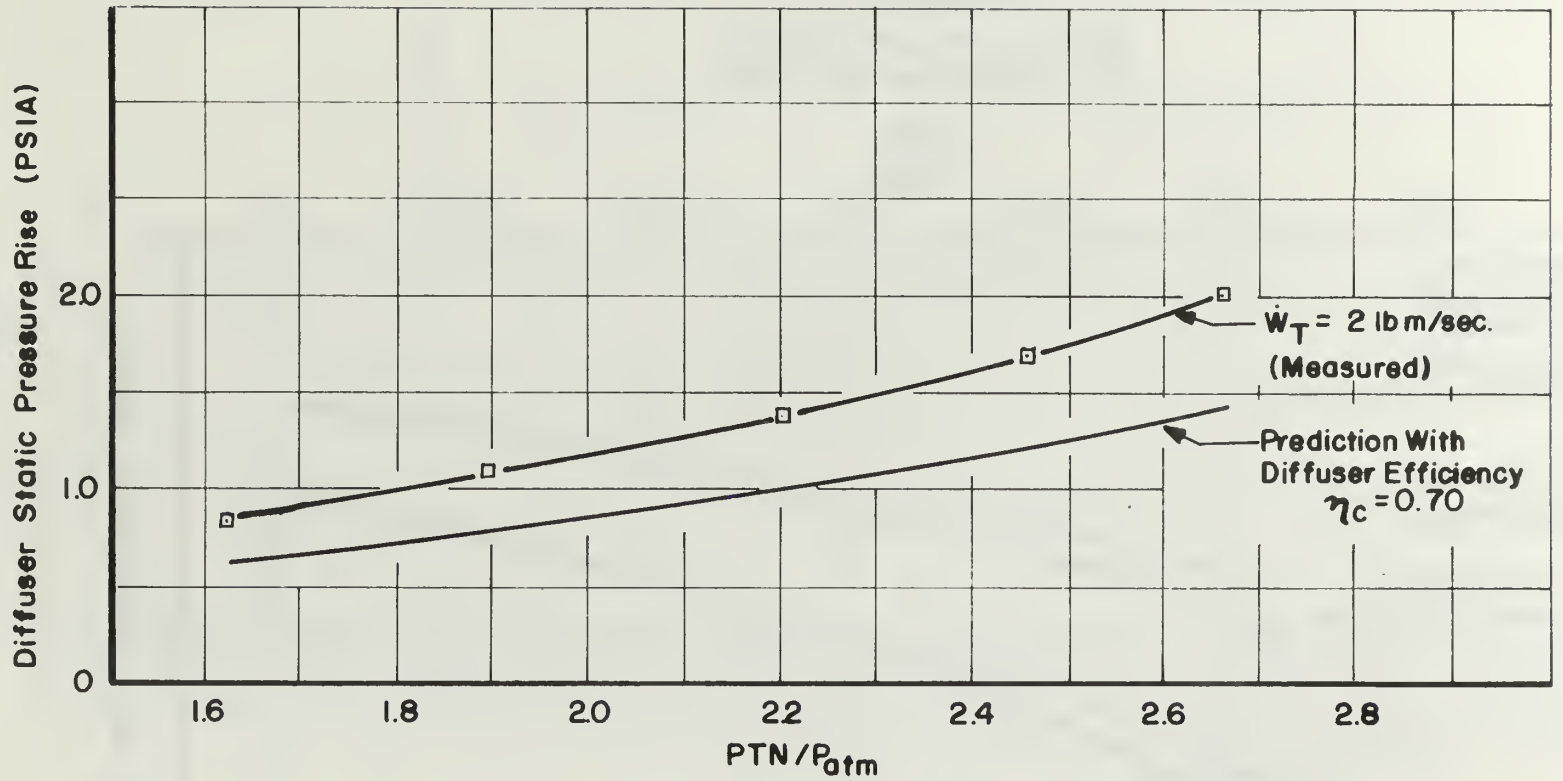

DIFFUSER STATIC PRESSURE RISE
COMPARED TO PREDICTION BASED ON EFFICIENCY η_c = 0.70

FIGURE 27

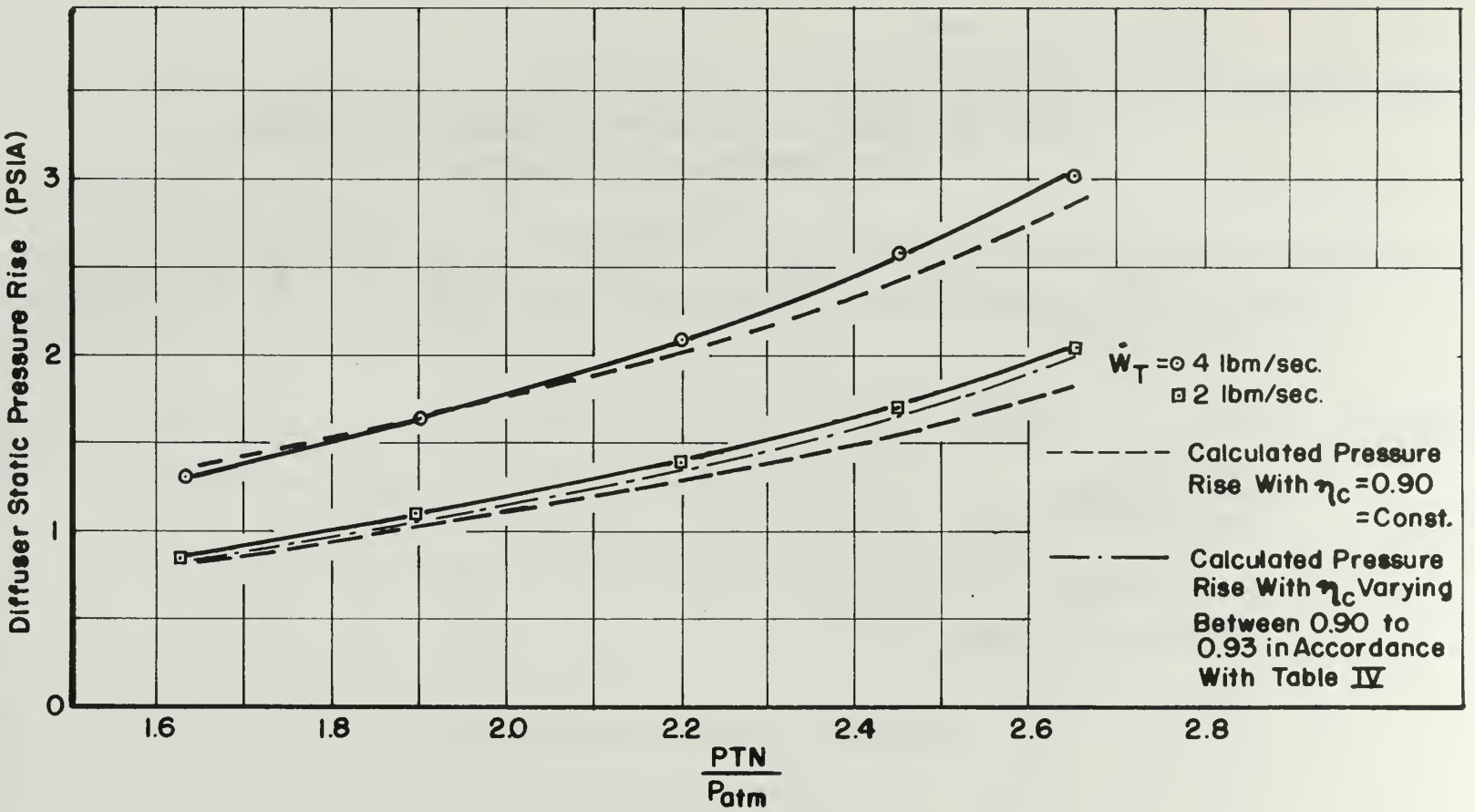

DIFFUSER PRESSURE RISE
ACTUAL AND CALCULATED

η_c=0.90

FIGURE 28

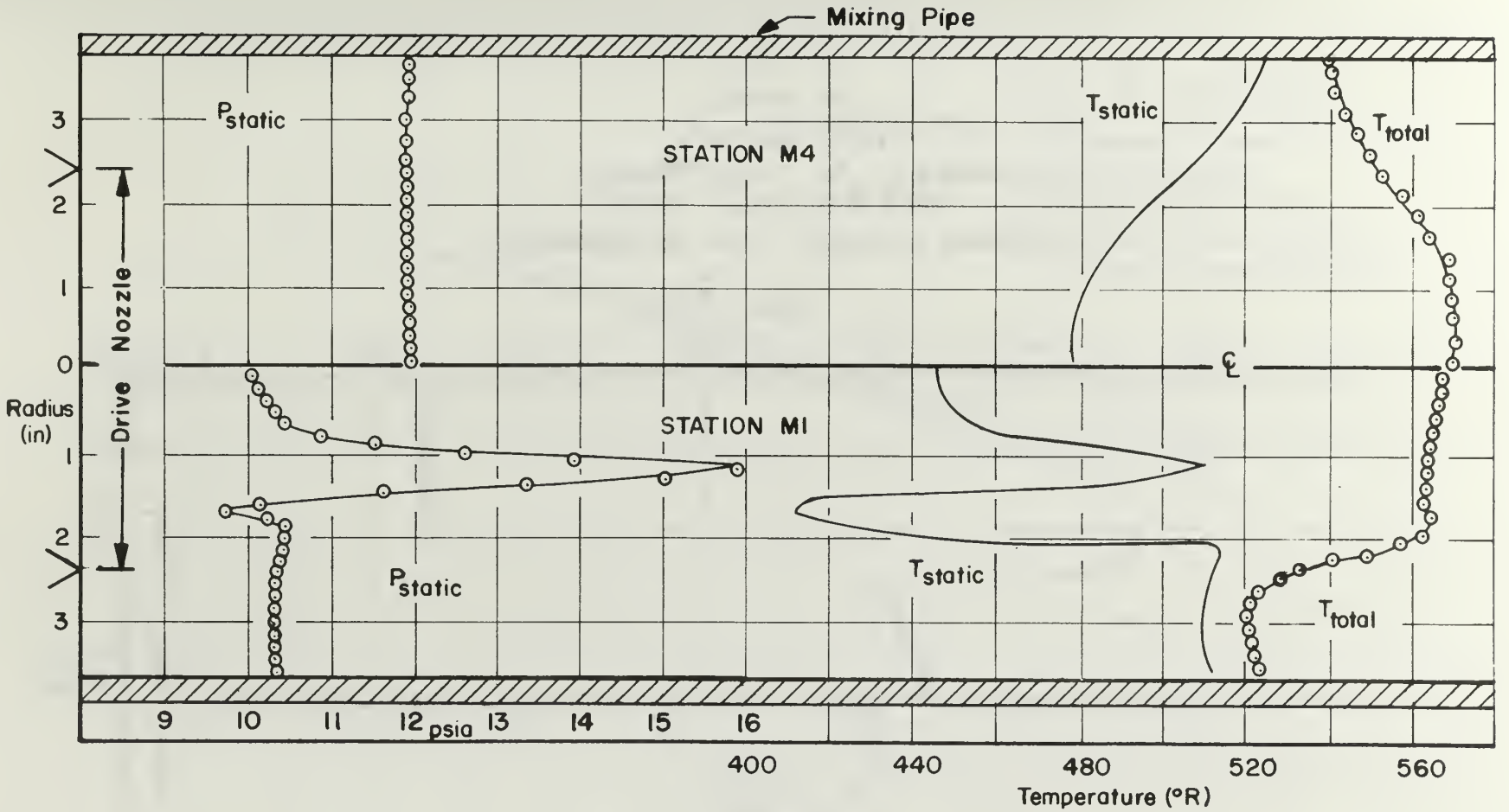

Comparison of P_{static}, T_{static}, and T_{total}

MIXING STATIONS MI & M4

$PTN/P_{atm} = 2.18$ $\dot{W}_T = 4$ lbm/sec.

EJECTOR TESTS

FIGURE 29

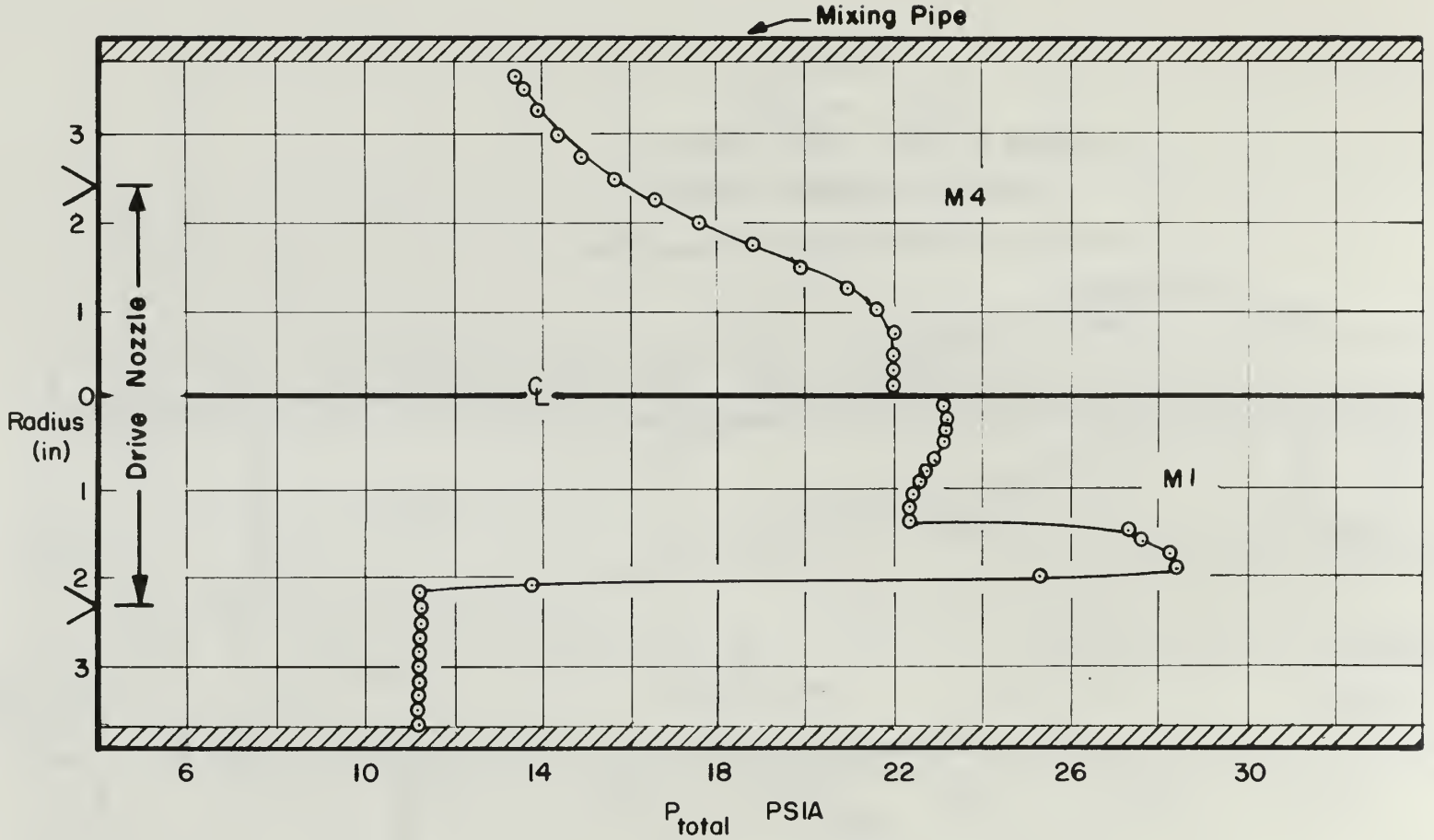

COMPARISON OF TOTAL PRESSURE PROFILE
MIXING STATIONS M1 & M4
$PTN/P_{atm} = 2.18$ $\dot{W}_T = 4$ lbm/sec.
EJECTOR TESTS

FIGURE 30

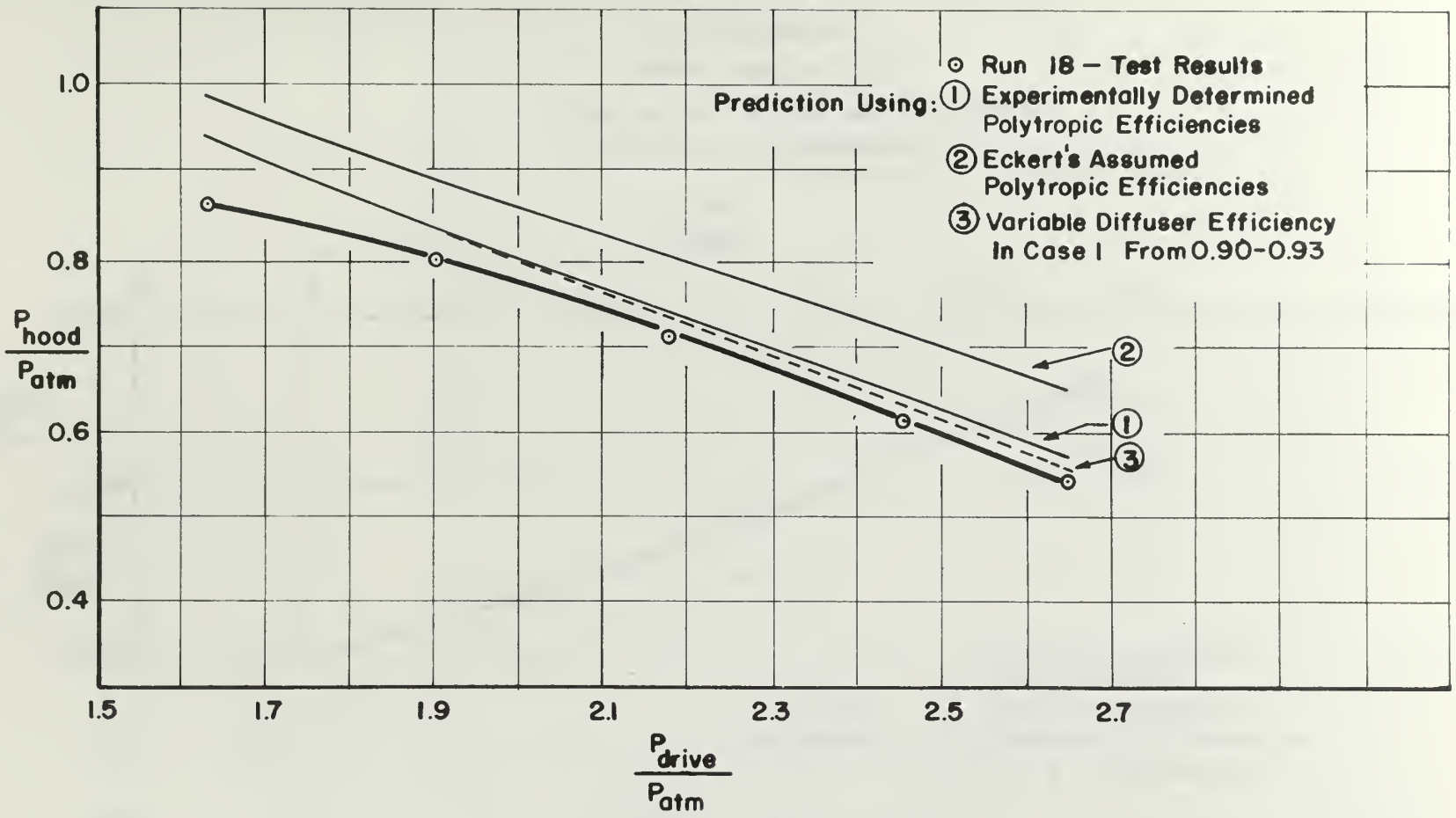

EXHAUSTER PERFORMANCE
TEST RESULTS AND PREDICTIONS
DRIVE NOZZLE I
$\dot{W}_T$ = 4 lbm/sec.

FIGURE 31

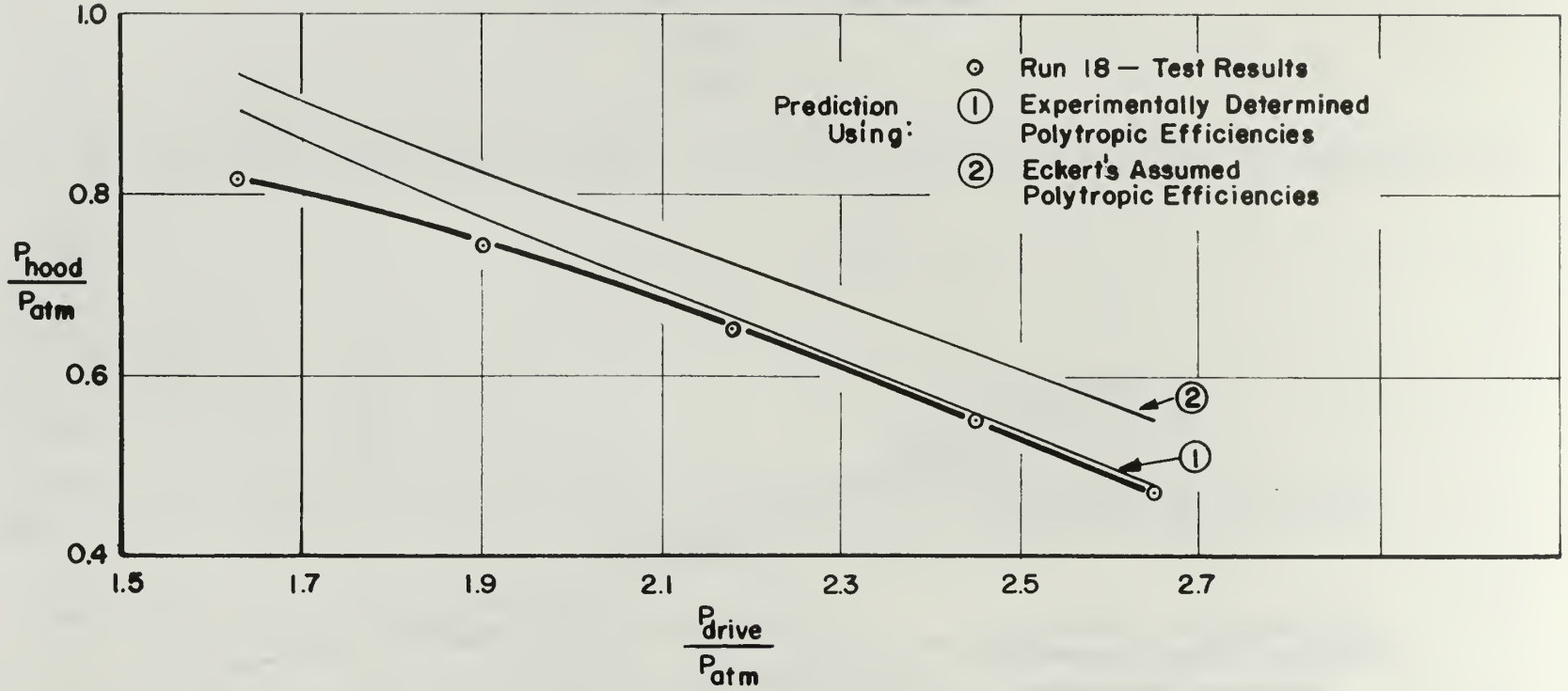

EXHAUSTER PERFORMANCE
TEST RESULTS AND PREDICTIONS
DRIVE NOZZLE I
$\dot{W}_T = 2$ lbm/sec.

FIGURE 32

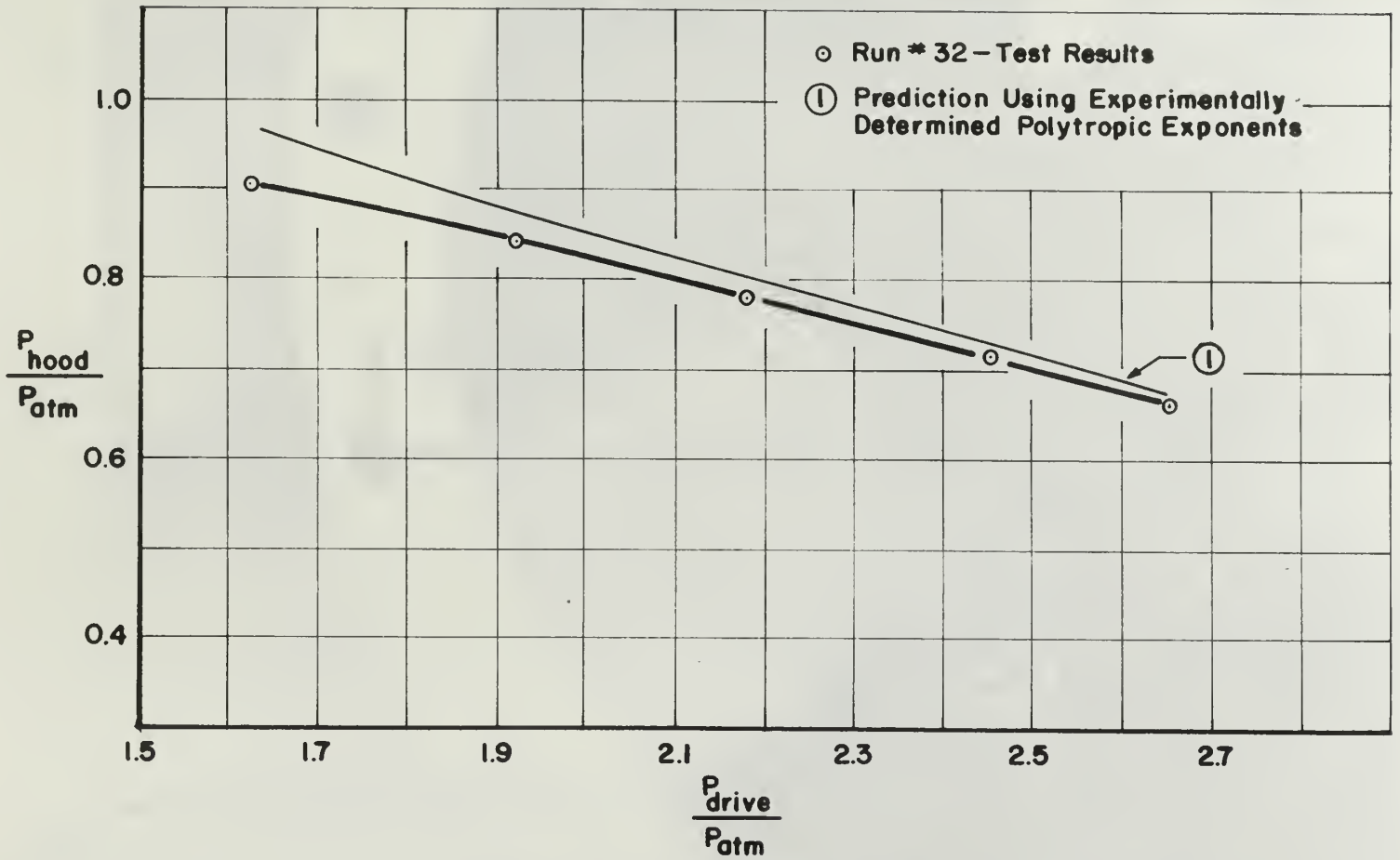

EXHAUSTER PERFORMANCE
TEST RESULTS AND PREDICTIONS
DRIVE NOZZLE II
$\dot{W}_T$ = 4 lbm/sec.
FIGURE 33

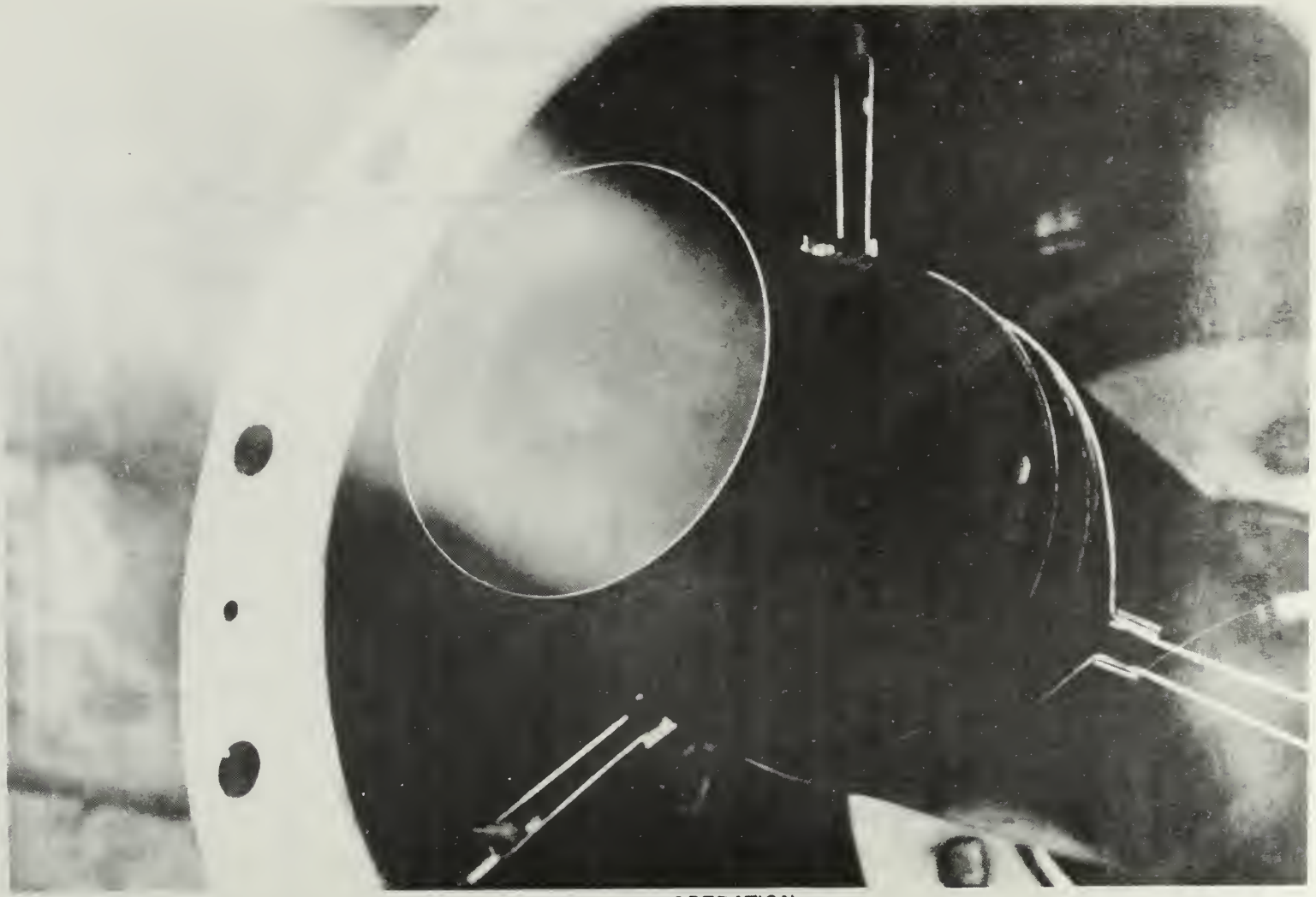

FREE JET OPERATION
DRIVE NOZZLE I

FIGURE 34

FREE JET SHOCK PATTERN
FIGURE 35

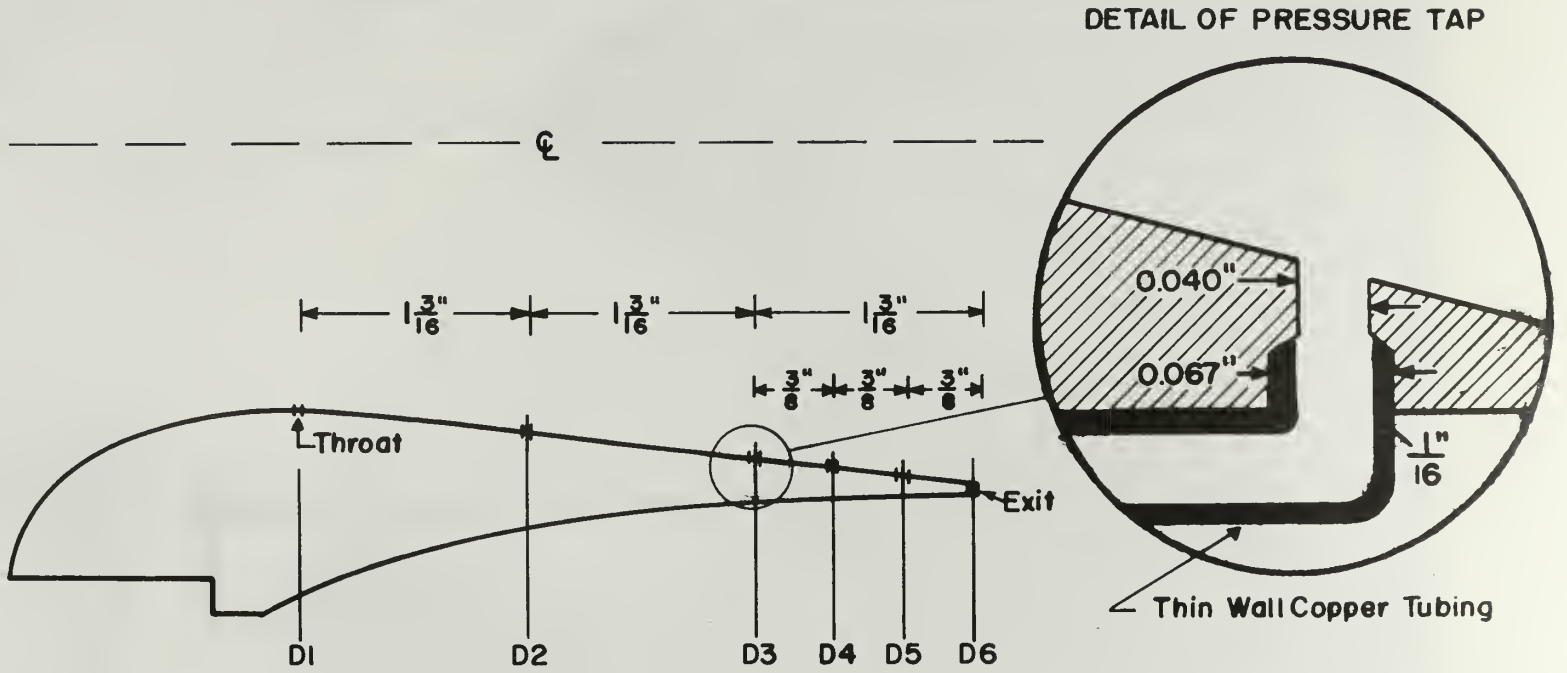

DRIVE NOZZLE I
STATIC TAP AXIAL LOCATION
EJECTOR TESTS
FIGURE 36

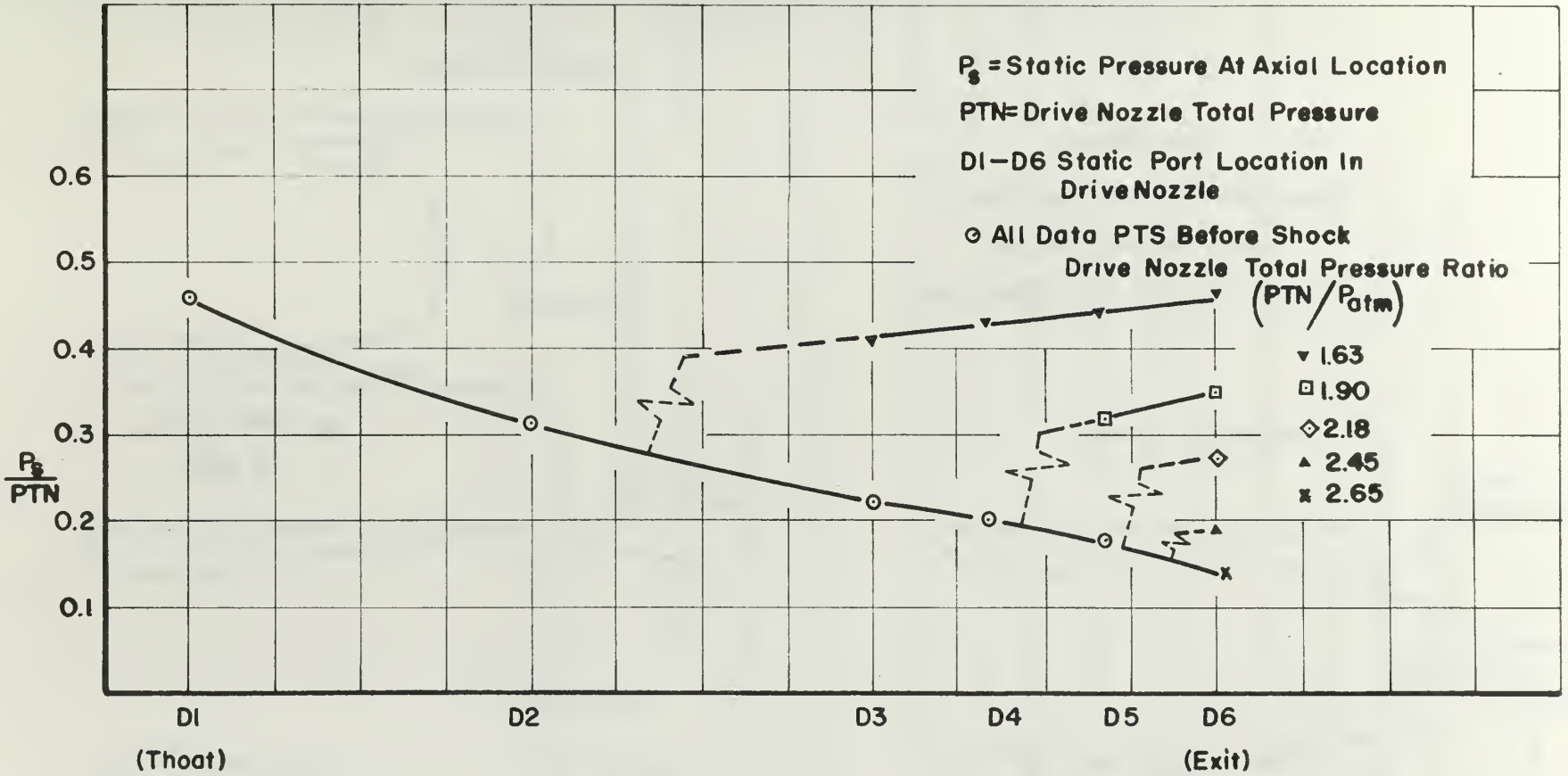

DRIVE NOZZLE STATIC PRESSURE VERSUS AXIAL POSITION

FOR DIFFERENT DRIVE NOZZLE SETTINGS

EJECTOR TESTS

FIGURE 37

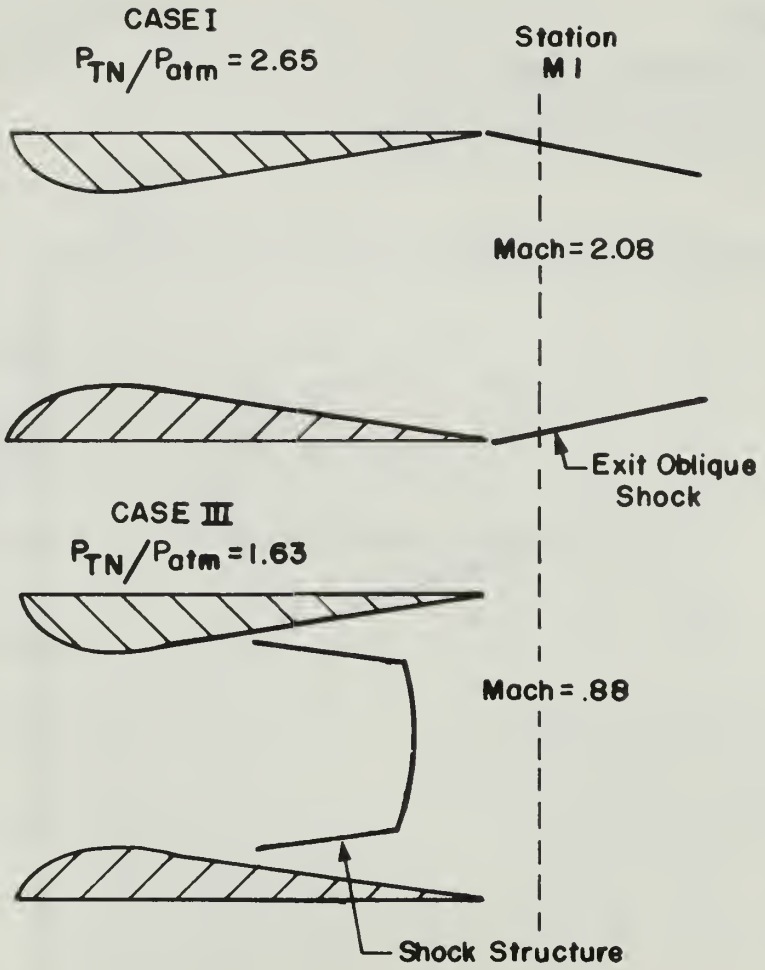

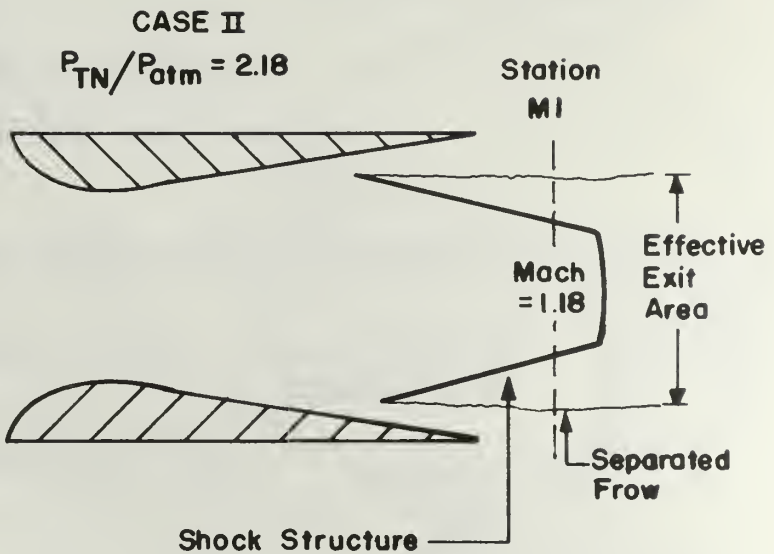

HYPOTHESIZED SHOCK STRUCTURE
AND MOVEMENT FOR
EXHAUSTER TEST CONDITIONS
FIGURE 38

APPENDIX A

Exhauster Performance Analysis

An analysis was made of the exhauster performance to predict hood total pressure which essentially parallels the preliminary design calculations of Vavra. However, the previous work assumed that the nozzle operates at design conditions and that the static pressure at the entrance to the mixing section is constant with radius. The analysis explained in the following permits a discontinuity in static pressure between the nozzle exit (Area A1) and the secondary flow annulus (Area A1T) at the start of the mixing pipe.

In order to simplify the equations, polytropic process relations as well as non-dimensional flow functions were used. These were taken from Vavra.

For an expansion process

$$\frac{\dot{w}\sqrt{T_{T1}}}{A_2 P_{T1}}\sqrt{\frac{R}{g}} = \Phi_e = \sqrt{\frac{2\gamma}{\gamma-1}\left[\left(\frac{P_2}{P_{T1}}\right)^{2/n} - \left(\frac{P_2}{P_{T1}}\right)^{\frac{n+1}{n}}\right]} \qquad \text{(A1)}$$

where

$$n = \frac{\gamma}{\gamma - \eta_p(\gamma-1)} \qquad \text{(A2)}$$

n = polytropic exponent

η_p = polytropic efficiency $\left(\frac{dT}{dT_{is}}\right)$

γ = ratio of specific heats

$\dot{w}$ = flow rate (lbm/sec)

T_{t_o} = inlet stagnation temperature (^oR)

A_2 = Flow area at station of interest (in.^{2})

P_{t_o} = Inlet stagnation pressure (psia)

p_2 = static pressure at station of interest (psia)

g = universal gravitational constant $\left(\frac{lbm}{lb_f}\frac{ft}{sec^2}\right)$

Subscript 1 refers to inlet conditions

Subscript 2 refers to station of interest

For a compression process

$$\frac{\dot{w}\sqrt{T_1}}{P_1 A_2}\sqrt{\frac{R}{g}} = \Phi_c = \sqrt{\frac{2\gamma}{\gamma-1}\left[\frac{T_{T1}}{T_1}\left(\frac{P_2}{P_1}\right)^{2/n} - \left(\frac{P_2}{P_1}\right)^{\frac{n+1}{n}}\right]} \qquad \text{(A3)}$$

where

p_1 = static pressure at 1

$$n = \frac{\gamma\eta_p}{1-\gamma(1-\eta_p)} \qquad \text{(A4)}$$

The flow through the nozzle will be choked when it is operating at supersonic conditions. Therefore Φ_e (or Φ_e^2) must be a maximum value. Differentiating Φ_e^2 and

setting the result equal to zero yield the critical pressure ratio for choked conditions

$$\left(\frac{P_2}{P_{T1}}\right)_{critical} = \left(\frac{2}{n+1}\right)^{\frac{n}{n-1}}$$

Substituting this value into Eq. A1, the expression for the flow function of a choked nozzle simplifies to

$$\Phi_{\substack{choked \\ Nozzle}} = \left(\frac{2}{n+1}\right)^{\frac{1}{n-1}} \sqrt{\frac{2\gamma}{\gamma-1}\left(\frac{n-1}{n+1}\right)} \qquad \text{(A5)}$$

It was assumed that the drive nozzle total temperature and total pressure were known, as well as the secondary flow rate and total temperature. Polytropic efficiencies for the drive nozzle are assumed or determined from testing and held constant over the operating range of the exhauster. Notation in the development is consistent with Fig. 3.

Drive Nozzle

For a choked nozzle,

$$\Phi_n = \left(\frac{2}{n_T+1}\right)^{\frac{1}{n_T-1}} \sqrt{\frac{2\gamma}{\gamma-1}\left(\frac{n_T-1}{n_T+1}\right)} \qquad \text{(A6)}$$

The flow functions from the nozzle entrance to the throat (Φ_n), and from the nozzle entrance to the exit (Φ_{ex}) are, respectively,

$$\Phi_n = \frac{\dot{w}_N \sqrt{T_{TN}}}{A_T \; P_{TN}} \sqrt{\frac{R}{g}} \tag{A7}$$

$$\Phi_{ex} = \frac{\dot{w}_N \sqrt{T_{TN}}}{A_1 \; P_{TN}} \sqrt{\frac{R}{g}} \tag{A8}$$

There are

$$\Phi_n A_T = \Phi_{ex} A_1 \tag{A9}$$

and

$$\Phi_{ex} = \Phi_n \frac{A_T}{A_1} \tag{A10}$$

Expressing the exit flow function in terms of the pressure ratio P_{TN}/P_{IN}

$$\Phi_{ex} = \sqrt{\frac{2\gamma}{\gamma-1}\left[\left(\frac{P_{IN}}{P_{TN}}\right)^{2/n_1} - \left(\frac{P_{IN}}{P_{TN}}\right)^{\frac{n_1+1}{n_1}}\right]} \tag{A11}$$

With Φ_{ex} given by Eq. A10, and with PTN known, PlN can be solved by iteration. Then

$$T_{IN} = T_{TN}\left(\frac{P_{IN}}{P_{TN}}\right)^{\frac{n_1+1}{n_1}} \tag{A12}$$

$$V_{IN} = \sqrt{2gJc_p\left(T_{TN} - T_{IN}\right)} \tag{A13}$$

$$\dot{w}_N = \Phi_{ex} \; P_{TN} \; A_1 \sqrt{\frac{g}{R\,T_{TN}}} \tag{A14}$$

Secondary Flow

Secondary air is that part of the high pressure air provided by the Allis-Chalmers compressor that passes through the test turbine to the hood. For the expansion process from the hood to the annulus area

$$\frac{\dot{w}_T \sqrt{T_{TD}}}{A_{IT}\, P_{TD}} \sqrt{\frac{R}{g}} = \Phi_d = \sqrt{\frac{2\gamma}{\gamma-1}\left[\left(\frac{P_{IT}}{P_{TD}}\right)^{2/n_d} - \left(\frac{P_{IT}}{P_{TD}}\right)^{\frac{n_d+1}{n_d}}\right]} \qquad \text{(A15)}$$

With the secondary flow rate and hood total temperatures known, a value of PlT was assumed, and PTD is calculated by iteration and matching. For the assumed PlT

$$T_{IT} = T_{TD}\left(\frac{P_{IT}}{P_{TD}}\right)^{\frac{n_d-1}{n_d}} \qquad \text{(A16)}$$

$$V_{IT} = \sqrt{2gJc_p\left(T_{TD} - T_{IT}\right)} \qquad \text{(A17)}$$

Mixing Pipe

The momentum equation was used for the mixing pipe to obtain conditions at the diffuser entrance. The flow rate through the drive nozzle is known from preceding calculations and values must be assumed for the secondary flow conditions. Applying the momentum equation to the control volume between the nozzle exit and annulus plane (station 1), and the entrance to the diffuser (station 2),

$$\left(\frac{\dot{W}_N + \dot{W}_T}{g}\right)V_2 - \frac{\dot{W}_N}{g}V_{1N} - \frac{\dot{W}_T}{g}V_{1T} = P_{1T}A_{1T} + P_{1N}A_1 - P_2A_2 - F_f \qquad \text{(A18)}$$

Equation A18 holds for uniform velocity profiles and uniform static pressure distribution over each area.

The friction force F_f may be expressed as a pressure loss

$$F_f = \frac{\pi}{4}D_2^2\,\Delta p = \Delta p\, A_2 \qquad \text{(A19)}$$

where

$$\Delta P = f\,\frac{L}{D_2}\,\frac{\bar{\rho}}{2}\,\bar{V}^2 \qquad \text{(A20)}$$

L = length of duct

D_2 = duct diameter

$\bar{V}$ = average velocity

$\bar{\rho}$ = average density

f = friction factor

The friction factor was determined to be 0.017, in the manner outlined by Naviaux.[33] The friction force was figured with one iteration only. For the initial solution of Eq. A18, F_f was considered zero. After obtaining the conditions at the diffuser entrance, average values of $\bar{V}$ and $\bar{\rho}$ for the mixing pipe were calculated, and a ΔP found using Eq. A20. $\Delta P\, A_2$ was then subtracted from $P_{1T}A_{1T} + P_{1N}A_{1N}$ to obtain a new solution of Eq. A18.

[33] Naviaux, op. cit., pp. 25 - 26.

Unknown quantities in Eq. A18 are V_2 and p_2. The pressure p_2 can be expressed by V_2 to obtain one independent variable, if the total temperature after mixing is taken as the mass weighted average of

$$T_{T2} = \frac{\dot{w}_T T_{TD} + \dot{w}_N T_{TN}}{\dot{w}_N + \dot{w}_T} \tag{A21}$$

This condition assumes the existence of an adiabatic process. With

$$\dot{w}_N + \dot{w}_T = \dot{w} \tag{A22}$$

and the continuity equation

$$\dot{w} = \rho_2 A_2 V_2 \tag{A23}$$

$$V_2 = \frac{\dot{w} R T_2}{A_2 P_2} = \frac{\dot{w} R}{A_2 P_2} \left[T_{T2} - \frac{V_2^2}{2gJc_p} \right] \tag{A24}$$

Therefore

$$P_2 = \frac{\dot{w} R}{A_2 V_2} \left[T_{T2} - \frac{V_2^2}{2gJc_p} \right] \tag{A25}$$

Substituting Eq. A25 into Eq. A18

$$\frac{\dot{w}}{g} V^2 - \frac{\dot{w}_N}{g} V_{IN} - \frac{\dot{w}_T}{g} V_{IT} = P_{IT} A_{IT} + P_{IN} A_I - \frac{\dot{w} R}{V_2} \left[T_{T2} - \frac{V_2^2}{2gJc_p} \right] \tag{A26}$$

Multiply Eq. A26 by V_2 and rearrange

$$\left[\frac{\dot{w}}{g} - \frac{\dot{w}R}{2gJc_p}\right] V_2^2 - \left[\frac{\dot{w}_N}{g} V_{IN} + \frac{\dot{w}_T}{g} V_{IT} + P_{IT} A_{IT} + P_{IN} A_1\right] V_2 + WRT_{T2} = 0 \tag{A27}$$

Let

$$B_1 = \frac{\dot{w}}{g}\left(1 - \frac{R}{2Jc_p}\right) \tag{A28}$$

$$B_2 = -\left[\frac{\dot{w}_N}{g} V_{IN} + \frac{\dot{w}_T}{g} V_{IT} + P_{IT} A_{IT} + P_{IN} A_1\right] \tag{A29}$$

$$B_3 = \dot{w} R T_{T2} \tag{A30}$$

$$B_1 V_2^2 + B_2 V_2 + B_3 = 0 \tag{A31}$$

Thus

$$V_2 = \frac{-B_2 - \sqrt{B_2^2 - 4B_1 B_3}}{2B_1} = -\frac{B_2}{2B_1} - \sqrt{\left(\frac{B_2}{2B_1}\right)^2 - \frac{B_3}{B_1}} \tag{A32}$$

and

$$T_{21} = T_{T2} - \frac{V_{21}^2}{2gJc_p} \tag{A33}$$

$$P_{T2} = P_{21}\left(\frac{T_{T2}}{T_{21}}\right)^{\frac{\gamma-1}{\gamma}} \tag{A34}$$

The negative sign before the square root yields the subsonic solution. Supersonic conditions at the diffuser are outside to operating range of the TTTR installation.

Finally, for the compression in the subsonic diffuser

$$\frac{\dot{w}\sqrt{T_{21}}}{A_3 P_{21}}\sqrt{\frac{R}{g}} = \Phi_c = \sqrt{\frac{2\gamma}{\gamma-1}\left[\frac{T_{T2}}{T_{21}}\left(\frac{P_3}{P_{21}}\right)^{2/n_c} - \left(\frac{P_3}{P_{21}}\right)^{\frac{n_c+1}{n_c}}\right]} \tag{A35}$$

P_3 is solved by iteration and compared to atmospheric pressure. If it does not match for the chosen values of secondary flow conditions, a new P1T is selected and the process repeated until p_3 equals p_{atm}. With p_3 obtained

$$T_3 = T_{21}\left(\frac{P_3}{P_{21}}\right)^{\frac{n_c-1}{n_c}} \tag{A36}$$

$$V_3 = \sqrt{2gJc_p(T_{T2} - T_{21})} \tag{A37}$$

$$P_{T3} = P_3\left(\frac{T_{T2}}{T_3}\right)^{\frac{\gamma}{\gamma-1}} \tag{A38}$$

APPENDIX B

Exhauster Performance Prediction Program

The analysis of exhauster performance presented in detail in Appendix A was programed in Fortran IV for calculation on the IBM 360 computer. Input data include the assumed polytropic efficiencies, drive nozzle total pressure, drive nozzle total temperature, secondary air total temperature, secondary flow rate and atmospheric pressure. The principal quantity to be determined is the predicted hood total pressure. The printed output does include final values of temperature, velocity and pressure calculated during the computations.

The program uses an executive MAIN routine to arrange the sequence of calculations, but all calculations are performed in subroutines. The name and function of each subroutine is:

CSTANT; a grouping of all the basic quantities used in the entire program.

CHOPHI; a calculation of the non-dimensional flow function for a choked nozzle.

NOZZLE; computes conditions at the nozzle exit.

SECFLO; computes conditions at the secondary flow annulus area at the entrance to the mixing pipe.

MMENTM; Using conditions determined by NOZZLE and SECFLO, conditions at the diffuser entrance are calculated

based on conservation of momentum. One iteration is included to determine the wall frictional shear force.

SBCOMP; computes the compression process in the diffuser to obtain conditions at the diffuser exit.

Input information required to operate the prediction program is:

Card 1;

ETAD - Secondary flow polytropic efficiency

ETAN - Nozzle polytropic efficiency, entrance to throat

ETA1 - Nozzle polytropic efficiency, entrance to exit

NSETS - Number of sets of data to be computed

Card 2;

PTN - Drive nozzle total pressure (psia)

TTN - Drive nozzle total temperature (^{o}R)

TTD - Hood (secondary air) total temperature (^{o}R)

WT - Secondary flow rate

PA - Atmospheric pressure

Program EJECTOR with a sample output sheet is given on the following pages.

PREDICTION PROGRAM EJECTOR

```
      READ (5,1) ETAD,ETAN,ETA1,ETAC,NSETS
    1 FORMAT(4F10.4,I5)
     OCALL CSTANT(ETAD,ETAN,ETA1,ETAC,PI,PI4,AN,A1,A2,A1T,A3,GAM,
     1ENDD,ENN,EN1,ENC,R,CJ,CP,G,C1,C2,BLGTH,WT)
      WRITE (6,3)
    3 FORMAT (1H1)
      WRITE (6,10)
   10 FORMAT(///40H      ENDD         ENN         EN1         ENC   )
      WRITE (6,11) ENDD,ENN,EN1,ENC
   11 FORMAT(4F10.4)
      DO 400 J=1,NSETS
      PSUM=6.0
      RESET = 0.0
      SET=0.0
      READ (5,20) PTN,TTN,TTD,WT,PA
   20 FORMAT(5F10.4)
      CALL CHOPHI (PHIN,ENN,C2)
     OCALL NOZZLE (PHIN,AN,A1,PHIE,EN1,PTN,TTN,TTD,T1N,P1N,WN,G,R,C1,
     1C2,V1N)
   55 P1T=(PSUM*A2-P1N*A1)/A1T
      CALL SECFLO (ENDD,WT,PTD,P1T,C2,A1T,TTD,R,G,T1T,V1T,C1)
     OCALL MMENTM (W,WN,WT,G,R,CJ,CP,C1,BLGTH,A2,V1N,V1T,V21,TTN,T1T,
     1TT2,TTD,T21,P1T,P21,PT21,DELP1,GAM,PSUM,RESET)
      IF (RESET - .5) 96,96,69
   96 CONTINUE
      CALL SBCOMP (TT2,T21,ENC,R,G,A3,P21,C2,W,P3)
      DIFF=PA-P3
      IF(1.0-SET)63,64,64
   64 IF(DIFF-.01)27,28,28
   27 PSUM=PSUM-1.0
      SET = 5.0
      GO TO 55
   28 PSUM=PSUM+1.0
      GO TO 55
   63 IF(DIFF-.01)70,70,69
   69 PSUM=PSUM+.01
      RESET = 0.0
      GO TO 55
   70 T3=T21*(P3/P21)**((ENC-1.)/ENC)
      V3=SQRT (C1*(TT2-T3))
      PT3=P3*(TT2/T3)**(GAM/(GAM-1.))
      WRITE (6,100)
  100 FORMAT(1H1)
      WRITE (6,101) PTN,TTN
 1010FORMAT (/21H  TOTAL PRESSURE,PTN=,F6.2,24H  TOTAL TEMPERATURE,TTN=
     1,F6.2)
```

Prediction Program EJECTOR - Main Program Continued

```
      WRITE (6,102)
1020FORMAT(//75H          PTD          TTD          P1T          T1T
     1    V1T          WT          )
      WRITE (6,103) PTD,TTD,P1T,T1T,V1T,WT
103 FORMAT(6F12.5)
      WRITE (6,104)
104 FORMAT(//65H          P1N          T1N          WN          V1N
     1    PSUM                    )
      WRITE (6,105)P1N,T1N,WN,V1N,PSUM
105 FORMAT(5F12.5)
      WRITE (6,106)
1060FORMAT(//75H          PT21          TT2          P21          T21
     1    V21          W          )
      WRITE (6,103) PT21,TT2,P21,T21,V21,W
      WRITE (6,107)
1070FORMAT(//75H          PT3          P3          T3          V3
     1    DELP1                    )
      WRITE (6,108) PT3,P3,T3,V3,DELP1
108 FORMAT(5F12.5)
400 CONTINUE
      END
```

```
      OSUBROUTINE CSTANT (ETAD,ETAN,ETA1,ETAC,PI,PI4,AN,A1,A2,AIT,
      1A3,GAM,ENDD,ENN,EN1,ENC,R,CJ,CP,G,C1,C2,BLGTH,WT)
C      CONSTANTS IS SIMPLY A GROUPING OF ALL THE BASIC QUANTITIES USED
C      IN THE ENTIRE PROGRAM
       PI=3.1416
       PI4=PI/4.
       AN=PI4*3.65**2
       AN=PI4*3.25**2
       A1=PI4*4.74**2
       A1=PI4*4.24**2
       A2=PI4*7.50**2
       AIT=A2-PI4*4.76**2
       AIT=A2-PI4*4.25**2
       A3=PI4*14.**2
       GAM=1.4
       ENDD=GAM/(GAM-ETAD*(GAM-1.))
       ENN=GAM/(GAM-ETAN*(GAM-1.))
       EN1=GAM/(GAM-ETA1*(GAM-1.))
       ENC=GAM*ETAC/(1.-GAM*(1.-ETAC))
       R=53.345
       CJ=778.16
       CP=.24
       G=32.174
       C1=2.*G*CJ*CP
       C2=2.*GAM/(GAM-1.)
       BLGTH=86.
       RETURN
       END



       SUBROUTINE CHOPHI (PHIN,ENN,C2)
C  CHOPHI COMPUTES THE FLOW FUNCTION FOR A CHOCKED NOZZLE
       PHIN=(2./(ENN+1.))**(1./(ENN-1.))*SQRT(C2*(ENN-1.)/(ENN+1.))
       RETURN
       END
```

```
      OSUBROUTINE NOZZLE (PHIN,AN,A1,PHIE,EN1,PTN,TTN,TTD,T1N,P1N,
     1WN,G,R,C1,C2,V1N)
       PHIE=PHIN*AN/A1
       EXP1=2./EN1
       EXP2=(EN1+1.)/EN1
       EXP3=(EN1-1.)/EN1
       RA=.52
   38  F=SQRT(C2*(RA**EXP1-RA**EXP2))
       DIFF=F-PHIE
       IF(ABS(DIFF)-.001)40,40,39
   39  RA=RA-.0001
       GO TO 38
   40  T1N=TTN*RA**EXP3
       P1N=RA*PTN
       WN=PHIN*PTN*AN*SQRT(G/(R*TTN))
       V1N=SQRT(C1*(TTN-T1N))
       RETURN
       END
```

```
      OSUBROUTINE SECFLO (ENDD,WT,PTD,P1T,C2,A1T,TTD,R,G,T1T,V1T,
     1C1)
       EXP1=2./ENDD
       EXP2=(ENDD+1.)/ENDD
       PTD=P1T+.001
   71  PHID=SQRT (C2*((P1T/PTD)**EXP1-(P1T/PTD)**EXP2))
       FE=WT/(A1T*PTD)*SQRT (TTD*R/G)
       IF(FE-PHID)70,70,75
   75  PTD=PTD+.001
       GO TO 71
   70  CONTINUE
       T1T=TTD*(P1T/PTD)**((ENDD-1.)/ENDD)
       V1T=SQRT (C1*(TTD-T1T))
       RETURN
       END
```

```
      SUBROUTINE MMENTM (W,WN,WT,G,P,CJ,CP,C1,BLGTH,A2,V1N,V1T,V21,
     1TTN,T1T,TT2,TTD,T21,P1T,P21,PT21,DELP1,GAM,PSUM,RESET)
       W=WN+WT
       B1=W/G*(1.-R/(2.*CJ*CP))
       B2=(WN*V1N+WT*V1T)/G+PSUM*A2
       TT2=(WN*TTN+WT*TTD)/W
       B3=W*R*TT2
       B=B2/B1
       C=B3/B1
       ROOT=SQRT ((B/2.)**2-C)
       V21=B/2.-ROOT
       P21=B3/(A2*V21)-W*R*V21/(A2*C1)
       T21=TT2-V21**2/C1
C      FRICTION FACTOR .017 APPLIED AND PRESSURE LOST FOUND BY ONE
C      ITERATION
       PAV1=(PSUM+P21)/2.
       TAV1=(T1T+T21)/2.
       RHO1=PAV1*144./(G*R*TAV1)
       VAV1=(V1T+V21)/2.
       DELP1=.017*BLGTH*RHO1*VAV1**2/(7.5*2.*144.)
       PST1=PSUM-DELP1
       B21=(WN*V1N+WT*V1T)/G+PST1*A2
       BN1=B21/B1
       CHAR = (BN1/2.)**2-C
       IF (CHAR)91,92,92
    91 RESET=1.
       GO TO 93
    92 V21=BN1/2.-SQRT ((BN1/2.)**2-C)
       P21=B3/(A2*V21)-W*R*V21/(A2*C1)
       T21=TT2-V21**2/C1
       PT21=P21*(TT2/T21)**(GAM/(GAM-1.))
    93 CONTINUE
       RETURN
       END

      SUBROUTINE SBCOMP (TT2,T21,ENC,R,G,A3,P21,C2,W,P3)
      R1=TT2/T21
      R2=1.
      EXP1=2./ENC
      EXP2=(ENC+1.)/ENC
      Y=(W*SQRT (T21*R/G)/(A3*P21))**2/C2
   50 F=R1*R2**EXP1-R2**EXP2
      IF(F-Y)51,51,52
   52 R2=R2+.001
      GO TO 50
   51 P3=P21*R2
      RETURN
      END
```

TOTAL PRESSURE,PTN= 39.00 TOTAL TEMPERATURE,TTN=570.75

PTD	TTD	P1T	T1T	V1T	WT
10.22568	517.45630	9.20924	504.46533	395.11914	4.05340

P1N	T1N	WN	V1N	PSUM
5.50045	345.47998	7.05413	1677.90259	8.01000

PT21	TT2	P21	T21	V21	W
15.18006	557.01782	12.88652	531.54955	553.23022	11.10753

PT3	P3	T3	V3	DELP1
14.94920	14.79268	555.34497	141.78693	0.25409

APPENDIX C

Data Reduction Programs

Data obtained from laboratory tests to compute secondary flow rate, velocity profiles, and polytropic exponents were reduced by the computer programs included in this section. Input requirements are listed on comment cards at the start of each program.

Program SECFLO computes the mass of air that passes from the hood to the mixing pipe. The program basically calculates Eq. 1 of the main text. In addition, the small quantity of air that enters the hood through the shaft labyrinth is approximated by Eq. 2. Naviaux's flow nozzle coefficient is determined as a function of Reynolds number by a series of "IF" statements. The values used range from 1.00 - 1.05 in increments of .01.

Program VELOCITY computes Mach number and Velocity from traverse probe data. Input pressures are tested for supersonic or subsonic conditions. Either Eq. 4 or Eq. 5 is used depending on the condition that exists.

Program POLY computes by iteration the secondary flow polytropic exponent from test data. Eq. 19 with all quantities known but n_d was used in the calculation.

Data Reduction Program
SECFLO

```
C      CARD 1    RUN
C                DAY
C                MONTH
C      CARD 2    NSETS - NUMBER OF SETS OF DATA TO BE COMPUTED FOR RUN
C      CARD 3    TCL - TEMP IN CASCADE LAB IN DEG F
C                TCR - TEMP IN CONTROL ROOM IN DEG F
C                PBAR - BAROMETRIC PRESSURE IN CASCADE LAB IN IN HG
C      CARD 4    TTC - TEMP TEST CELL IN MILLIVOLTS
C                PTD - HOOD TOTAL PRESSURE IN IN HG FROM MANOMETER BOARD
C      CARD 5    PNOZ - CALIBRATION NOZZLE TOTAL PRESSURE IN IN HG
C                DIFF IN PRES ACROSS CALIBRATION NOZZLE IN IN H2O
C      CARD 6    TNOZ - CALIBRATION NOZZLE TOTAL TEMP IN MILLI-VOLTS
C                TTD - HOOD TOTAL TEMP IN MILLI-VOLTS
C                TTN - DRIVE NOZZLE TOTAL TEMP IN MILLI-VOLTS
C      CARD 7    DATA 1 - TRAVERSE NUMBER
C                DATA 2 - 1 IF BEFORE TRAVERSE, 2 IF AFTER TRAVERSE
C      REPEAT CARDS 4 - 7 FOR EACH FLOW RATE CALCULATED
       TEMPF(X)=32.+35.98*X-.435*X**2                                    0216A
       TCA1F(X)=32. + 44.41*X + .2185*X**2.
       TCA2F(X)=32.+45.24*X-.3295*X**2
       DO 777 I=1,2
       READ (5,102) RUN,DAY,MONTH
   102 FORMAT(I2,I2,I2)
       WRITE (6,103) RUN,DAY,MONTH
   103 FORMAT(12H1 RUN NUMBER,I3,4H ON,I2,1H/,I2,3H/67)
       READ (5,1) NSETS
     1 FORMAT(I3)
       WRITE (6,598)
   598 FORMAT(105H  DATA POINT    SECONDARY FLOW    SHAFT LABYRINTH    HOOD
      1TOTAL TEMP    DRIVE NOZZLE    HOOD TOTAL PRESSURE                 )
       WRITE (6,599)
   599 FORMAT(80H                          (LB/SEC)        FLOW (LB/SEC)
      1                TOTAL TEMP                )
       PATM=70.0
       DN = 4.25
       C5=.036269
       ALFA=0.76
       GAMS=1.15
       AL=3.1416*(1.2205**2.-1.2**2.)/4.
       G=32.174
       R=53.35
       READ (5,2) TCL,TCR,PBAR
     2 FORMAT(3F10.4)
       GH2O=1.00013+TCR*.078/1000.-TCR**2.*.0014/1000.
       CHGC=.49280-TCL*.5/10000.
       CHGCR=.49280-TCR*.5/10000.
       PBAR=PBAR*CHGC
       DO 700 J=1,NSETS
```

```
      CN=1.05
      READ (5,15) TTC,PTD
   15 FORMAT (2F10.5)
      PTD=CHGCR*(PATM-PTD)+PBAR
      TTC=TEMPF(TTC)+459.6
      RATIO=PTD/PBAR
      PHI=SQRT((1.-RATIO**2.)/(10.+2.*ALOG(1./RATIO)/1.4))
      WSHL=AL*PBAR*SQRT(G/(TTC*R))*ALFA*GAMS*PHI
      READ (5,3) PNOZ,DH,BLANK
      READ (5,3) TNOZ,TTD,TTN
    3 FORMAT (3F10.4)
      READ (5,4) DATA1,DATA2
    4 FORMAT(I5,I5)
      TNOZ=TEMPF(TNOZ)+459.6
      TTD = TEMPF(TTD)+459.6
      IF (TTN-1.52)65,65,66
   65 TTN=TCA1F(TTN)+459.6
      GO TO 67
   66 TTN = TCA2F(TTN)+459.6
   67 DH=DH*GH2O*C5
      PNOZ=CHGCR*(PATM-PNOZ)+PBAR
      ALPHN=1.+.00252*(TNOZ-527.7)/100.
      Z=1.9+.24*((TNOZ-459.7)/100.-1.)
      X=DH/PNOZ
      XR=1.-X
      B=(4.25/7.975)**4.
      Y=SQRT((XR**(2./1.4))*3.5*(1.-XR**(.4/1.4))/(1.-XR)*(1.-B)/(1.
     1-B*XR**(2./1.4)))
      FLOW=.8633*DN**2*ALPHN*CN*Y*SQRT(PNOZ*DH/TNOZ)
      FLOW=FLOW + WSHL
      RE=6.316*FLOW/(4.25*Z)*360000.
      RE=RE*.00001
      IF(RE-9.00)11,21,21
   11 IF (RE-7.25) 12,22,22
   12 IF (RE-6.25) 24,23,23
   21 CN=1.05
      GO TO 75
   22 CN=1.04
      GO TO 75
   23 CN=1.03
      GO TO 75
   24 CN=1.02
   75 FLOW=.8633*DN**2*ALPHN*CN*Y*SQRT(PNOZ*DH/TNOZ)
      FLOW=FLOW + WSHL
      WRITE (6,600) DATA1,DATA2,FLOW,WSHL,TTD,TTN,PTD
  600 FORMAT(/I6,2H -,I2,1F15.4,1F17.4,2H  ,1F19.4,1F16.4,1F19.4)
  700 CONTINUE
  777 CONTINUE
```

Data Reduction Program
VELOCITY

```
C      VELOCITY COMPUTES BY ITERATION THE VELOCITY IN EITHER
C      SUPERSONIC OR SUBSONIC FLOW FROM THE TRAVERSE INFORMATION
C      INPUTS TO VELOCITY  ARE
C      CARD 1     NSETS (NUMBER OF DATA POINTS)      FORMAT  I3
C      CARD 2  PTAM (BAROMETRIC PRESSURE-IN.HG.)
C              TARE (REFERENCE PRESSURE OF MAMOMETER BOARD)
C      FORMAT      2F10.4
C      CARD 3 THRU NSETS
C              POSIT (TRAVERSE POSITION)
C              STA (MIXING TUBE STATION TRAVERSE TAKEN AT)
C              P  (TRAVERSE STATIC PRESSURE)  READING FROM BOARD   IN.HG.
C              PT (TRAVERSE TOTAL PRESSURE)  READING FROM BOARD  IN.HG.
C              TT (TRAVERSE TOTAL TEMPERATURE)      ENTER IN MILLIVOLTS
C              DATA POINT
C      FORMAT  I2,I3,3F10.4,I2
C      THIS RUN USES TRAVERSE STATIC PRESSURE
       TEMPF(X)=32.+35.98*X-.435*X**2
       DO 779 I=1,1
       READ (5,1) NSETS
     1 FORMAT(I3)
       READ (5,2) PATM,TARE
     2 FORMAT(2F10.4)
       WRITE (6,777)
   777 FORMAT (50H1VELOCITY PROFILES AT      7 AUG  1967 --- RUN 31   // )
       WRITE (6,3C1)
  3010FORMAT (114H       MACH NO.       VELOCITY            PT
     1 P                TT                T       POS   STA  DATA            )
       DO 500 J=1,NSETS
       READ (5,4) POSIT,STA,P,PT,TT,DATA
     4 FORMAT(I2,I3,3F10.4,I2)
       PA=PATM*.4913
       P=P-TARE
       P=PA-P*.4921
       IF(PT-TARE)10,10,11
    10 PT=(TARE-PT)*.4921 +PA
       GO TO 77
    11 PT=PA-(PT-TARE)*.4921
    77 CONTINUE
       AM=.001
       Y=P/PT
       Z=PT/P
       IF (Y-.528)15,15,7
     7 Q=(1.+.2*(AM**2))**3.5
       IF(Q-Z)12,12,13
    12 AM=AM+.001
       GO TO 7
    13 IF(AM-1.)14,14,15
    14 GO TO 21
```

Program VELOCITY Continued

```
 15 X=P/PT
    AM=1.
 17 R=((2.8/2.4*AM**2-.4/2.4)**2.5)/((1.2*AM**2)**3.5)
    IF(X-R)20,21,21
 20 AM=AM+.001
    GO TO 17
 21  CONTINUE
    TT=TEMPF(TT)+459.7
    T=TT/(1.+.2*AM**2)
    C=SQRT(1.4*32.174*53.345*T)
    V=AM*C
400 WRITE(6,600)AM,V,PT,P,TT,T,POSIT,STA,DATA
600 FORMAT (6F15.5,3I5)
500 CONTINUE
779 CONTINUE
    END
```

Data Reduction Program
POLY

```
C      PROGRAM POLY COMPUTES THE POLYTROPIC EXPONENT OF THE SECONDARY
C      FLOW FROM THE PLENUM TO THE MIXING TUBE FROM EXPERIMENTAL DATA
C      CARD 1    NSETS - NUMBER OF SETS OF DATA TO BE COMPUTED
C      CARD 2    TCL - TEMP IN CASCADE LAB IN DEG F
C                TCR - TEMP IN CONTROL ROOM IN DEG F
C                PBAR - BAROMETRIC PRESSURE IN CASCADE LAB IN IN HG
C      CARD 3    WT - SECONDARY AIR MASS FLOW RATE IN LBS/SEC
C                TTD - TOTAL TEMP IN PLENUM IN MILLI VOLTS
C                PTD - TOTAL PRESSURE IN PLENUM IN IN HG
C                P7 (N7) - STATIC PRESSURE SEC AIR THROAT IN IN HG
C      REPEAT CARD 3 FOR EACH DATA POINT
C      THIS DATA FROM RUN 23 AT PTN 39,36$32
       TEMPF(X)=32.+35.98*X-.435*X**2
       R=53.35
       G=32.174
       PI4=3.1416/4.0
       RG=SQRT(R/G)
       GAM=1.4
       A2=PI4*7.50**2
       A1T=A2-PI4*4.76**2
       PATM1=70.0
       PATM2=50.0
       WRITE (6,9)
     9 FORMAT (1H1)
       WRITE (6,15)
    15FORMAT ( 85H                WT                TTD                PTD
      1P7      POLYTROPIC EXPONENT                 )
       READ (5,1) NSETS
     1 FORMAT(I3)
       READ (5,11) TCL,TCR,PBAR
    11 FORMAT (3F10.4)
       CHGC=.49280-TCL*.5/10000.
       CHGCR=.49280-TCR*.5/10000.
       PBAR=PBAR*CHGC
       DO 500 J=1,NSETS
       READ (5,2) WT,TTD,PTD,P7
     2 FORMAT(4F10.5)
       TTD=TEMPF(TTD)+459.7
       PTD=CHGCR*(PATM1-PTD)+PBAR
       P7=CHGCR*(PATM2-P7)+PBAR
       RA=P7/PTD
       X=WT*RG*SQRT(TTD)/(PTD*A1T)
       ETAS=1.001
     6 EXP1=2./ETAS
       EXP2=(ETAS+1.)/ETAS
     5 Y=SQRT(2.*GAM/(GAM-1.)*(RA**EXP1-RA**EXP2))
       IF(X-Y)10,10,20
    20 ETAS=ETAS+.001
       GO TO 6
    10 WRITE (6,30) WT,TTD,PTD,P7,ETAS
    30 FORMAT(/5F15.7)
   500 CONTINUE
       END
```

APPENDIX D

Restricted Jet Operation

In order that the reader might better understand the general terms used in this thesis to describe jet operation and associated mixing phenomena, the following general description of jet operation is presented.

Figure D1 of this appendix pictures the physical situation to be discussed. Essentially, two co-flowing streams enter a mixing pipe. Abramovich[33] states that with this situation, the velocity components along the y-axis (the radial components for the exhauster) prove so small that they can be disregarded in engineering problems involving jet theory.

The two co-flowing streams enter the mixing pipe with their fluid particles traveling at different velocities. The viscous forces acting between the two flows cause a slowing down of the particles of the primary jet and a speeding up of the secondary flow particles. The area of the flow where the interaction between the particles of the two streams takes place is called the mixing zone. The mixing zone thickens with axial distance, causing a gradual "eating up" of the primary and secondary core regions.

Two main mixing regions are designated in the mixing pipe. The initial region has the axial distance where the

[33] Abramovich, op. cit., p. 5

secondary core region and the primary core region still exist. The main mixing region is that part of the pipe where the mixing zone has touched the pipe walls and the primary core region no longer exists. The regions are shown in Fig. D1. In the literature use is sometimes made of a transition zone which is the region that occurs if the mixing zone contacts the pipe wall before the primary core is "eaten up" or vice versa. This thesis uses the simplified model in which it is assumed that the length of the transitional region is equal to zero. In the main mixing region, the jet becomes similar in appearance to a flow of fluid from a source of infinitely small thickness (in an axially symmetric case,the source is a point).

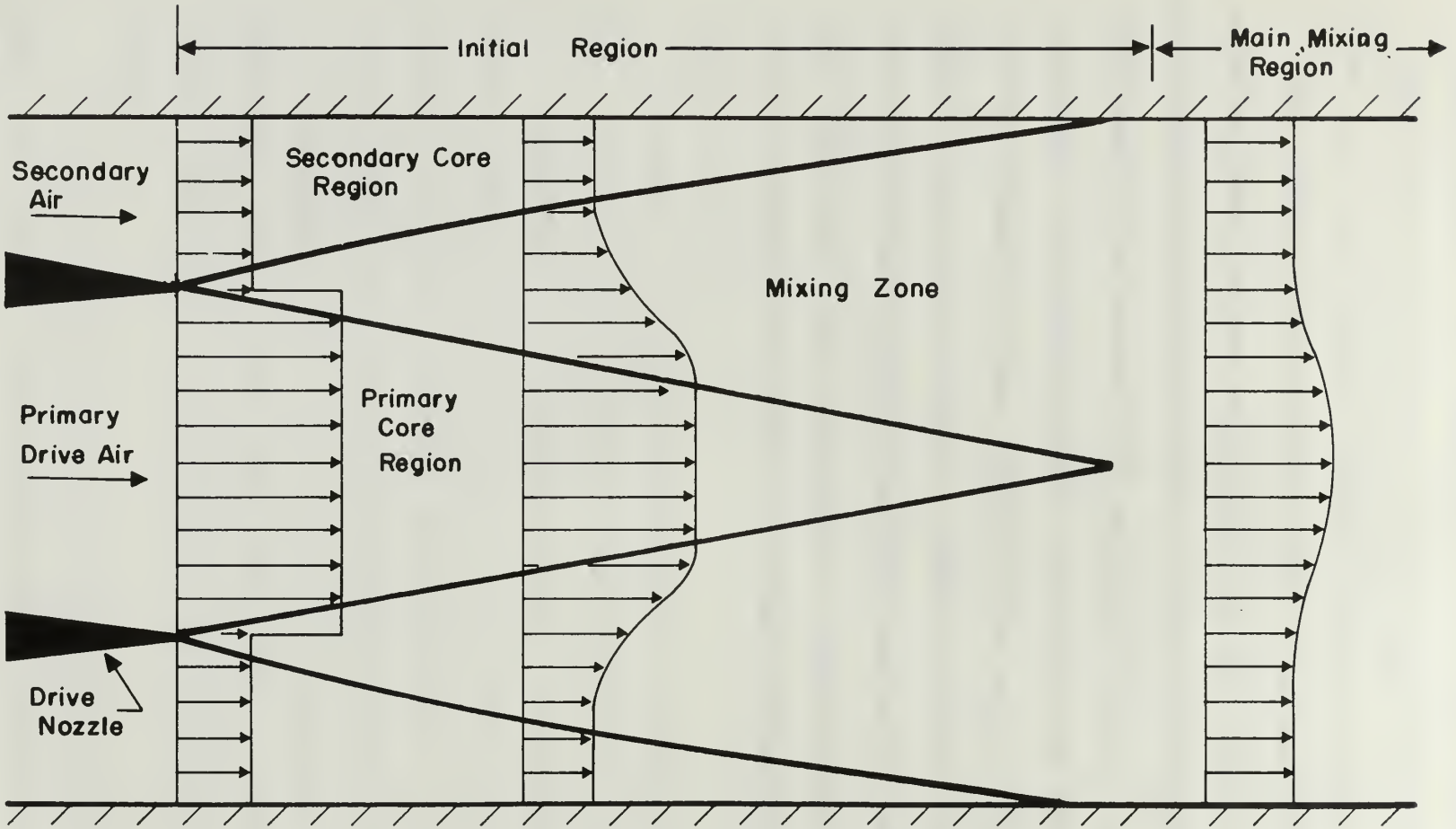

DIAGRAM OF RESTRICTED JET
WITH SECONDARY FLOW

FIGURE D-1

INITIAL DISTRIBUTION LIST

		No. Copies
1.	Defense Documentation Center Cameron Station Alexandria, Virginia 22314	20
2.	Library Naval Postgraduate School Monterey, California 93940	2
3.	Commander, Naval Air Systems Command Navy Department Washington, D. C. 20360	1
4.	Commander, Naval Ship Systems Command Navy Department Washington, D. C. 20360	1
5.	CAPT A. Bodnaruk, USN Naval Ship Systems Command (Code 6140) Navy Department Washington, D. C. 20360	1
6.	Office of Naval Research (Power Branch) Attn. Mr. J. K. Patton, Jr. Navy Department Washington, D. C. 20360	1
7.	Chairman, Department of Aeronautics Naval Postgraduate School Monterey, California 93940	2
8.	Professor M. H. Vavra Department of Aeronautics Naval Postgraduate School Monterey, California 93940	3
9.	LCDR P. A. Monroe, USN Propulsion Group Naval Air Systems Command Navy Department Washington, D. C. 20360	3

UNCLASSIFIED

Security Classification

DOCUMENT CONTROL DATA - R&D

(Security classification of title, body of abstract and indexing annotation must be entered when the overall report is classified)

1. ORIGINATING ACTIVITY *(Corporate author)*
Naval Postgraduate School
Monterey, California, 93940

2a. REPORT SECURITY CLASSIFICATION
UNCLASSIFIED

2b. GROUP

3. REPORT TITLE
An Investigation of the Performance and Mixing Phenomena Associated with a Supersonic Exhauster Interacting with Subsonic Secondary Flow.

4. DESCRIPTIVE NOTES *(Type of report and inclusive dates)*
Thesis - Aeronautical Engineer

5. AUTHOR(S) *(Last name, first name, initial)*
Monroe, Philip A.

6. REPORT DATE	7a. TOTAL NO. OF PAGES	7b. NO. OF REFS
September 1967	128	

8a. CONTRACT OR GRANT NO.	9a. ORIGINATOR'S REPORT NUMBER(S)
b. PROJECT NO.	
c.	9b. OTHER REPORT NO(S) *(Any other numbers that may be assigned this report)*
d. Unlimited dist.	

10. AVAILABILITY/LIMITATION NOTICES
This document is subject to special export controls and each transmittal to foreign nationals may be made only with prior approval of the Naval Postgraduate School.

11. SUPPLEMENTARY NOTES	12. SPONSORING MILITARY ACTIVITY
	Naval Postgraduate School Monterey, California 93940

13. ABSTRACT

The Transonic Turbine Test Rig at the Naval Postgraduate School, Monterey, California, uses a supersonic jet exhauster to lower the turbine exit static pressure and thus increase pressure ratios available for turbine testing. Exhauster operation results in interaction between two co-flowing streams of air. The primary air is supersonic and the secondary air, subsonic. This thesis is an experimental study of the mixing process that occurs between the two streams in a cylindrical mixing chamber. In addition, a theoretical model of the exhauster performance based on polytropic efficiencies and conservation of momentum was programmed, and the predicted values were compared to test results.

DD FORM 1 JAN 64 1473

UNCLASSIFIED

Security Classification

14 KEY WORDS	LINK A		LINK B		LINK C	
	ROLE	WT	ROLE	WT	ROLE	WT
Exhauster						
Ejector						
Mixing of Co-Flowing Streams						
Turbulent Jet						
Compressible Mixing						
Supersonic Flow						